



National Library
of Canada

Bibliothèque nationale
du Canada

Canadian Theses Service

Service des thèses canadiennes

Ottawa, Canada
K1A 0N4

NOTICE

The quality of this microform is heavily dependent upon the quality of the original thesis submitted for microfilming. Every effort has been made to ensure the highest quality of reproduction possible.

If pages are missing, contact the university which granted the degree.

Some pages may have indistinct print especially if the original pages were typed with a poor typewriter ribbon or if the university sent us an inferior photocopy.

Reproduction in full or in part of this microform is governed by the Canadian Copyright Act, R.S.C. 1970, c. C-30, and subsequent amendments.

AVIS

La qualité de cette microforme dépend grandement de la qualité de la thèse soumise au microfilmage. Nous avons tout fait pour assurer une qualité supérieure de reproduction.

S'il manque des pages, veuillez communiquer avec l'université qui a conféré le grade.

La qualité d'impression de certaines pages peut laisser à désirer, surtout si les pages originales ont été dactylographiées à l'aide d'un ruban usé ou si l'université nous a fait parvenir une photocopie de qualité inférieure.

La reproduction, même partielle, de cette microforme est soumise à la Loi canadienne sur le droit d'auteur, SRC 1970, c. C-30, et ses amendements subséquents.

UNIVERSITY OF ALBERTA

ESTIMATION OF HARMONICS IN ELECTRICAL POWER SYSTEMS

BY

KHALED MOHAMED MOHIE EL-DEEN EL-NAGGAR

A Thesis submitted to the Faculty of Graduate Studies and
Research in partial fulfillment of the requirements for the
degree of Doctor of Philosophy

DEPARTMENT OF ELECTRICAL ENGINEERING

Edmonton, Alberta

Spring 1992



National Library
of Canada

Bibliothèque nationale
du Canada

Canadian Theses Service Service des thèses canadiennes

Ottawa, Canada
K1A 0N4

The author has granted an irrevocable non-exclusive licence allowing the National Library of Canada to reproduce, loan, distribute or sell copies of his/her thesis by any means and in any form or format, making this thesis available to interested persons.

The author retains ownership of the copyright in his/her thesis. Neither the thesis nor substantial extracts from it may be printed or otherwise reproduced without his/her permission.

L'auteur a accordé une licence irrévocable et non exclusive permettant à la Bibliothèque nationale du Canada de reproduire, prêter, distribuer ou vendre des copies de sa thèse de quelque manière et sous quelque forme que ce soit pour mettre des exemplaires de cette thèse à la disposition des personnes intéressées.

L'auteur conserve la propriété du droit d'auteur qui protège sa thèse. Ni la thèse ni des extraits substantiels de celle-ci ne doivent être imprimés ou autrement reproduits sans son autorisation.

ISBN 0-315-73217-2

Canada

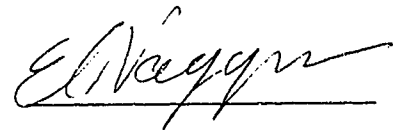
UNIVERSITY OF ALBERTA

RELEASE FORM

NAME OF AUTHOR: KHALED MOHAMED MOHIE EL-NAGGAR
TITLE OF THESIS: HARMONICS ESTIMATION IN ELECTRICAL
POWER SYSTEMS
DEGREE: DOCTOR OF PHILOSOPHY
YEAR THIS DEGREE GRANTED: 1992

Permission is hereby granted to the University of Alberta Library to reproduce single copies of this thesis and to lend or sell such copies for private, scholarly or scientific research purposes only.

The author reserve all other publication and other rights in association with the copyright in the thesis, and expect as hereinbefore provided neither the thesis nor any substantial portion thereof may be printed or otherwise reproduced in any material form whatever without the author's prior written permission.



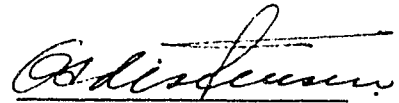
116 EL-HEGAZ street
HELIOPOLIES
CAIRO, EGYPT

Date: *April 21, 1992*

UNIVERSITY OF ALBERTA

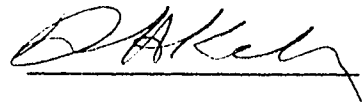
FACULTY OF GRADUATE STUDIES AND RESEARCH

The undersigned certify that they have read, and recommend to the Faculty of Graduate Studies and Research for acceptance, a thesis entitled ESTIMATION OF HARMONICS IN ELECTRICAL POWER SYSTEMS submitted by KHALED MOHAMED MOHIE EL-NAGGAR in partial fulfilment of the requirements for the degree of DOCTOR OF PHILOSOPHY.



Supervisor:

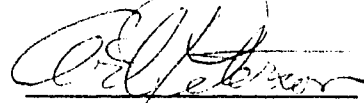
G.S. Christensen



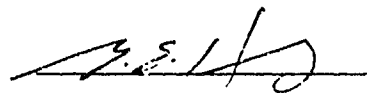
D.H. Kelly



D. Koval



A.E. Peterson



External Examiner:

M.E. EL-Hawary

Date: 16/04/92.

To My Parents

and

To My Wife and Sons

ABSTRACT

Power system networks are subjected to harmonics injection due to the presence of non linear loads, and to the use of all kinds of converters and inverters. The estimation of harmonic contents of the voltage or the current waveforms needs an efficient parameter estimation technique.

Parameter estimation techniques used in harmonics identification, can be classified as either static or dynamic.

This thesis present a new application of the least squares technique for estimating the harmonic contents. A new non iterative least absolute value technique is presented as well. Results obtained from those techniques showed that they can be considered as alternative to the discrete Fourier transform algorithm.

In the dynamic case a new least absolute value filter is presented as an equivalent to the Kalman filter with the superiority in the cases where the error distribution is non-Gaussian.

The thesis is concluded by comments and recommendations for future work.

ACKNOWLEDGMENT

My sincerest gratitude is extended to Professor G.S.Christensen for the efforts he has undertaken, to make it possible for me to attend this fine university. I would also like to thank Professor Christensen for encouragement, help, support, advice and for patience and understanding shown during the course of my studies.

I wish to thank Professor D.H. Kelly, for the time and effort he spent with me through frequent discussions.

I am grateful to Dr. S.A.Soliman, for the helpful advice and for the time and effort he has spent helping me during my study. His suggestions were always of great help to me. My thanks are also extended to the Alberta Power Company for providing the data used in this study.

I owe a debt of gratitude to my wife Hala. This work would not be possible without her support, help, encouragement, understanding and patience. Thanks also to our children, Mohamed and Ahmed for their patience. The understanding, patience and support that my parents gave me were the motivation to start and complete this work. My thanks go also to my father and mother in law for their encouragement and moral support.

I wish to extend my thanks to Ain Shams University, Cairo, Egypt for giving me the chance to continue my studies.

Finally I wish to thank the National Research Council of Canada, and the Department of Electrical Engineering, University of Alberta, for the financial support during the course of this study.

TABLE OF CONTENTS

LIST OF FIGURES

LIST OF SYMBOLS

CHAPTER I: INTRODUCTION	1
1.1 Outline of thesis	3
CHAPTER II: THE POWER SYSTEM HARMONICS PROBLEM	4
2.1 Introduction	4
2.2 Harmonic sources	4
2.2.1 Established and known harmonic sources	5
2.2.2 New harmonic sources	6
2.3 Harmonic effects	7
2.3.1 Resonances	8
2.3.2 Effects on rotating machines	8
2.3.3 Effects on static components	9
2.3.4 Effects on protection systems	10
2.3.5 Effects on communication systems	10
2.3.6 Other harmonic effects	10
2.4 Harmonic measurements	11
2.4.1 The development of power system harmonic measurements	11
2.5 State estimation techniques used in power systems	14
2.5.1 Static state estimation techniques	14

2.5.2	Dynamic state estimation techniques	17
2.6	Standards for limitation of power system harmonics	18
2.7	Harmonic elimination and reduction	19
CHAPTER III	MATHEMATICAL MODELLING	21
3.1	Mathematical analysis	21
3.1.1	Harmonic analysis	21
3.1.2	Subharmonic analysis	25
3.2	System modelling	29
3.2.1	Static estimation model	30
3.2.2	Dynamic estimation models	30
3.3	Harmonic sources identification	38
CHAPTER IV	PARAMETER ESTIMATION: THE STATIC CASE	41
4.1	Static estimation techniques	41
4.1.1	Discrete Fourier transform	41
4.1.2	Least error squares estimation	44
4.1.3	Least absolute value estimation	46
4.2	Test of algorithms: Simulated examples	50
4.2.1	The discrete Fourier case	50
4.2.2	The least squares case	55
4.2.3	The Least absolute value case	78
4.3	Test of algorithms: Actual recorded data	87
4.3.1	Comparison between the DFT and the LS techniques	92
4.3.2	Comparison between the LAV and the LS techniques	115

CHAPTER V	PARAMETER ESTIMATION: THE DYNAMIC CASE	132
5.1	Stochastic estimation	132
5.2	Dynamic estimation problem	133
5.2.1	Kalman filtering	136
5.2.2	Least absolute value filtering	138
5.3	Test of the algorithms: Simulated example	142
5.4	Test of the algorithms: Actual recorded data	151
5.4.1	Kalman filter case	153
5.4.2	Weighted least absolute value filter case	176
5.5	Comparison between the KF and the WLAVF	192
CHAPTER VI	SUMMARY AND CONCLUSIONS	200
REFERENCES		204
APPENDICES		208

LIST OF FIGURES

Discrete Fourier transform results Simulated example

4.1	Line spectrum of the full wave voltage	52
4.2	The percentage error in the voltage magnitudes	53
4.3	Variations of the percentage error with the number of harmonics	55
4.4	Variations of harmonic magnitudes with the sampling frequency	56
4.5	Variations of harmonic magnitudes with the sampling frequency	57
4.6	Variations of the percentage error with the sampling frequency	58
4.7	Variations of the percentage error with the data window size	60
4.8	The effect of the frequency drift on the harmonic magnitudes	61
4.9	The effect of the bad data on the harmonic magnitudes	63
4.10	The percentage error in the voltage magnitudes	64

Least error squares results Simulated example

4.11	Line spectrum of the full wave voltage	66
4.12	The percentage error in the voltage magnitudes	67
4.13	Variations of harmonics magnitudes with the number of harmonics	69
4.14	Variations of the percentage error with the number of harmonics	70
4.15	Variations of harmonics magnitudes with the sampling frequency	71
4.16	Variations of the percentage error with the sampling frequency	72
4.17	Variations of the percentage error with the data window size	74
4.18	The effect of the frequency drift on the harmonic magnitudes	75
4.19	The effect of the bad data on the harmonic magnitudes	77

4.20	The percentage error in the voltage magnitudes	79
------	--	----

Least absolute value results Simulated Examples (1&2)

4.21	The percentage error in the voltage magnitude (Ex.1)	81
4.22	The effect of the bad data on the harmonic magnitudes (Ex.1)	82
4.23	Harmonics magnitudes (Ex.2)	83
4.24	Harmonics phase angles (Ex.2)	84
4.25	Bad data effects on the harmonic magnitudes (Ex.2)	85
4.26	Bad data effects on the phase angles (Ex.2)	86
4.27	Harmonics magnitudes with frequency drift (Ex.2)	88
4.28	Harmonics phase angles with frequency drift (Ex.2)	89

Actual Recorded data

4.29	Actual recorded voltage for phase A	90
4.30	Actual recorded phase currents	91

Comparison between the DFT and the LS techniques

4.31	Line spectrum for the voltage V_A	93
4.32	Phase angles for the voltages V_A	94
4.33	Line spectrum for I_A	95
4.34	Phase angles for I_A	96
4.35	Harmonics power for phase A	98
4.36	Variations of harmonics magnitudes with the number of harmonics	99

4.37	Variations of harmonics phase angles with number of harmonics	100
4.38	Variations of harmonics power with the number of harmonics	101
4.39	Variations of harmonics magnitudes with sampling rate	102
4.40	Variations of harmonics phase angles with sampling rate	103
4.41	Variations of harmonics power with sampling rate	104
4.42	Variations of harmonics magnitudes with the data window size	106
4.43	Variations of harmonics phase angles with the data window size	107
4.44	Variations of harmonics power with the data window size	108
4.45	The effect of the bad data on the harmonic magnitudes (LS)	109
4.46	The effect of the bad data on the Harmonic magnitudes (DFT)	110
4.47	Actual and reconstructed current for phase A (W.S.=1cycles)	112
4.48	Actual and reconstructed current for phase A (W.S.=4cycles)	113
4.49	Actual and Reconstructed current for phase considering each cycle separately	114

Comparison between the LAV and the LS algorithms

4.50	Line spectrum for I_b	116
4.51	Phase angles for I_b	117
4.52	Line spectrum for V_b	118
4.53	Harmonics power for phase B	119
4.54	Variations of harmonic magnitudes with the number of harmonics	122
4.55	Variations of harmonic phase angles with the number of harmonics	123
4.56	Variations of harmonics power with the number of harmonics	124
4.57	Variations of harmonics magnitudes with sampling rate	125
4.58	Variations of harmonics power with sampling rate	126
4.59	Variations of harmonics magnitudes with the data window size	128

4.60	Variations of harmonics power with the data window size	129
4.61	Effect of bad data on the harmonic magnitudes	130

Testing of KF and WLAVF (Simulated example)

5.1	Estimated magnitude of 60 Hz and third harmonic components using models 1 and 2	144
5.2	Estimated magnitudes of 7th, 11th and 13th harmonic using models 1 and 2.	145
5.3	Estimated phase angles using models 1 and 2	146
5.4	Kalman filter gain for x_1 and y_1 (Model 1)	147
5.5	The WLAVF gain for x_1 and y_1 (Model 1)	148
5.6	Kalman filter gain for x_1 (model 2)	149
5.7	The WLAVF gain for x_1 (model 2)	150
5.8	Estimated magnitudes of the fundamental and 3rd harmonic components with frequency drift	152

Kalman filter results (actual recorded data)

5.9	Harmonics magnitudes of V_A versus time steps at different W.S.	154
5.10	Harmonics magnitudes of I_A versus time steps at different W.S.	155
5.11	Harmonics phase angles of I_A versus time steps at different W.S.	156
5.12	Fundamental powers versus time steps at different W.S.	157
5.13	4th harmonic power versus time steps at different W.S.	158
5.14	6th harmonic power versus time steps at different W.S.	159
5.15	Variations of harmonics magnitudes with the time steps ($f_s=2118.6$ Hz.)	162
5.16	Variations of harmonics magnitudes with the time steps ($f_s=2824.58$ Hz.)	163
5.17	Variations of harmonics magnitudes with the time steps	

($f_s=4237.28$ Hz.)	164
5.18 Variations of harmonics power with the sampling frequency	165
5.19 Variations of harmonics power with the time steps ($f_s=2824.58$ Hz.)	166
5.20 Variations of harmonics power with the time steps ($f_s=4237.28$ Hz.)	167
5.21 Variations of harmonics magnitudes with the time steps (Number of harmonics=7)	168
5.22 Variations of harmonics magnitudes with the time steps (Number of harmonics=9)	169
5.23 Variations of harmonics magnitudes with the Number of harmonics	170
5.24 Actual and reconstructed current for phase A	172
5.25 The subharmonic amplitudes	173
5.26 The phase angle of the 30 Hz. component	174
5.27 The final error in the estimate using KF algorithm	175

WLAVF results (Actual recorded data)

5.28 Harmonics magnitudes of V_A versus time steps at different W.S.	177
5.29 Harmonics magnitudes of I_A versus time steps at different W.S.	178
5.30 Harmonics phase angles of I_A versus time steps at different W.S.	179
5.31 Fundamental powers versus time steps at different W.S.	180
5.32 6th harmonic power versus time steps at different W.S.	181
5.33 Variations of harmonics magnitudes with the time steps ($f_s=2118.6$ Hz.)	183
5.34 Variations of harmonics magnitudes with the time steps ($f_s=2824.85$ Hz.)	184
5.35 Variations of harmonics magnitudes with the time steps ($f_s=4237.28$ Hz.)	185

5.36	Variations of harmonics power with the time steps ($f_s=2118.6$ Hz.)	186
5.37	Variations of harmonics power with the time steps ($f_s=2824.85$ Hz.)	187
5.38	Variations of harmonics power with the sampling frequency	188
5.39	Variations of harmonics magnitudes with the time steps (Number of harmonics=7)	189
5.40	Variations of harmonics magnitudes with the time steps (Number of harmonics=9)	190
5.41	Variations of harmonics magnitudes with the number of harmonics	191
5.42	Actual and reconstructed current for phase A	193
5.43	The subharmonic amplitudes	194
5.44	The phase angle of the 30 Hz. component	195
5.45	The final error in the estimate using the WLAVF algorithm	196
5.46	Comparison between the filters gains	197
5.47	The final error in the estimate using the two filters	199

LIST OF SYMBOLS

$Z(t)$	The measurement vector
$A(t)$	The measurement coefficient matrix (static case)
Θ	The parameter vector to be estimated
w	The measurement noise vector
U	The total number of unknowns
m	The total number of measurements
σ	The damping constant
$H(t)$	The measurement coefficient matrix (dynamic case)
k	The time step
Δt	The sampling time
$\Phi(k)$	The state transition matrix at step (k)
$\varepsilon(k)$	The state equation noise vector due to modeling errors
$Q(k)$	The covariance matrix of $\varepsilon(k)$
$R(k)$	The covariance matrix of $w(k)$
$A^+(t)$	The left pseudo-inverse of the matrix $A(t)$
r_i	The i^{th} residual
\bar{r}	The mean value of the residuals
$K(k)$	The dynamic filter gain matrix at step k
$e(k)$	The estimation error at step k
$P(k)$	The error covariance matrix at step k
$\hat{\Theta}(k)$	The updated estimate after the measurement considered
$\tilde{\Theta}(k)$	The projected estimate prior to assimilating the measurement

CHAPTER I

INTRODUCTION

Over the past several years, electric utilities have experienced an increase in the levels of harmonic frequencies on the electrical delivery system. Although harmonic frequencies have always been present on power supply systems, they have recently become of interest to utilities.

The increasing use of solid-state power-conversion equipment (rectifiers inverters, cycloconverters) and other power electronic-type devices (voltage controllers, motor-speed controllers) on distribution systems is causing utilities to become much more concerned about harmonic voltage and current levels on these systems. The undesirable effects of harmonic distortion in power systems have been well documented and will be discussed in the next chapter [6,7]. The electricity supply authorities have a responsibility to insure that, in using electrical energy, a consumer does not cause undue interference with, or damage to, the equipment of another consumer or of the supply authority [1,2,3].

Accurate measurement of power system harmonics is essential to evaluate the harmonic distortion in both current and voltage waveforms. Most static harmonic analysis algorithms are based either on the discrete Fourier transform or on fast Fourier transform [7,13] (FFT) to obtain the voltage and current frequency spectra from discrete time samples. This thesis presents a new application of the

least squares state estimation technique, as well as, a new, non iterative, least absolute value state estimation technique for power system harmonics identification. Static techniques give an accurate estimation when the given waveform is stationary, but if the waveform is non-stationary, then dynamic state estimation techniques should be used. The thesis presents different dynamic state estimation techniques, such as the Kalman filter and a new weighted least absolute value dynamic filter [40,43].

In this thesis the primary objective is to compare the accuracy of harmonics estimation made via least squares criterion, least absolute value criterion and discrete Fourier transform to each other. Also to be compared, is the performance of the weighted least absolute value filter to that of the Kalman filter.

The harmonic identification problems which will be considered are of two different kinds, the first one is when the waveform has harmonics order with an integral multiple of the fundamental frequency only, while the second one is when the waveform is contaminated with frequencies lower than the fundamental frequency.

1.1: Outline of thesis

Chapter II introduces the power system harmonics problem. Here the harmonic sources, harmonic effects and harmonic measurement techniques are reviewed.

In chapter III the mathematical models suitable for both on and off-line estimation are developed.

Chapter IV presents the static estimation problem followed by discrete Fourier method then the theories and derivations of the least squares and least absolute value methods. Also included in this chapter are the results obtained using these different methods.

The dynamic estimation problem is presented in chapter V and the derivations of the Kalman filter and the weighted least absolute value filter are presented as well as the results obtained using these techniques.

In chapter VI conclusions are drawn and recommendations are made.

CHAPTER II

THE POWER SYSTEM HARMONICS PROBLEM

In this chapter, the harmonics problem is reviewed. The chapter begins by reviewing the basic harmonic sources and effects. Then the development of the measurement techniques for power system harmonics will be reviewed. State estimation techniques, as they are the mathematical tools to perform the measurement, are discussed as well. Finally the chapter is concluded by defining different distortion factors used in judging the distortion levels.

2.1: Introduction

The presence of power system harmonics is not a new problem, it has been well-known since the first generator was built. But, nowadays due to the widespread use of electronic equipment, arcing devices, such as arc furnaces and equipment with saturable ferromagnetic cores, such as transformers, power engineers pay more attention to power system harmonics. Identification of harmonics may be of great importance in locations where harmonic standards are to be adopted. Also, it may be used to allocate loads which exceed specified harmonic current limits. Furthermore, the identification of power system harmonics is needed for designing harmonic filters, therefore an accurate method is required to perform this identification [6,7].

2.2: Harmonic sources

The AC power system harmonic problems are mainly due to the substantial increase of nonlinear loads resulting from new technologies, such as using power electronics elements in AC/DC transmission links or in the control of power systems using microprocessor controls, all this equipment creates load-generated harmonics throughout the system. Another reason is the change of the design philosophy. In order to be competitive, power equipment are more critically designed nowadays. For example in iron-core devices, their operating points are more into nonlinear regions. Operation in such regions results in a sharp rise in harmonics. Harmonics sources, in general, can be divided into two categories; established and known, new and future [3,6,7].

2.2.1: Established and known harmonic sources.

Prior to the development of static converters power system harmonic problems were mainly associated with the operation of electric machines and transformers. Modern transformers and rotating machines when operated normally do not in themselves cause a significant distortion in the network. However, they can be considered as sources of harmonics if they operate outside their normal operating range or during transients. Besides these sources some nonlinear loads, other than static converters, can be considered as harmonic sources. Established harmonic sources will be summarized in the next part of this subsection.

a) Rotating machines are considered to be one of the most important harmonic sources in the power system. Many factors can be considered, such as the nonsinusoidal distribution of the flux in the machine air gap, variations in the air gap reluctance over the machine pole pitch, tooth ripple, and sudden loading of the machine, which may cause flux distortion.

b) Transformer magnetizing currents are nonsinusoidal because of the nonlinear relationship between the flux and the current needed to produce it.

c) Network nonlinearities from loads, such as rectifiers and inverters, arc furnaces, and voltage controllers and frequency converters, introduce harmonics.

2.2.2: New harmonic sources

While the established harmonic sources still exist, new harmonic sources have appeared, such as:

a) energy conservation measures, such as those for improved motor efficiency and load matching, which employ power semiconductor devices and switching for their operation,

b) large power converters such as those used in the metal reduction industry and high voltage direct current transmission,

c) medium size converters, such as those used in the manufacturing industry for motor control and also in railway applications,

d) the new sources of energy, such as wind and solar power converters which are connected to the distribution systems,

- e) static Var compensators which have largely replaced synchronous condensers as continuously variable Var sources, and
- f) low power converters, such as battery chargers which is not a problem at the moment, but if the use of electric vehicles becomes generally accepted this load will be a considerable harmonic source.

Together established and new harmonic sources form the sources of harmonics considered today. With more application of static converters in industry the problem of harmonics will be one of the most important aspects to be considered [3,6,7].

2.3: Harmonic effects

The early investigation of power system harmonics was prompted by interference with neighboring communication circuits. Communication interference is the oldest and the most studied problem related to power system harmonics. Initially, harmonics were not considered to be a serious problem for power equipment. This presumption changed, however, as problems arose, particularly in resonant systems with rectifiers and shunt capacitors. In addition to increased losses due to harmonic currents and conductor skin effect, harmonics can be detrimental to capacitors, rotating machines, transformers and protective relays.

The main effects of current and voltage harmonics within the power system can be summarized as:

- a) amplification of harmonic levels due to resonance,

- b) reduction in the efficiency of different system components, and
- c) shortening the useful life of plant components by ageing their insulation.

In the next part of this section the effects of these problems on system behavior as well as the effects on different system components will be discussed [6,7].

2.3.1: Resonances

The problem of resonance can occur in a number of ways. An example way being a capacitor, used for power factor correction or Var compensation, connected to a certain bus-bar where there is a harmonic source. A parallel resonance can then occur between the system equivalent inductance and the capacitor. Where resonance exists, excessive harmonic currents can flow, resulting in damage to the capacitors used for correction or compensation.

2.3.2: Effects of harmonics on rotating machines

The presence of harmonic voltages or currents cause additional losses in both stator and rotor circuits in the form of eddy and copper losses. The additional losses cause over heating and the capability of a machine to cope with extra harmonic current will depend on the total additional losses and its effects on the overall machine temperature rise. At the same time harmonic currents present in the stator of an A.C. machine create shaft torques corresponding to those harmonics. Although harmonics have little effect upon mean torque, they can produce significant torque pulsations.

2.3.3: Effects of harmonics on static components

Harmonic currents or voltages can affect the static components of power system, such as transformers, transmission lines and capacitor banks in different ways. In the case of transformers the harmonic voltages stress the insulation by increasing the eddy and hysteresis current losses. At the same time the harmonic currents flow give rise to copper losses and this becomes important in the case of transformers used with converters even in the presence of filters because filters are usually connected on the A.C. system side. The use of the delta connection to provide an internal path for the triple harmonic currents can cause excessive winding current.

The flow of harmonic currents in the transmission system results in extra losses caused by the increased root mean square current. Another problem appears when under ground cables are used in transmission systems. The harmonic voltages increase the dielectric stress and hence the number of faults which may lead, at the end, to a shorter life of the cable. The corona losses can be affected by the harmonic voltages since corona starting and extinction levels are a function of peak to peak voltage.

In the case of capacitor banks the voltage distortion gives more dielectric losses since the dielectric loss is directly proportional to the square of the r.m.s. voltage. Resonance between the capacitors and the inductance of the system can cause high currents thus increasing dramatically the losses and overheating of capacitors and could lead to their failure [7].

2.3.4: Effects of harmonic on protection systems

The presence of harmonic voltages or currents in the power circuits can lead to a false operation of the circuit breakers in some cases, such as the case of energization of power transformers. In this case while the secondary currents is zero there is a heavy inrush current in the primary circuit and that leads to a false operation of the differential protection.

2.3.5: Effects of harmonic on communication systems

The effect of noise on communication systems varies from annoyance, at low noise levels, to loss of information at high noise levels. Noise voltages may be impressed on telephone circuits in many different ways, such as electrostatic induction or inductive coupling.

2.3.6: Other harmonic effects

Over the years, it has been reported that harmonics cause operational problems for many other system and consumer equipment, these can be summarized as [1,4,6,7]

- 1) Unstable operation of the thyristor controlled rectifiers firing circuits based on zero voltage crossing detection.
- 2) Errors in induction KWh meters.
- 3) Interference with ripple control systems.
- 4) Quality changes of the picture received by television sets.
- 5) Excessive heating of the capacitors used in fluorescent and mercury

arc lighting.

6) Interference with power plant excitation systems.

2.4: Harmonic measurements

In this section the development of power system harmonic measurement techniques will be reviewed as well as the most common techniques used nowadays.

2.4.1: The development of power system harmonic measurements

The efforts of power system harmonic measurement started nearly 90 years ago. At that time most of the techniques used were based on the manual calculation of harmonic levels using some form of recorded data. One method was developed using the amplitude and time information from a single cycle of a wave form recorded on an oscillograph to obtain an approximation to the integrations in the Fourier coefficient equations [7,26]. The harmonic amplitudes and phase angles were then calculated.

As early as 1925, another method was proposed to measure the power system harmonics using a dynamometer. In this instrument the fixed coil is energized by a variable frequency current (sinusoidal) and the current or the voltage to be analyzed is passed to the moving coil. An average torque is produced when the two components have the same frequency, the deflection of the moving coil provides a measurement of the harmonic amplitude.

In 1939, due to the development of valve technology, an electrostatic wave analyzer was used [26,7]. This used a principle

similar to that of the dynamometer, but with an electrometer. During the same period, another method for analyzing sine waves was produced electronically using a Dynatron oscillator, where the frequency and the phase angle could be adjusted relative to the fundamental frequency, then the reference point of the phase angle measurement was obtained by using a Thyatron valve.

As the quality and availability of electronic components improved, it became possible to produce stable, variable frequency oscillators, which led to the development of the techniques of harmonic measurement. These techniques are still used by the current generation of analog wave, frequency and spectrum analyzers. The fast Fourier transform (FFT) is one of the techniques currently used with digital instruments and microprocessors to provide the spectral information [26,7].

Discussions of harmonic impedance measurement appear in references 8 and 9. It has been found that the method described in these references gives good results up to the mid-harmonic range. Beyond this range bad results are obtained.

The design and operation of a system based on a portable personal computer for the measurement of harmonic current and voltage magnitudes and phase angles are described in reference 10. The method used tries to avoid sources of error common to digital frequency analysis by using an anti-aliasing filter, a high resolution A/D converter and a phase locked loop to synchronize sampling to the input fundamental frequency.

A digital method of analyzing harmonics in a power system has been developed by Crevier and Marcier [12], this method permits the equivalent network impedance to be calculated by mean of switching capacitor banks. The method records voltages and currents digitally and by data processing computes the amplitude and phase of the harmonic. The proposed method is modified to take into account the variation with time of the harmonics content of the signal. The results obtained using this method are accurate in amplitude, but less accurate for the angle. This method uses Fourier transform of a signal sampled for a finite duration to calculate the harmonic amplitudes and phase angles.

Much attention has been focused on the propagation of harmonic signals in power systems for a given source, but little has been given to identifying the source of harmonic injection. A reverse power flow procedure is described by Heydt [11] to identify the sources of harmonic signals in electrical power systems. When energy at harmonic frequencies is found to be injected into the network at a bus, that bus been identified as a harmonic source. Line and bus data at several points in the network are used with a least squares estimator to calculate the injection spectrum of buses suspected of being harmonic sources. Inaccuracies occur due to losses, estimation errors and modeling errors. These inaccuracies result in errors in the spectrum of the injected current [26,11].

Currently instruments used for the measurement of power system harmonics fall into two broad categories, harmonic analyzers and spectrum analyzers. Harmonic analyzers give measurement for signal

amplitudes at harmonic frequencies only. On the other hand the spectrum analyzers scan a range of frequencies to provide a measurement of signal amplitudes at all frequencies within that range. Each of these methods may use either analog or digital techniques [7]. Most frequency domain harmonic analysis algorithms are based either on the discrete Fourier transform (DFT) or on the fast Fourier transform (FFT) to obtain the voltage and current harmonic spectra from discrete time samples [13].

2.5: State estimation techniques used in power systems

In order to perform the measurement of power system harmonics an efficient mathematical tool is needed. In this section a review of most common techniques used in power system state estimation is offered. No mathematical derivations will be offered at this point, since complete derivations will be provided in the following chapters. State estimation techniques are classified as static and dynamic techniques.

2.5.1: Static state estimation techniques

The parameter estimation techniques suitable for off-line identification are sometimes referred as static estimation techniques as they are required to produce independent estimation from fixed windows of previous data.

Fourier transform

The Fourier transform and its inverse are used to map any function in the interval minus infinity to plus infinity, in either the time or frequency domain, into a continuous function in the inverse domain [7]. The discrete Fourier transform is the modified form of Fourier transform suitable for dealing with the data available in the form of sampled time function which is the practical case. The fast Fourier transform was developed to reduce the computational burden of the discrete Fourier transform [13]. If N , number of samples, is an integer multiple of two then the number of operations is reduced from N^2 to $N/2 \log_2 N$. This become very useful when dealing with large values of N . Most harmonic analysis algorithms are based on Fourier transforms because of the simplicity of use, the speed of the estimation and the accuracy of the results [7,13].

Least error squares estimation

In the least squares technique the objective is to minimize the sum of the squares of the residuals. It has been shown [14] that the least squares gives very good estimates if the error distribution is Gaussian. It has been found that by using weighted matrices an even better method developed. This became known as weighted least squares method. With the advent of modern computers, the least squares techniques became more popular and are now considered as one of the most popular estimation techniques with many applications in the field of power system state estimation.

Least squares techniques are easy to implement on digital

computers and give an accurate estimate providing that the error distribution is Gaussian as mentioned before. The main disadvantage of these techniques is that they do not inherently reject outliers when estimating [15,16].

Least absolute value estimation

The basic difference between the least absolute value and the least squares estimation is that the best least absolute value is obtained by minimizing the sum of the absolute values of the residuals, whereas the best least squares approximation is obtained by minimizing the sum of the squares of the residuals. It has been found that if the errors in n -dimensional linear system are exponentially distributed, then the parameters estimated by minimization of the sum of the absolute values of the residuals are optimal [17,21].

O.J. Karst [18] was the first author to present a technique for solving this kind of estimation problems. This technique was with iterative nature and valid only for a two dimensional case.

Barrodale [19,20] used linear programming to solve the problem iteratively. However, while linear programming is capable of handling the n -dimensional system it has two main drawbacks. First, it is iterative technique, requires considerable computing time. Second, it needs a great deal of memory to perform the matrices manipulation.

Several references [23,24] have presented techniques to save the computing time by decreasing the number of iterations and memory required. Some of these techniques employ the least squares estimation

to find the least absolute value estimation. Soposito [23] has suggested using a least squares estimator to establish the starting point for a linear programming algorithm. While, the results indicated great saving in computing time; the method is still an iterative method. Schlossmacher presents another approach, in which he uses successive iterations performed by an least squares estimator to find the least absolute estimation [17,22].

This thesis presents a new, non iterative, least absolute value technique to be used as a static estimator for power system harmonics. Least squares and discrete Fourier transform techniques will be presented as well.

2.5.2: Dynamic state estimation techniques

The parameter estimation techniques suitable for on-line identification are sometimes referred to as dynamic estimation techniques as they update the estimate according to each new measurement received by the algorithm.

The dynamic estimation problem for continuous data systems were first solved by Wiener in 1940. Wiener used the least error squares criterion. The theory has provided valuable insight into the analysis of systems subject to random signals. However, the theory has no practical applications in power systems due to several limitations. Kalman, in 1960, presented a new approach to the problem. Kalman obtained the same results as Wiener in a simpler and more direct way. At the beginning Kalman filter had no applications in power system state estimation, but recently more attention has been paid to the

technique as a powerful tool in power system state estimation area [40,42].

This thesis will present a new application of the Kalman filter in power system state estimation as an estimator for power system harmonics. A new weighted least absolute value filter will be used as well for solving the same problem .

2.6: Standards for limitation of power system harmonics

The purpose of the power system harmonic measurements is to provide data to be used in calculating different distortion factors. These calculated values are compared to certain standards to give an idea about the level of distortion. If those limits or standards are violated then, there should be a solution for the harmonic problem. This solution will be in the form of filters to eliminate or to reduce the levels of distortion.

The objective of all the standards relating to the levels of power system harmonics is to ensure certain requirements such as [7,25] :

- a) providing consumers with a waveform suitable for their particular need,
- b) controlling the distortion to a level that the system and its associated components can tolerate, and
- c) ensuring that there is no interference with the other systems such as communication systems.

The development of harmonic standards is based on many factors.

These factors are well documented in many references [7.25]. A complete discussion of these factors is beyond the scope of the thesis. However very important factors, used in the judging process, should be mentioned.

The total harmonic distortion factor (THD)

The total harmonic content, of either current or voltage, can be expressed as a percentage of the fundamental component using the total distortion factor.

$$THD = 100 \left(\sum_{n=2}^n U_n^2 \right) / U_1 \quad (2.1)$$

Where U_1 is the r.m.s value of the fundamental component
 U_2 to U_n are the r.m.s values of the harmonic components.

The individual harmonic distortion factor (IHD)

The individual harmonic distortion factor for a certain harmonic, n , is given by the ratio of the r.m.s. harmonic to the fundamental r.m.s. value of the waveform.

$$IHD = 100 (U_n) / U_1 \quad (2.2)$$

For each of the three levels of the system voltages namely transmission, distribution and utilization there should be certain harmonic standards for the distortion factors. Of course these standards are different from one country to another.

2.7: Harmonic elimination and reduction

Once the harmonic distortion levels has been identified, the final step is to eliminate or reduce those harmonic components which exceeds the permissible limits or standards. The simple solution to this problem is to use a harmonic filter. The ideal goal of the filter is the elimination of all harmful effects caused by waveform distortion. However, this ideal goal is unrealistic from both an economical and technical point of view. A more practical goal then, is to reduce the distortion to an acceptable level [7]. The design and the performance of these filters are beyond of the scope of this thesis.

CHAPTER III

MATHEMATICAL MODELLING

This chapter starts with the general mathematical formulation for the problem of power system harmonics. Two different problems are considered, the first one is when the wave form has harmonics order with an integral multiple of the fundamental frequency only, this case will be referred to as the harmonic case, while the second one is when the waveform is contaminated with frequencies lower than the fundamental frequency, this case will be referred to as the sub-harmonic case. The mathematical models suitable for both off-line state estimation and on-line state estimation will then be developed. Finally the concept of power system harmonics identification will be introduced.

3.1: Mathematical analysis

In this section two different algorithms are introduced. The first one is for the harmonic analysis and the second one is for the sub-harmonic analysis.

3.1.1: Harmonic analysis

In this subsection it is assumed that the waveform under consideration consists of a fundamental frequency component and harmonic components with order of integral multiples of the fundamental frequency. It is assumed also that the fundamental

frequency is known and constant during the estimation period. The analysis here is the process of deriving expressions suitable for use with different state estimation techniques in order to calculate the magnitudes and phase angles of the fundamental and higher order harmonics of a periodic waveform. Consider a non-sinusoidal voltage given by a Fourier-type equation [26]:

$$v(t) = \sum_{n=0}^N V_n \sin (n\omega_0 t + \phi_n) \quad (3.1)$$

Where $v(t)$ is the voltage at time t , and V_n and ϕ_n are, respectively, the magnitude and phase angle of harmonic n . N is the highest number of harmonics to be considered in the wave $v(t)$; this is a selected number, depending on the decision of the analyst.

Equation (3.1) can be written as:

$$v(t) = \sum_{n=0}^N [(V_n \cos \phi_{nv})(\sin n\omega_0 t) + (V_n \sin \phi_{nv})(\cos n\omega_0 t)] \quad (3.2)$$

Define the components x_{nv} and y_{nv} as:

$$x_{nv} = V_n \cos \phi_{nv} \quad (3.3)$$

$$y_{nv} = V_n \sin \phi_{nv} \quad (3.4)$$

Then equation (3.2) becomes

$$v(t) = \sum_{n=0}^N [x_{nv} \sin n\omega_0 t + y_{nv} \cos n\omega_0 t] \quad (3.5)$$

By expanding the summation, equation (3.5) can be rewritten as:

$$v(t) = y_{OV} + x_{1V} \sin \omega_0 t + y_{1V} \cos \omega_0 t + \dots + x_{NV} \sin N \omega_0 t + y_{NV} \cos N \omega_0 t \quad (3.6)$$

Where y_{OV} represents the DC component, zero frequency harmonic. By making the following substitutions in equation (3.6),

$$\begin{aligned} a_{11}(t) &= 1 \\ a_{12}(t) &= \sin \omega_0 t \\ a_{13}(t) &= \cos \omega_0 t \\ a_{14}(t) &= \sin 2 \omega_0 t \\ a_{15}(t) &= \cos 2 \omega_0 t \\ &\dots\dots\dots \\ &\dots\dots\dots \\ a_{1\ 2N}(t) &= \sin N \omega_0 t \\ a_{1\ 2N+1}(t) &= \cos N \omega_0 t \end{aligned} \quad (3.7)$$

Then equation (3.8) can be obtained as:

$$v(t) = a_{11}(t)y_{OV} + a_{12}(t)x_{1V} + a_{13}(t)y_{1V} + \dots\dots\dots + a_{1\ 2N}(t)x_{NV} + a_{1\ 2N+1}(t)y_{NV} \quad (3.8)$$

Where $2N+1$ becomes the total number of unknowns

If the voltage is sampled at a pre-selected rate, the samples would be obtained at equal time intervals, say every Δt second. A set of m samples for the voltage may be designed; $v(t_1)$,

$v(t_1 + \Delta t), \dots, v(t_1 + (m-1)\Delta t)$, where t_1 is an arbitrary time reference Equation (3.8) becomes [26]

$$\begin{bmatrix} v(t_1) \\ v(t_2) \\ \dots \\ \dots \\ v(t_m) \end{bmatrix} = \begin{bmatrix} a_{11}(t_1) & a_{12}(t_1) & \dots & a_{1 \ 2N+1}(t_1) \\ a_{21}(t_2) & a_{22}(t_2) & \dots & a_{2 \ 2N+1}(t_2) \\ \dots & \dots & \dots & \dots \\ \dots & \dots & \dots & \dots \\ a_{m1}(t_m) & a_{m2}(t_m) & \dots & a_{m \ 2N+1}(t_m) \end{bmatrix} \begin{bmatrix} y_{ov} \\ x_{1v} \\ \dots \\ \dots \\ y_{NV} \end{bmatrix} \quad (3.9)$$

Equation (3.9) can be rewritten in vector form as:

$$Z_v(t) = A(t) \Theta_v + w_v \quad (3.10)$$

Where $Z_v(t)$ is an $m \times 1$ vector of sampled voltage measurements, $A(t)$ is an $m \times (2N+1)$ matrix of measurement coefficients, Θ_v the $(2N+1) \times 1$ parameter vector to be estimated and w_v is an $m \times 1$ noise vector to be minimized. The order of matrix $A(t)$ and the vector Θ_v depends, of course, on the number of harmonics considered. In general, the order of $A(t)$ and Θ_v for N harmonics contaminating the wave signal is $m \times (2N+1)$ and $(2N+1) \times 1$, respectively, where $m > (2N+1)$. The elements of the matrix $A(t)$ depend on the time reference t_1 , the sampling interval Δt used, and the data window size, and can be calculated in an off-line mode.

Equation (3.10) describes an overdetermined system of equations, since we assume that $m > (2N+1)$. As will be shown later the solution for

this set of equations can be obtained through either static techniques or dynamic techniques. Having obtained the vector Θ_v , the unknown vector, the magnitude of any harmonic n can be calculated as:

$$V_n = (x_{nv}^2 + y_{nv}^2)^{1/2} ; \quad n=1, \dots, N \quad (3.11)$$

While the phase angle of the n^{th} harmonic is

$$\phi_{nv} = \tan^{-1} \left(\frac{y_{nv}}{x_{nv}} \right) ; \quad n=1, \dots, N \quad (3.12)$$

If the given waveform is a current waveform of course the same steps explained above can be followed. Then the current magnitude of any harmonic can be calculated as:

$$I_n = (x_{ni}^2 + y_{ni}^2)^{1/2} ; \quad n=1, \dots, N \quad (3.13)$$

and the current phase angle of the n^{th} harmonic will be

$$\phi_{ni} = \tan^{-1} \left(\frac{y_{ni}}{x_{ni}} \right) ; \quad n=1, \dots, N \quad (3.14)$$

3.1.2: Sub-harmonics analysis

Now assuming that the waveform is contaminated with both harmonics and sub-harmonics. It is easy to split the problem into two problems harmonics and sub-harmonics. We assume that the sub-harmonics waveform is a combination of sinusoidal and exponential terms. This is just to make the expressions derived more

general and valid even for high frequency oscillations [27].

$$f(t) = A_1 e^{\sigma_1 t} \cos(\omega_1 t) + \sum_{i=2}^N A_i e^{\sigma_i t} \cos(\omega_i t + \Phi_i) \quad (3.15)$$

where A_1, A_2, \dots, A_N are the oscillation amplitudes
 $\sigma_1, \sigma_2, \dots, \sigma_N$ are the damping constants
 $\Phi_i, i=2, \dots, N$ are the phase angles of the oscillations
 $\omega_1, \omega_2, \dots, \omega_N$ are the sub-harmonic frequencies,
 assumed to be identified in the frequency domain.

It is clear that this expression represents the general possible low or high frequency dynamic oscillations. This model represents the dynamic oscillations in the system in cases such as, the currents of an induction motor when controlled by variable speed drive. As a special case, if the damping constants are equal to zero then the considered wave is just a summation of low frequency components. Without loss of generality, for simplicity, it can be assumed that only two modes of equation (3.15) are considered, then equation (3.15) becomes

$$f(t) = A_1 e^{\sigma_1 t} \cos(\omega_1 t) + A_2 e^{\sigma_2 t} \cos(\omega_2 t + \Phi_2) \quad (3.16)$$

Using the well-known trigonometric identity

$$\cos(\omega_2 t + \Phi_2) = \cos\omega_2 t \cos\Phi_2 - \sin\omega_2 t \sin\Phi_2$$

Then equation (3.16) can be rewritten as:

$$f(t) = A_1 e^{\sigma_1 t} \cos \omega_1 t + (e^{\sigma_2 t} \cos \omega_2 t) A_2 \cos \phi_2 - (e^{\sigma_2 t} \sin \omega_2 t) A_2 \sin \phi_2 \quad (3.17)$$

It is obvious that equation (3.17) is a nonlinear function of A 's, σ 's and ϕ 's. By using the first two terms in the Taylor series

expansion of $A_i e^{\sigma_i t}$; $i=1,2$. Equation (3.17) turns out to be

$$\begin{aligned} f(t) = & A_1 \cos \omega_1 t + (t \cos \omega_1 t)(A_1 \sigma_1) + (\cos \omega_2 t)(A_2 \cos \phi_2) \\ & + (t \cos \omega_2 t)(A_2 \sigma_2 \cos \phi_2) - (\sin \omega_2 t)(A_2 \sin \phi_2) \\ & - (t \sin \omega_2 t)(A_2 \sigma_2 \sin \phi_2) \end{aligned} \quad (3.18)$$

Where Taylor series expansion is given by:

$$e^{\sigma t} = 1 + \sigma t + \dots$$

Making the following substitutions in equation (3.18), equation (3.21) can be obtained.

$$\begin{aligned} x_1 &= A_1 & ; & & x_2 &= A_1 \sigma_1 \\ x_3 &= A_2 \cos \phi_2 & ; & & x_4 &= A_2 \sigma_2 \cos \phi_2 \\ x_5 &= A_2 \sin \phi_2 & ; & & x_6 &= A_2 \sigma_2 \sin \phi_2 \end{aligned} \quad (3.19)$$

and

$$\begin{aligned}
h_{11}(t) &= \cos \omega_1 t & ; & & h_{12}(t) &= t \cos \omega_1 t \\
h_{13}(t) &= \cos \omega_2 t & ; & & h_{14}(t) &= t \cos \omega_2 t \\
h_{15}(t) &= -\sin \omega_2 t & ; & & h_{16}(t) &= -t \sin \omega_2 t
\end{aligned} \tag{3.20}$$

$$f(t) = h_{11}(t)x_1 + h_{12}(t)x_2 + h_{13}(t)x_3 + h_{14}(t)x_4 + h_{15}(t)x_5 + h_{16}(t)x_6 \tag{3.21}$$

If the function $f(t)$ is sampled at a pre-selected rate, its samples would be obtained at equal time intervals, say Δt second. Considering m samples, then there will be a set of m equations with an arbitrary time reference t_1 given by

$$\begin{bmatrix} f(t_1) \\ f(t_2) \\ \dots \\ \dots \\ f(t_m) \end{bmatrix} = \begin{bmatrix} h_{11}(t_1) & h_{12}(t_1) & \dots & h_{16}(t_1) \\ h_{21}(t_2) & h_{22}(t_2) & \dots & h_{26}(t_2) \\ \dots & \dots & \dots & \dots \\ \dots & \dots & \dots & \dots \\ h_{m1}(t_m) & h_{m2}(t_m) & \dots & h_{m6}(t_m) \end{bmatrix} \begin{bmatrix} x_1 \\ x_2 \\ \dots \\ \dots \\ x_6 \end{bmatrix} \tag{3.22}$$

It is clear that this set of equations is similar to the set of equations given by equation (3.9). Of course the only difference lies in the elements of the matrix H which has replaced the matrix A in equation (3.9). Thus a similar equation to (3.10) can be written as:

$$Z(t) = H(t) \Theta + w \tag{3.23}$$

Where $Z(t)$ is the vector of sampled measurements, $H(t)$ is an $m \times 6$, in this simple case, matrix of measurement coefficients, Θ is an 6×1

parameter vector to be estimated and w is an $m \times 1$ noise vector to be minimized. The dimensions of the previous matrices depend on the number of modes considered as well as on the number of terms truncated from Taylor series.

Using either static or dynamic state estimation techniques the solution of the overdetermined system described by (3.23) can be obtained. Having estimated the parameter vector Θ , the amplitude, damping constant and the phase angle can be determined using the following equations:

$$A_1 = x_1 \quad (3.24)$$

$$\sigma_1 = \frac{x_2}{x_1} \quad (3.25)$$

$$A_2 = [x_3^2 + x_5^2]^{1/2} \quad (3.26)$$

$$\sigma_2 = \frac{[x_4^2 + x_6^2]^{1/2}}{[x_3^2 + x_5^2]^{1/2}} \quad (3.27)$$

$$\phi_2 = \tan^{-1} (x_6 / x_4) \quad (3.28)$$

or

$$= \tan^{-1} (x_5 / x_3) \quad (3.29)$$

3.2: System modelling

It has been shown in the previous section that both harmonics and sub-harmonics analysis have the same form of equations described by (3.9) or (3.22). Now the problem is, how to estimate the parameter

vector Θ . In this section different models, based on the derived equations (3.9), will be developed to be used in solving the estimation problem either statically or dynamically.

3.2.1: Static estimation model

As described in section 3.1 the problem has been formulated as the set of equations given by (3.9) or (3.22). In vector form both of these equation can be written as given in equation (3.10)

$$Z(t) = A(t) \Theta + w \quad (3.30)$$

In general if there are m samples and U unknowns, $Z(t)$ will be an $m \times 1$ vector of measurements, $A(t)$ is an $m \times U$ matrix of coefficients, Θ is the $U \times 1$ parameters vector to be estimated and w is an $m \times 1$ noise vector to be minimized [26].

Assuming that this system is an overdetermined system, $m > U$, this arrangement is suitable for solving the problem using any static estimation technique and will be referred to, when ever used, as the static model (SM).

3.2.2: Dynamic state estimation models

The suitable form for dynamic state estimation techniques is the state space form. The system equations will be arranged in such a way as to be in this form. Two different models will be developed according to the time reference chosen. If the time reference is considered to be a rotating reference this will lead to model 1 but,

if the time reference is chosen to be a stationary reference, then model 2 will be obtained [13,42].

Model 1

For this model a rotating time reference is used. In this model the state transition matrix becomes the identity matrix, while the connection matrix H is a time varying matrix [13].

Equations (3.8) and (3.21) are basically the same equations, or, in more specific terms, equation (3.21) is a special case of equation (3.8). Thus it is possible to write one general equation to represent any of the two cases, harmonics or sub-harmonics, as:

$$v(t)=h_{11}(t)x_1+h_{12}(t)x_2+h_{13}(t)x_3....+h_{1\ U-1}(t)x_{U-1}+h_{1U}(t)x_U \quad (3.30)$$

Here U is considered to be the total number of unknowns, then x_1, x_2, \dots, x_U are the unknowns, and of course, they could be either harmonics or sub-harmonics parameters depending on the h's and the sampled wave used.

If the voltage is sampled at a pre-selected rate, its samples would be obtained at equal time intervals, say Δt seconds, Then equation (3.31) can be written at stage k , $k=1,2,\dots,K$, where K is the total number of intervals, $K=[\text{window size in seconds}/\Delta t] = [\text{window size in seconds} \times \text{sampling frequency(Hz)}]$.

$$v(k\Delta t)=h_{11}(k\Delta t)x_1(k)+h_{12}(k\Delta t)x_2(k)+.....+h_{1U}(k\Delta t)x_U(k) \quad (3.31)$$

If there are m samples, equation (3.31) turns out to be a set of equations. Each equation defines the system at a certain time $k\Delta t$.

$$z_i(k\Delta t) = H_i(k\Delta t) \Theta(k) + w_i(k) \quad ; i=1,2,\dots,m \quad (3.32)$$

This equation can be written in a vector form as:

$$z(k\Delta t) = H(k\Delta t) \Theta(k) + w(k) \quad (3.33)$$

where

$z(k)$ is $m \times 1$ measurement vector taken over the window size.

$\Theta(k)$ is $U \times 1$ state vector to be estimated. It could be harmonic or sub-harmonic parameters depending on both $H(k)$ and $z(k)$.

$H(k)$ is $m \times U$ matrix giving the ideal connection between $z(k\Delta t)$ and $\Theta(k)$ in the absence of noise $w(k)$. If the elements of $H(k\Delta t)$ are given by equation (3.7) then the problem is the harmonic problem, while the problem will be the sub-harmonic problem if the elements are given by equation (3.20). It is clear that in both cases $H(k\Delta t)$ is a time varying matrix.

$w(k)$ is an $m \times 1$ noise vector to be minimized and is assumed to be random white noise with known covariance construction.

Equation (3.33) describes the measurement system equation at time $k\Delta t$.

The state space variable equation for this model may be expressed as:

$$\begin{bmatrix} x_1(k+1) \\ x_2(k+1) \\ x_3(k+1) \\ \dots \\ \dots \\ x_U(k+1) \end{bmatrix} = \begin{bmatrix} 1 & 0 & 0 & 0 & 0 & \dots \\ 0 & 1 & 0 & 0 & 0 & \dots \\ 0 & 0 & 1 & 0 & 0 & \dots \\ \dots & \dots & \dots & \dots & \dots & \dots \\ \dots & \dots & \dots & \dots & \dots & \dots \\ 0 & 0 & 0 & 0 & 0 & \dots 1 \end{bmatrix} \begin{bmatrix} x_1(k) \\ x_2(k) \\ x_3(k) \\ \dots \\ \dots \\ x_U(k) \end{bmatrix} + \varepsilon(k) \quad (3.34)$$

Equation (3.34) can be rewritten in vector form as:

$$\Theta(k+1) = \Phi(k+1) \Theta(k) + \varepsilon(k) \quad (3.35)$$

Where

$\Phi(k)$ is $U \times U$ state transition matrix

$\varepsilon(k)$ is $U \times 1$ plant noise vector.

Together equations (3.33) and (3.35) form model 1 (M1). It is worthwhile to state here, that in this state space representation the time reference was picked to be a rotating time reference which caused the state transition matrix to be the identity matrix and the H matrix to be a time varying matrix [13].

Model 2

In the previous model, model 1, the time reference was a rotating time reference and that caused the state transition matrix to be a

constant identity matrix and the $H(k\Delta t)$ matrix to have time varying elements. In this part, another model for the state transition and the $H(k\Delta t)$ matrices is derived [13,42]. This model is referred to as model 2 (M2). In this model the time reference is chosen to be a stationary time reference. The state transition matrix in this case depends on the sampling rate, Δt , and the number of samples (K) chosen. It is a constant matrix, rather than unity, for a specified sampling frequency and a specified number of harmonics. The model developed here is suitable for the case of harmonics. Of course a similar derivation can be made if we start with the sub-harmonics equation.

Recall equation (3.1) which is

$$v(t) = \sum_{n=0}^N V_n \sin(n\omega_0 t + \phi_n)$$

This can be considered as the sum of sinusoidal waveforms having different frequencies. To find the state space variable model for this signal waveform, it is better to start with a simple case, in which the waveform is assumed to be a pure sinusoid, $n=1$ only. then equation (3.1) becomes

$$v(t) = V_n e^{j(n\omega_0 t + \phi_n)} \quad ; n=1 \quad (3.36)$$

or in another form

$$v(t) = V_n e^{j(n\omega_0 t)} e^{j\phi_n} \quad ; n=1 \quad (3.37)$$

Substituting for x_n and y_n from equations (3.3) and (3.4) into equation (3.37), equation (3.38) can be obtained as:

$$v(t) = (x_n + j y_n) e^{j(n\omega_0 t)} ; n=1 \quad (3.38)$$

Where

$$\begin{aligned} x_n &= V_n \cos \phi_n & ; n=1 \\ y_n &= V_n \sin \phi_n & ; n=1 \end{aligned} \quad (3.39)$$

For this case, $n=1$, the in phase and quadrature components x_n and y_n , after time Δt , which is the time required for the state transition from step 0 to step 1, will have a new angle. The new expressions for x_n and y_n will be

$$\begin{aligned} x_n(1) &= V_n \cos(\phi_n + \omega_n \Delta t) & ; n=1 \\ y_n(1) &= V_n \sin(\phi_n + \omega_n \Delta t) & ; n=1 \end{aligned} \quad (3.40)$$

Where $\omega_n = n\omega_0 = \omega_0$ is the fundamental frequency.

Equations (3.40) can be written in a different form as:

$$\begin{aligned} x_n(1) &= V_n \cos \phi_n (\cos \omega_n \Delta t) - V_n \sin \phi_n (\sin \omega_n \Delta t) & ; n=1 \\ y_n(1) &= V_n \cos \phi_n (\sin \omega_n \Delta t) + V_n \sin \phi_n (\cos \omega_n \Delta t) & ; n=1 \end{aligned} \quad (3.41)$$

Substitute from (3.39) into (3.41), then equation (3.42) can be obtained as:

$$\begin{aligned}x_n(k+1) &= x_n(k)\cos(\omega_n \Delta t) - y_n(k)\sin(\omega_n \Delta t) & ;n=1 \\y_n(k+1) &= x_n(k)\sin(\omega_n \Delta t) + y_n(k)\cos(\omega_n \Delta t) & ;n=1\end{aligned}\quad (3.42)$$

Thus the state variable representation takes the following form:

$$\begin{bmatrix} x_n(k+1) \\ y_n(k+1) \end{bmatrix} = \begin{bmatrix} \cos \omega_n \Delta t & -\sin \omega_n \Delta t \\ \sin \omega_n \Delta t & \cos \omega_n \Delta t \end{bmatrix} \begin{bmatrix} x_n(k) \\ y_n(k) \end{bmatrix} \quad (3.43)$$

The measurement equation then becomes

$$z(k) = [0 \quad 1] [x_n(k) \quad y_n(k)]^T + \varepsilon(k) \quad ;n=1 \quad (3.44)$$

Equations (3.43), (3.44) are derived for the pure sinusoidal waveform, $n=1$. Now let us return to the general case where the signal includes N frequencies; the fundamental plus $N-1$ harmonics, neglecting the D.C. component the state variable representation may be expressed as:

$$\begin{bmatrix} x_1(k+1) \\ y_1(k+1) \\ \dots \\ x_N(k+1) \\ y_N(k+1) \end{bmatrix} = \begin{bmatrix} M_1 & \dots & 0 \\ 0 & \dots & M_N \end{bmatrix} \begin{bmatrix} x_1(k) \\ y_1(k) \\ \dots \\ x_N(k) \\ y_N(k) \end{bmatrix} + \varepsilon(k) \quad (3.45)$$

Where the sub matrices M_i are given by

$$M_i = \begin{bmatrix} \cos(\omega_i \Delta t) & -\sin(\omega_i \Delta t) \\ \sin(\omega_i \Delta t) & \cos(\omega_i \Delta t) \end{bmatrix} \quad (3.46)$$

In this expression $i=1,2,\dots,N$ and $\omega_i=i\omega$ the harmonic frequency.

The measurement equation can be then expressed as:

$$z(k) = \begin{bmatrix} 0 & 1 & 0 & 1 & \dots & 1 & 0 \end{bmatrix} \begin{bmatrix} x_1(k) \\ y_2(k) \\ \dots \\ x_N(k) \\ y_N(k) \end{bmatrix} + w(k) \quad (3.47)$$

Together equations (3.45) and (3.47) represent model 2 for harmonics calculations. It is clear that the state transition matrix depends on the sampling frequency as well as on the number of samples, K , chosen.

Finally to conclude this section the general state space representation, suitable for dynamic state estimation problem, will be in the following compact form

$$\begin{aligned} \Theta(k+1) &= \Phi(k) \Theta(k) + \varepsilon(k) \\ z(k) &= H(k) \Theta(k) + w(k) \end{aligned} \quad (3.48)$$

These equations are valid for both model 1 and model 2 with the

difference only in the transition matrix and the $H(k)$ vector. Model 1 can be obtained if the state transition matrix $\Phi(k)$ is an identity matrix while the $H(k)$ vector is a time dependent vector. on the other hand Model 2 will be obtained if the state transition matrix is picked to be a block diagonal matrix as given in equation (3.46) while the vector $H(k)$ is a constant vector given by equation (3.47) [13,42].

In equations (3.48) $\varepsilon(k)$ and $w(k)$ are assumed to be random white noise with known covariance structure and they are assumed to be uncorrelated to each other. The covariance matrices for the $\varepsilon(k)$ and $w(k)$ vectors are given by

$$E [\varepsilon(k) \varepsilon(i)^T] = \begin{cases} Q(k), & i=k \\ 0, & i \neq k \end{cases} \quad (3.49)$$

$$E [w(k) w(i)^T] = \begin{cases} R(k), & i=k \\ 0, & i \neq k \end{cases} \quad (3.50)$$

$$E [w(k) \varepsilon(i)^T] = 0 \quad \text{for all } k \text{ and } i \quad (3.51)$$

3.3: Harmonic sources identification

Having calculated, statically or dynamically, the harmonic

magnitudes and phase angles for both current and voltage, at a certain bus in the power system network, the average power generated from a harmonic n can be calculated simply using either the magnitude and the phase or the direct and quadrature components, x and y , for each harmonic. If the direct and quadrature components are used then the average power can be expressed as:

$$P_n = 0.5 [x_{nv} x_{ni} + y_{nv} y_{ni}] \quad ; n=1,2,\dots,N \quad (3.52)$$

Where nv referred to the voltage component of the harmonic n and ni referred to the current component of the harmonic n as mentioned earlier. Of course equation (3.52) is for the static case. A similar equation can be written for the dynamic case, where there will be a value for the power at each step k corresponding to each estimation of the parameter vector $\Theta(k)$. In this case the average power expression is given by

$$P_n(k) = 0.5 [x_{nv}(k) x_{ni}(k) + y_{nv}(k) y_{ni}(k)] \quad ; n=1,2,\dots,N \quad (3.53)$$

In both equations (3.52) and (3.53) the values of x and y are expressed as maximum values. A harmonic source is said to exist, at any bus, when the voltage $v(t)$ and the current $i(t)$ are such that

$$[x_{nv} x_{ni} + y_{nv} y_{ni}] > 0 \quad ; n=2,3,\dots,N \quad (3.54)$$

In other words, the average injected power associated with harmonic frequency $n\omega_0$, P_n , other than the power frequency, ω_0 , is positive [11,26].

CHAPTER IV

PARAMETER ESTIMATION: THE STATIC CASE

In this chapter, the parameter estimation techniques applicable to off-line harmonics identification is considered.

The chapter starts with the presentation of different static state estimation techniques namely, the Discrete Fourier transform (DFT), the Least error squares (LS) and the Least absolute value (LAV). Each of the three algorithms will be tested, separately, first using simulated examples, then practical data will be used for comparison between the different techniques.

4.1: Static estimation techniques

In this section different static estimation techniques applicable to harmonics identification is considered with a complete derivation whenever necessary.

4.1.1: Discrete Fourier transform (DFT)

In this subsection the equations applicable to use for calculating the direct and quadrature components of the harmonics are presented. The derivation of these equations is well documented in many references [8,30].

The frequency content of a periodic stationary discrete time signal $x(n)$, with M samples, can be expressed using the discrete Fourier transform as [7,8,13,30,31]:

$$X(f_k) = \frac{1}{M} \sum_{n=1}^M x(t_n) e^{-jk\Omega n} \quad (4.1)$$

Where $\Omega = 2\pi/N$.

The inverse Fourier transform is thus

$$x(t_n) = \sum_{k=1}^M X(f_k) e^{jk\Omega n} \quad (4.2)$$

Both the time domain function and the frequency domain spectrum are assumed periodic, with a total of M samples per period. Without going through derivations, if the sampled signal is a voltage signal then the direct and quadrature components of the harmonic n can be expressed as:

$$x_{nv} = \frac{2}{M} \sum_{k=1}^M V_k \sin n\omega_0 t_k \quad (4.3)$$

$$y_{nv} = \frac{2}{M} \sum_{k=1}^M V_k \cos n\omega_0 t_k \quad (4.4)$$

Where V_k is the sample of the voltage at time t_k ; $k=1, \dots, M$. Simply, if V_k is replaced by I_k , the sample of the current at t_k , similar expressions for the harmonic current components can be obtained.

The parameter vector, Θ , for either the current or the voltage can be then identified by substituting for $n=1, 2, \dots, N$ in equations (4.3) and (4.4).

$$\Theta_{\text{DFT}} = \begin{bmatrix} x_1 \\ y_1 \\ \dots \\ \dots \\ x_N \\ y_N \end{bmatrix} \quad (4.5)$$

Once the parameter vector has been identified, the harmonic magnitude and phase angle can be calculated using equations (3.11) to (3.14). Then the harmonic sources can be identified according to equation (3.55).

It is worthwhile to state here the basic assumptions embodied in the application of the DFT. These assumptions are [13]:

- a) the signal is assumed to be of a constant magnitude during the window size considered (stationary),
- b) the sampling frequency is equal to the number of samples multiplied by the fundamental frequency,
- c) the sampling frequency theorem is satisfied by choosing the sampling frequency to be at least twice the highest frequency in the signal to be analyzed, and
- d) the frequencies of the harmonics are an integral multiple of the fundamental frequency.

4.1.2: Least error squares estimation

Given the overdetermined system of equations described by equation (3.30)

$$z(t) = A(t) \Theta + w \quad ,$$

the generalized least error squares estimation is obtained as the value of the parameter vector Θ which minimizes the following cost function [26,39]

$$J_2(\Theta) = [z(t) - A(t)\Theta]^T W(t) [z(t) - A(t)\Theta] \quad . \quad (4.6)$$

In equation (4.6) W is a diagonal matrix of order $m \times m$ and m is the total number of samples. It is called the weighting matrix. It can be written as

$$W(t) = \text{diagonal} [w_i(t), i=1,2, \dots, m] \quad (4.7)$$

In equation (4.7) the matrix $W(t)$ is a symmetric positive definite matrix. The elements of $W(t)$ are assigned to each measurement so that the measurements with the larger weights have a greater influence on the cost function and thus on the solution.

Equation (4.6) can be rewritten as follows

$$J_2(\Theta) = z^T(t) W(t) z(t) - 2\Theta^T A^T(t) W(t) z(t) + \Theta^T A^T(t) W(t) A(t) \Theta \quad (4.8)$$

By setting $\frac{d J(\Theta)}{d \Theta} = 0$ and solving for Θ

$$\Theta_{GLS} = [A^T(t) \ W(t) \ A(t)]^{-1} A^T(t) \ W(t) \ z(t) \quad (4.9)$$

Equation (4.9) thus gives the best estimation of the parameter vector Θ that minimizes the error squared. The estimate obtained this way is called the generalized least squares estimation or some times it is called the weighted least squares estimation.

$$\text{If } W(t) = \omega I$$

Where ω is a positive scalar and I is the identity matrix, the estimate Θ is given by

$$\Theta_{LS} = [A^T(t) \ A(t)]^{-1} A^T(t) \ z(t) \quad (4.10)$$

or

$$\Theta_{LS} = A^+(t) \ z(t) \quad (4.11)$$

where

$$A^+(t) = [A^T(t) \ A(t)]^{-1} A^T(t) \quad (4.12)$$

is the left pseudo-inverse [39].

Θ obtained above in equation (4.10) is called the least squares estimate Θ_{LS} , and it is clear that this is a special case of the generalized least squares solution. The basic assumptions in this technique is that the sampling theorem is satisfied and the signal

under consideration is a stationary signal [26,32,33,39].

The least squares technique is easy to implement on a digital computer and usually requires a reasonable computing effort. The technique produces excellent estimates when the error distribution is Gaussian. On the other hand if there are outliers in the measurements the technique fails to produce the optimal estimate [21,22].

4.1.3: Least absolute value estimation

Given the overdetermined system of equations as stated in equation (3.30). The LAV estimation problem is to estimate Θ_{LAV} such that the absolute value of the error is minimized. The least absolute value cost function can be written as:

$$J_1(\Theta) = \sum_{i=1}^m | z_i - \sum_{j=1}^U A_{ij} \Theta_j | \quad (4.13)$$

Where z_i is the i^{th} measurement
 Θ_j is the j^{th} unknown
 U is the total number of unknowns
 A_{ij} is the element in the i^{th} row and j^{th} column of the
 $(m \times u)$ matrix A .

The i^{th} residual is given by

$$r_i = z_i - \sum_{j=1}^U A_{ij} \Theta_j \quad (4.14)$$

The iterative nature of linear programming techniques, as

discussed earlier in chapter 2, have deterred many potential users of the least absolute value technique. In 1987 Christensen and Soliman developed a new LAV technique which is non-iterative and produces a unique solution if the matrix A is of full rank [22]. This technique used the least squares estimate as a basis for the solution. The estimate obtained through this technique closely matches that resulting from conventional linear programming algorithms. The new method follows directly from the theorem governing LAV estimation, which reads as follows [21,22,34].

Theorem: If the column rank of the $(m \times U)$ matrix A is k , $k \leq U$ (for maximal rank $k=U$), then there exist a vector Θ_{LAV} corresponding to a best approximation that interpolates at least k points of the measurement set.

From this theorem Christensen and Soliman proposed, that the problem can be solved directly by choosing the best k points and then use them in solving a full determined system of equation providing that the matrix A is a full rank matrix [21,22]. The technique then has been modified [34] to get rid of the error resulted in some special cases. The steps to be followed in this new algorithm are as follows,

1. Given the overdetermined system of equation shown in a vector form as:

$$Z = A \Theta + w \quad , \quad (4.15)$$

where $Z = m \times 1$ vector of measurements,
 $\Theta = U \times 1$ vector of unknowns,
 $A = m \times U$ matrix of rank U describing the relationship between
 Z and Θ , and
 $w = m \times 1$ vector of errors.

2. Find the least error squares estimation Θ_{LS} as

$$\Theta_{LS} = (A^T A)^{-1} A^T Z \quad . \quad (4.16)$$

3. Calculate the least error squares residuals vector generated from this solution as

$$r = Z - A\Theta_{LS} \quad . \quad (4.17)$$

4. Calculate the standard deviation of these residuals,

$$S.D. = \left[\frac{1}{m-U+1} \sum_{i=1}^m (r_i - \bar{r})^2 \right]^{1/2} , \quad (4.18)$$

where r_i is the i^{th} residual given by equation (4.12),
 \bar{r} is the mean value of the residuals.

5. If the observation (measurement z_i) has a residual greater than the standard deviation, this measurement is considered as an outlier,

and it may be corrected and replaced with a new measurement $z_{i_{new}}$ according to the following relation

$$z_{i_{new}} = z_{i_{old}} - r_i, \quad i \in m. \quad (4.19)$$

6. Recalculate the least squares solution using the new measurements if there is any.

7. Find the new least squares residuals generated from this solution, r_{new} .

8. Rank the residuals r_{new} beginning with the smallest and ending with the largest .

9. Select the first U measurements corresponding to the first U smallest residuals.

10. Use the U measurements with the smallest residuals to find the LAV estimate as follows,

$$\Theta_{LAV} = A_U^{-1} z_U \quad (4.20)$$

where z_U are the U measurements having the smallest residuals

A_U is $U \times U$ reduced matrix corresponding to the z_U measurements.

The least absolute value residuals can be then calculated as :

$$r_{i \text{ LAV}} = z_i - A_i \Theta_{\text{LAV}} \quad i=1,2,\dots,m \quad (4.21)$$

Where A_i is the i^{th} row of the A matrix.

Some advantages of this technique can be stated here such as, it is very simple to use, it is a non-iterative technique that reduces the computational time dramatically, it has the ability to reject the outliers without any prior knowledge about them and it gives a better solution than the least squares if the measurement error distribution is not Gaussian.

4.2: Test of the algorithms: simulated examples

In this section, the three algorithms mentioned above are tested using simple simulated examples. Different factors that affect the estimation process are examined. Here the waveform is considered to have a constant magnitude during the data window size (stationary waveform). Later in section 4.3 the algorithms will be tested for nonstationary waveforms [26,30].

4.2.1: The discrete Fourier transform case

In this subsection the discrete Fourier transform algorithm is tested. The example used here is the full wave rectifier voltage waveform. The algorithm is used to calculate the harmonics magnitudes and hence to examine the effects of the different factors on the behavior of the algorithm. The full wave rectifier voltage waveform

contains only the even harmonics. The exact values of the Fourier coefficients are given by: (see Appendix I)

$$a_n = \frac{4 V_m}{\pi(n^2 - 1)} \quad n=2,4,6,\dots,N \quad (4.22)$$

where

V_m is the maximum value of the voltage waveform,

N is the total number of harmonics considered in the waveform,

and the D.C. component is given by

$$a_0 = \frac{2 V_m}{\pi} . \quad (4.23)$$

A computer program was developed to generate the sampled voltage. These samples can be used to calculate the magnitudes and the phases of the harmonics of the sampled voltage signal. Assuming that the maximum voltage is equal to one per unit then all the coefficients will be expressed in per unit values.

At the beginning a specific number of harmonics, 26, is considered with 60 samples and to satisfy the sampling theorem [7] the sampling frequency is chosen to be 3600 Hz. The per unit harmonics magnitudes are shown in figure (4.1) and the corresponding percentage error in the estimated magnitudes is given in figure (4.2). Examining those two plots shows that, no odd harmonics appear as expected and the percentage error starts with a very small value for the second

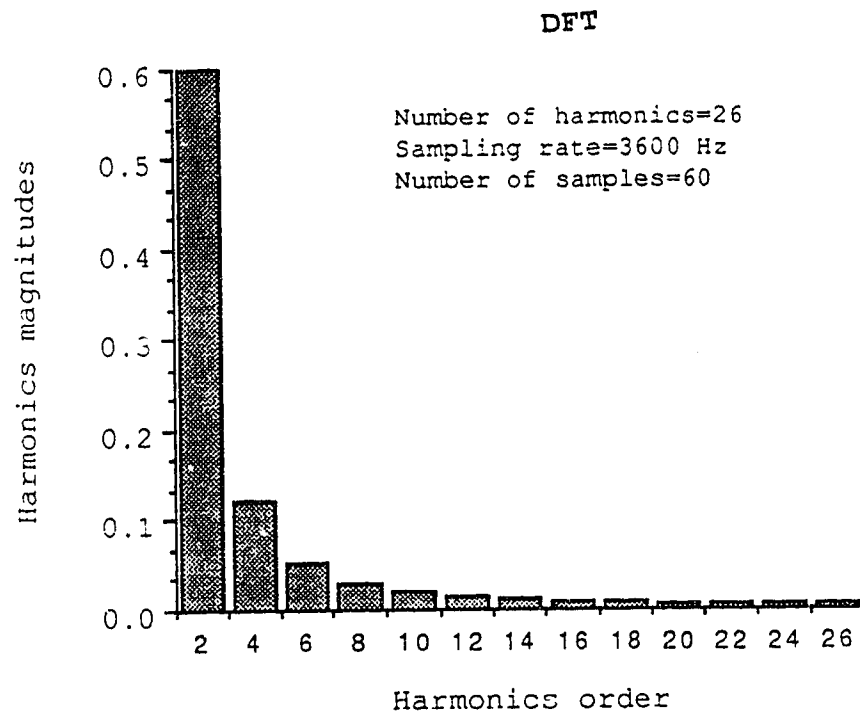


Fig. 4.1 Line spectrum of the full wave rectifier voltage

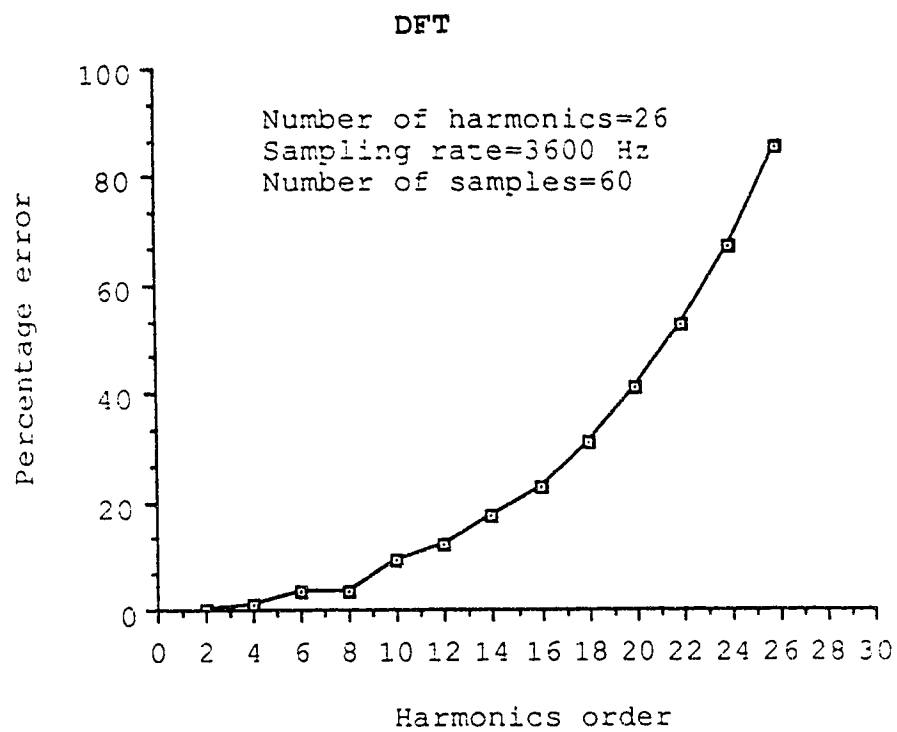


Fig. 4.2 The percentage error in the voltage magnitudes

harmonic and increased gradually as the harmonic order increases. It is clear that the maximum error is about 85% which is quite high. Different factors that affect the estimate are next considered to see when this error will be within an acceptable range.

Number of harmonics considered

To study the effect of the number of harmonics considered, a constant window size, 1 cycle, is chosen with 80 samples and a sampling frequency of 4800 Hz. Figure (4.3) shows the percentage error in the magnitude of both the 6th and 8th harmonics versus the number of harmonics considered. Examining this curve shows that the number of harmonics considered has no effect on the estimate and hence the percentage error.

Sampling frequency

The effect of the sampling frequency on the behavior of the algorithm is examined when the sampling rate varies between 1800 and 6000 Hz in steps of 600 Hz. Figures (4.4) and (4.5) show the variations of the magnitudes of the 4th, 6th, 10th, 16th, 18th and the 20th harmonics with the sampling rate for a data window size of 1 cycle with 20 harmonics considered. The percentage error in estimating the magnitudes of the 4th, 6th and the 8th harmonics is shown as well in figure (4.6). Careful examination of these figures indicates that, for the sampling frequency less than twice the frequency of the highest harmonic considered, $2 \times 20 \times 60 = 2400$ Hz, the percentage error is relatively higher than that with the sampling rate equal to 2400 Hz.

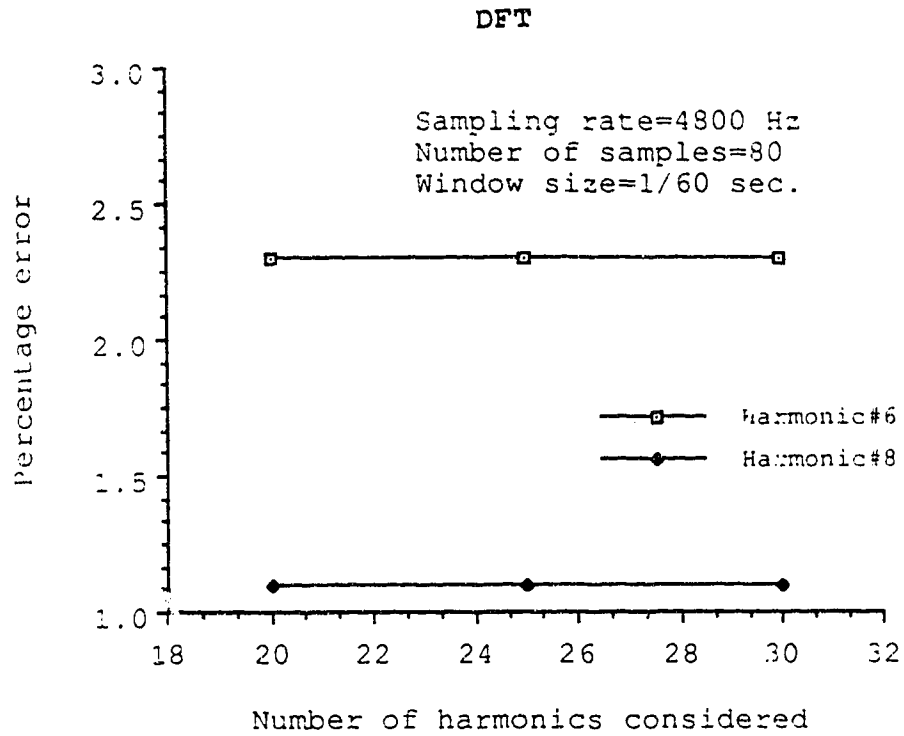


Fig. 4.3 Variations of the percentage error with the number of harmonics

DFT

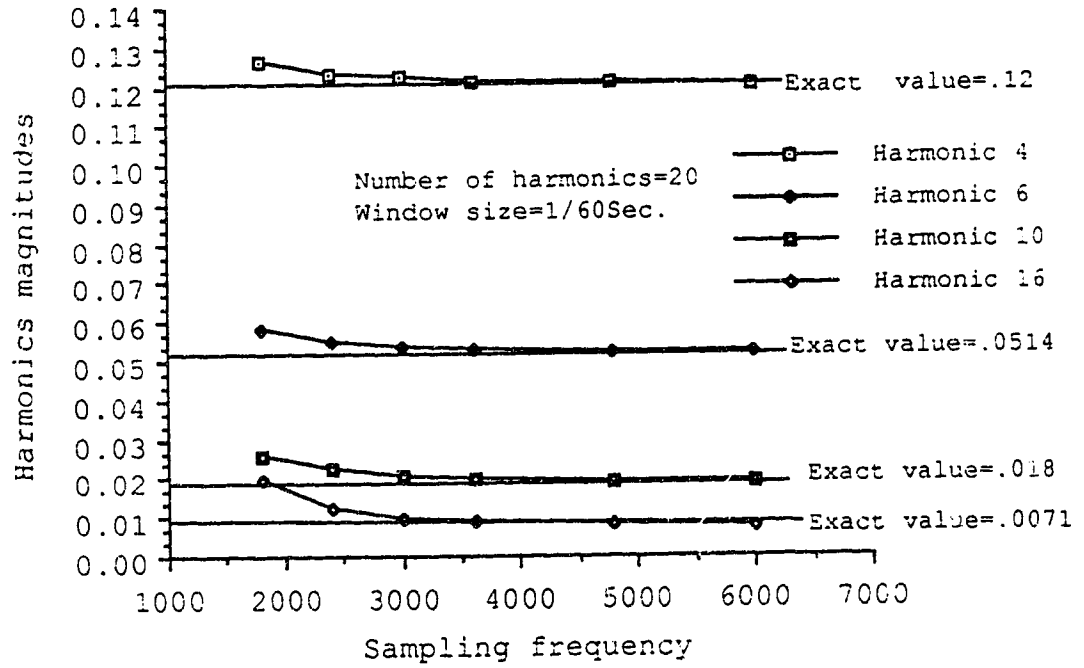


Fig. 4.4 Variations of harmonics magnitudes with sampling frequency

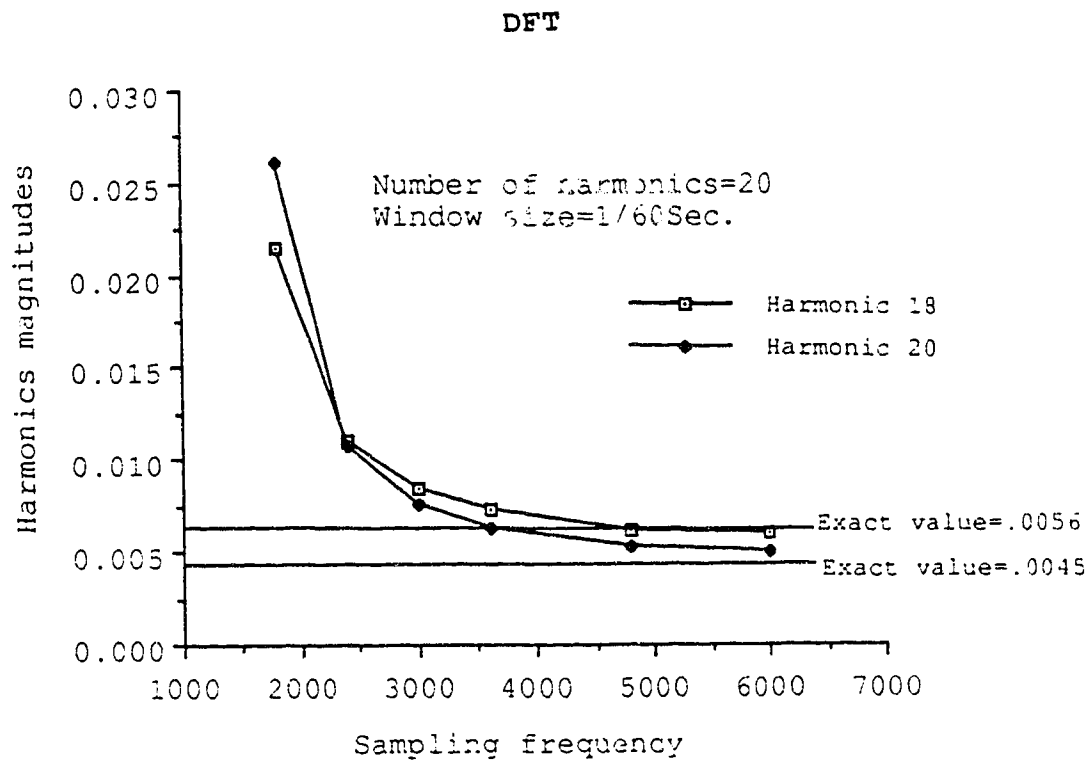


Fig. 4.5 Variations of harmonics magnitudes with sampling frequency

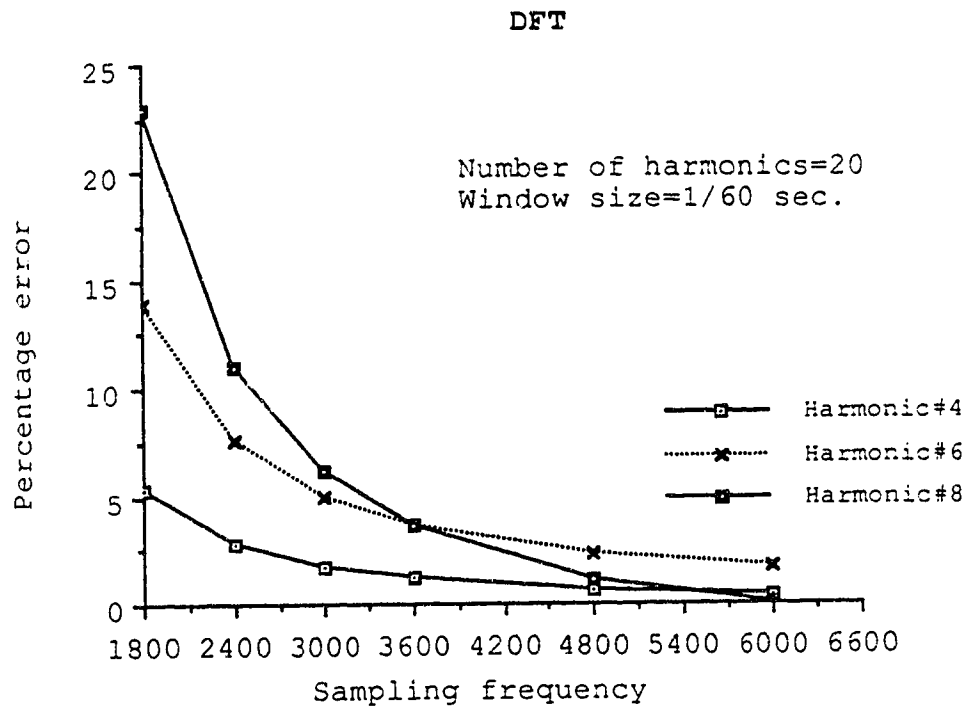


Fig. 4.6 Variations of the percentage error with the sampling frequency

By increasing the sampling rate the percentage error decreases. It is clear that for a good estimate the sampling frequency should be higher than twice the frequency of the highest harmonic considered in the waveform and the higher the frequency, after that, the better the estimate obtained.

Data window size

The effect of varying the data window size on the behavior of the algorithm is examined for 30 harmonics and a sampling frequency of 3600 Hz. Figure (4.7) shows that increasing the data window size from 1 cycle to 4 cycles in step of one complete cycle reduces the percentage error slightly. It should be mentioned here that an integral multiple of one complete cycle should be used in order to get a minimum error.

Frequency drift

There is always uncertainty in determining the actual fundamental frequency in the power system waveforms. It may not be 60 Hz exactly during the steady state operation. An acceptable drift in a power system is about ± 0.05 Hz. The effects of the frequency drift on the estimates of the harmonics magnitudes will be investigated. This is done simply by sampling the signal at 59.5 Hz instead of 60 Hz, -0.5 Hz drift. Considering 26 harmonics and a sampling rate of 3600 Hz with 60 samples. The effect of -0.5 Hz frequency drift appears in figure (4.8) as a slight deviation of the estimate from the exact value. It is a small error for a small drift but increasing the drift more than

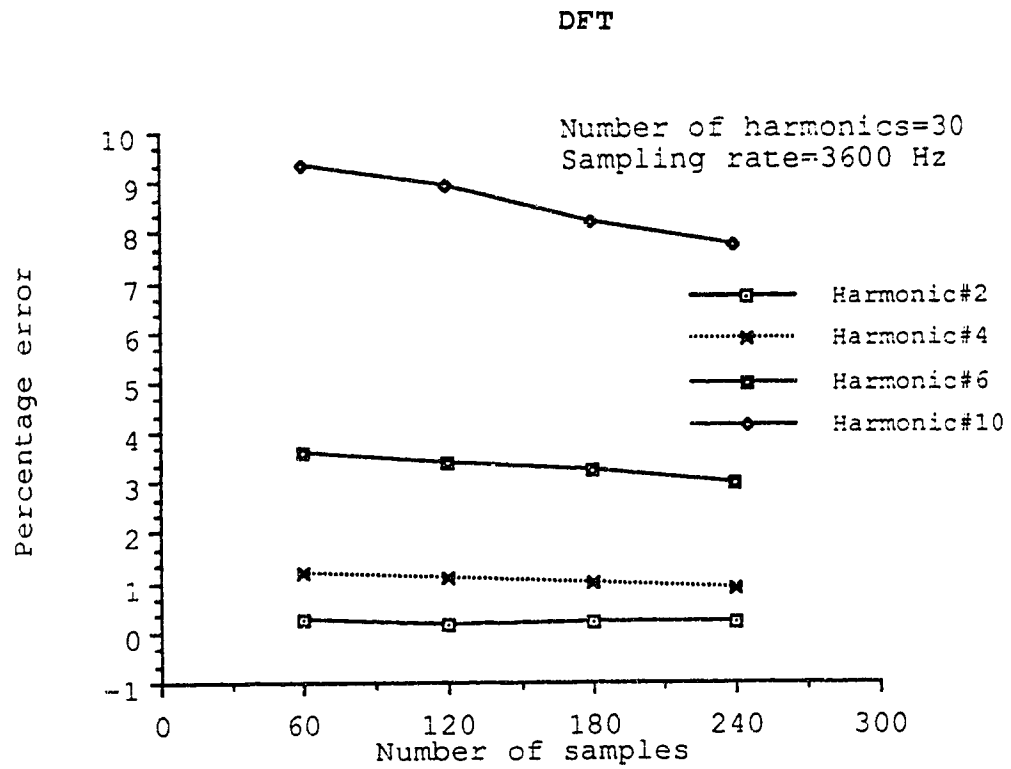


Fig. 4.7 Variations of the percentage error with the data window size

DFT

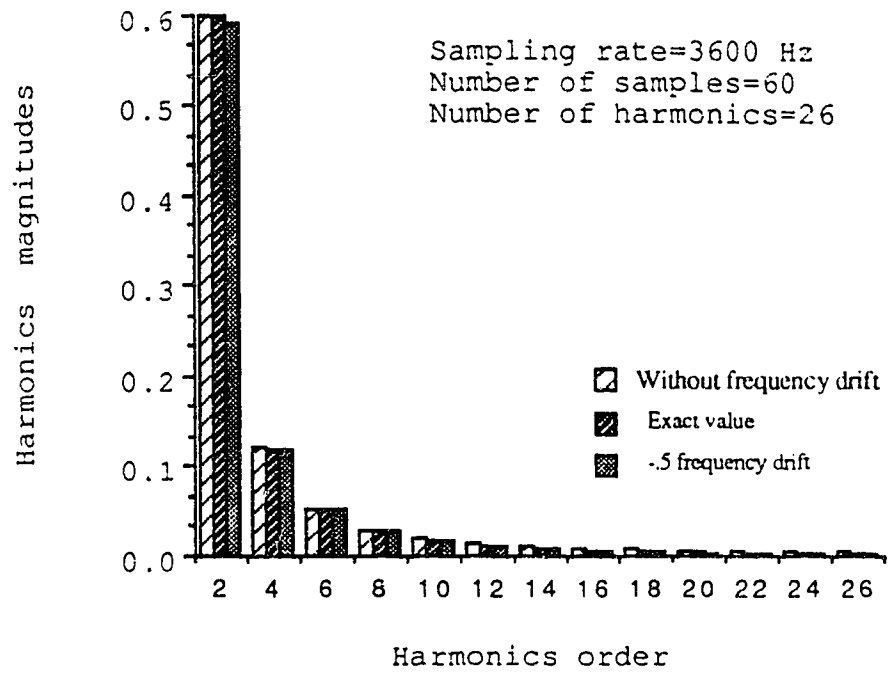


Fig. 4.8 The effect of the frequency drift on the harmonics magnitudes

0.5 Hz could cause a higher error. However, to maximize accuracy, it is better to update the fundamental frequency for each set of measurements.

Bad data

It is possible to have bad measurements, unusual events in the system waveforms, when performing the measurement process. For the 26 harmonics considered and a sampling rate of 3600 Hz the set of the measurements, 60 samples, is contaminated with two points of bad data. This is simply done by reversing the sign of the measurement. Figure (4.9) shows that the harmonics magnitudes estimate is strongly affected by the bad data presence. This is considered to be one of the disadvantages of the discrete Fourier analysis.

The previous discussions show that the discrete Fourier transform algorithm gives excellent results if the sampling frequency is high enough, the data window size is an integral multiple of a complete cycle and if the signal is a stationary signal. One more case which satisfies the above conditions is considered here to verify this conclusion. In this case the sampling frequency is chosen to be 10800 Hz and there are 180 samples considered in one full cycle. Figure (4.10) shows that the maximum percentage error resulted in estimating 20 harmonics is only about 3% . On the other hand, if the data is contaminated with bad measurements the estimate obtained starts to have a large error. It was also found that the frequency drift gives an acceptable error in the estimate if that drift is within the

DFT

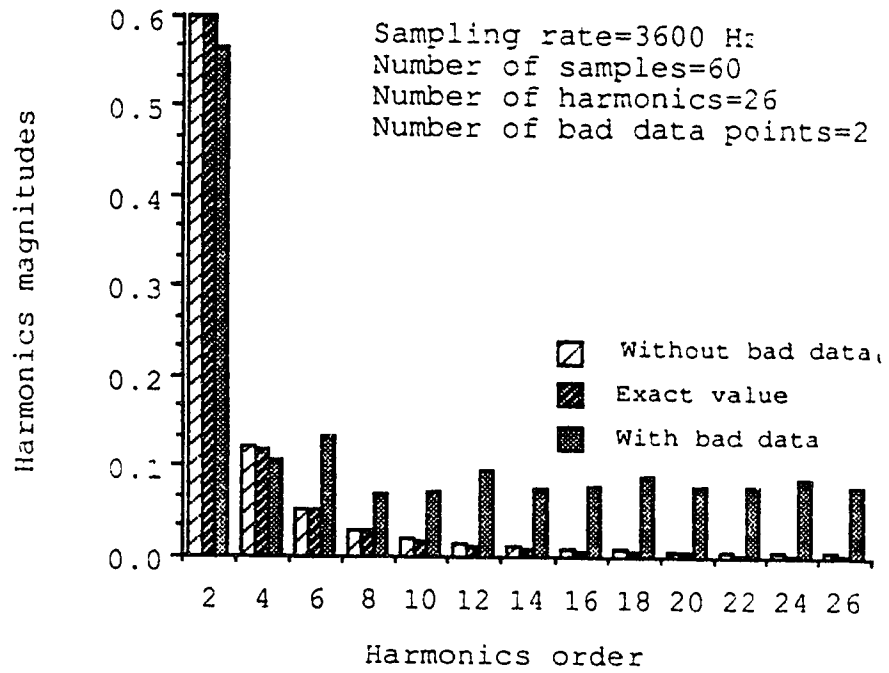


Fig. 4 9 The effects of the bad data on the harmonics magnitudes

DFT

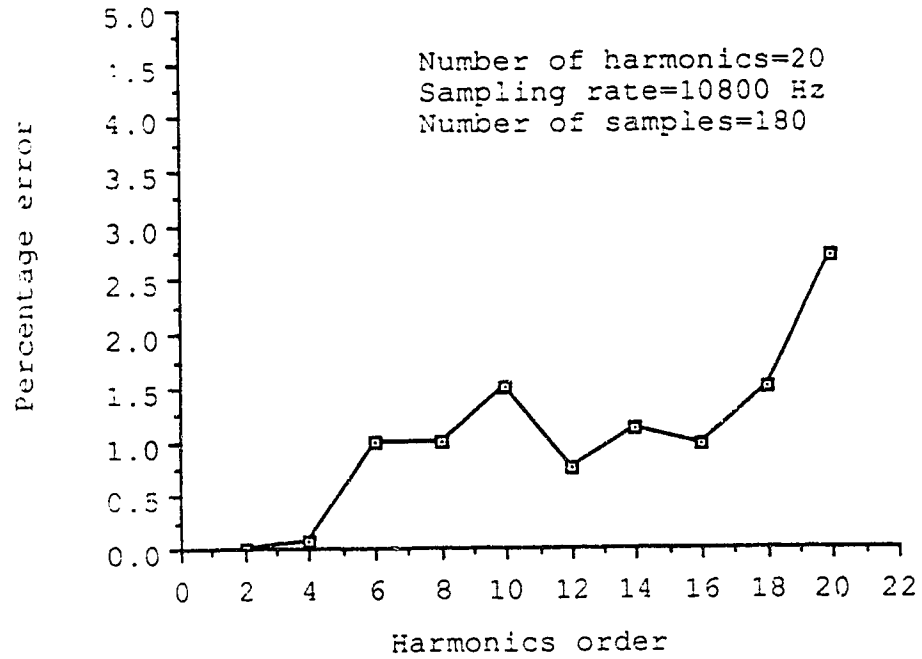


Fig. 4.10 The Percentage error in the voltage magnitude

allowable range, ± 0.05 Hz.

4.2.2: The Least squares case

In this subsection The least squares algorithm is tested using the same simulated example, full wave rectified voltage, used for testing the discrete Fourier transform algorithm in section 4.2.1. Different factors that affect the estimation process are considered such as, the data window size, the sampling rate and the number of harmonics considered. The effects of the bad data points and the frequency drift on the estimate are discussed as well.

Consider the same case as studied before with the DFT, where the number of harmonics considered was chosen to be 26 and a data window size of one complete cycle is considered by having 60 samples at a sampling rate of 3600 Hz. Figure (4.11) gives the harmonics magnitudes while figure (4.12) shows the error in this estimate. Again The error started with a small value for the second harmonic and increased considerably to be about 85% for the 26 harmonic. Comparing figure (4.2) to figure (4.12) shows that the percentage error is almost the same in both the DFT and the LS cases. Next the effects of the Number of harmonics, the sampling rate and the data window size will be examined.

Number of harmonics considered

For a constant sampling frequency, 2400 Hz, and with 60 samples taken over 1.5 cycle the effect of varying the number of harmonics considered is examined by changing the number of harmonics from 9 to

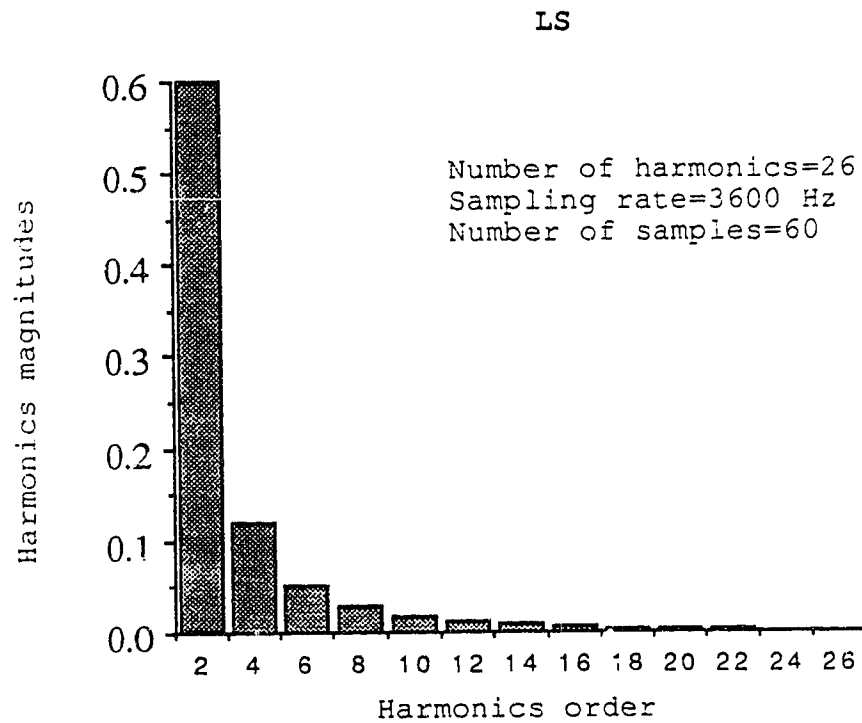


Fig. 4.11 Line spectrum of the full wave voltage
For comparison with DFT see page 52

LS

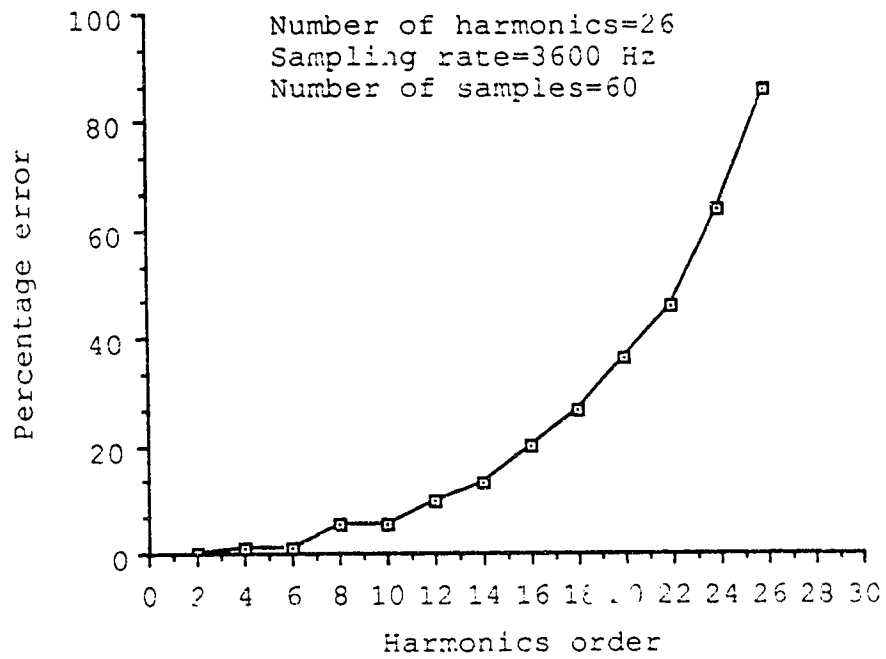


Fig. 4.12 The percentage error in the voltage magnitude
For comparison with DFT see page 53

27 in steps of 3. Figure (4.13) gives the variations of the magnitudes of the 4th, 6th and the 8th harmonic, with the number of harmonics considered while figure (4.14) shows the percentage error in estimating those harmonics magnitudes as varying with the number of harmonics considered. Examining those two curves reveals that increasing the number of harmonics decreases the percentage error considerably. Compared to the DFT this was not the case, the percentage error was constant with the number of harmonics considered.

Sampling frequency

To study the effects of the sampling frequency on the behavior of the algorithm, a constant number of harmonics, 20, is considered and the number of samples is chosen to be 60. Figure (4.15) gives the variations of the harmonics magnitudes with the sampling frequency when the sampling frequency varies between 1800 and 3600 Hz in step of 600 Hz. Figure (4.16) shows the effect of the sampling frequency on the error in estimating the harmonics magnitudes under the same conditions. Both figures (4.15) and (4.16) show that the error can be reduced by increasing the sampling rate. Of course the sampling frequency should be at least twice the frequency of the highest harmonic considered.

Data window size

The effect of varying the data window size on the estimated parameters is studied by considering a constant sampling rate of 2520 Hz and 20 harmonics. In this way by varying the number of samples, the

LS

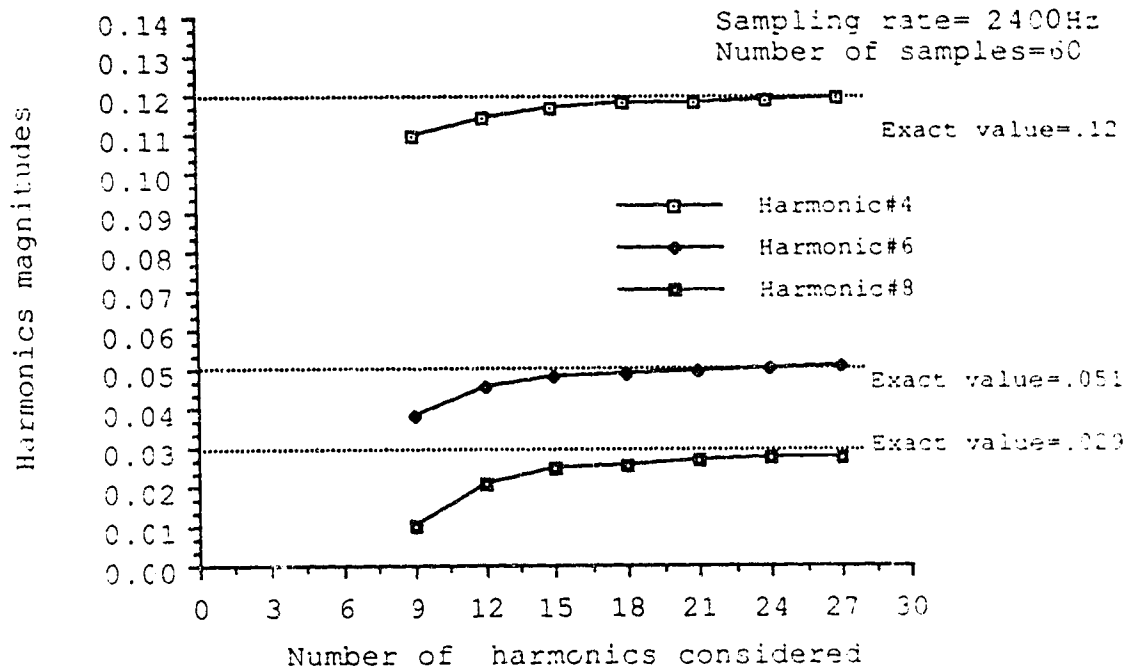


Fig. 4.13 Variations of harmonics magnitudes with the number of harmonics

LS

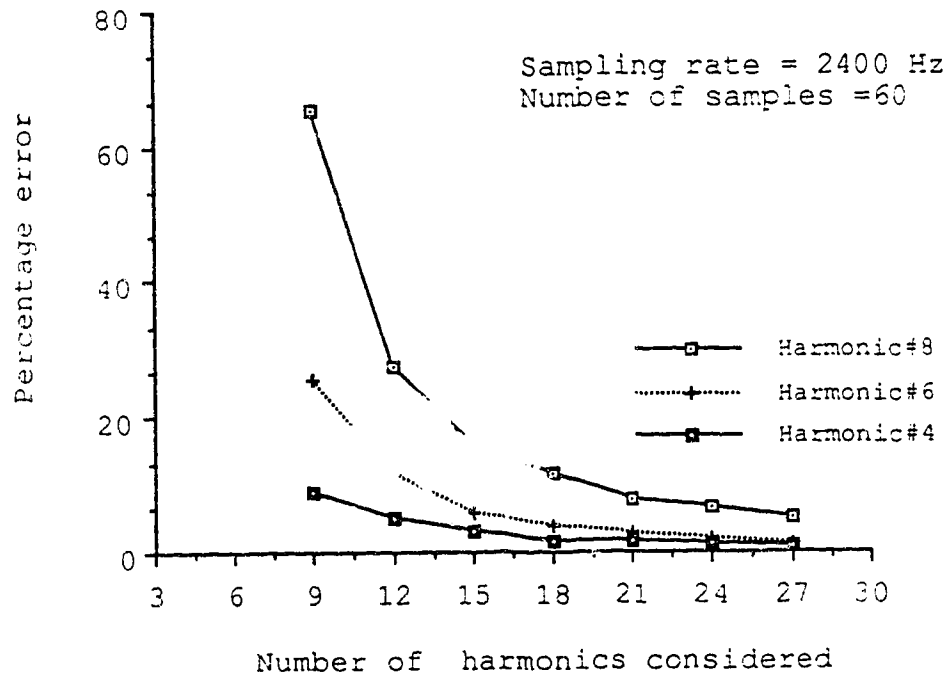


Fig. 4.14 Variations of the percentage error with the number of harmonics

LS

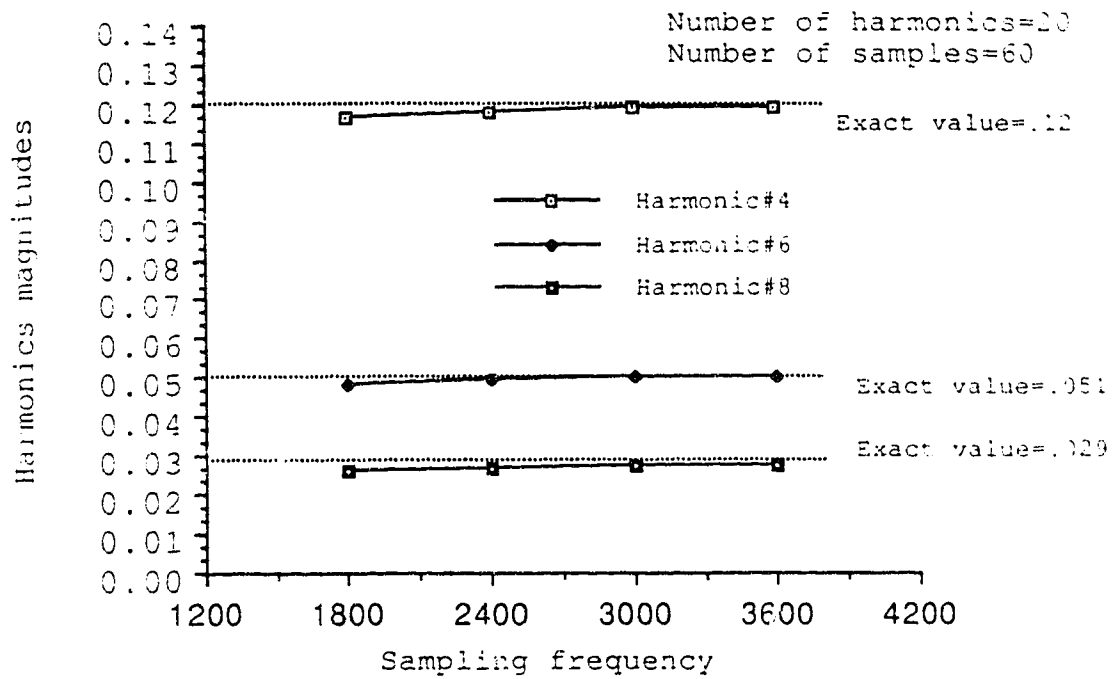


Fig. 4.15 Variations of the harmonic magnitudes with the sampling frequency

For comparison with DFT see page 56

LS

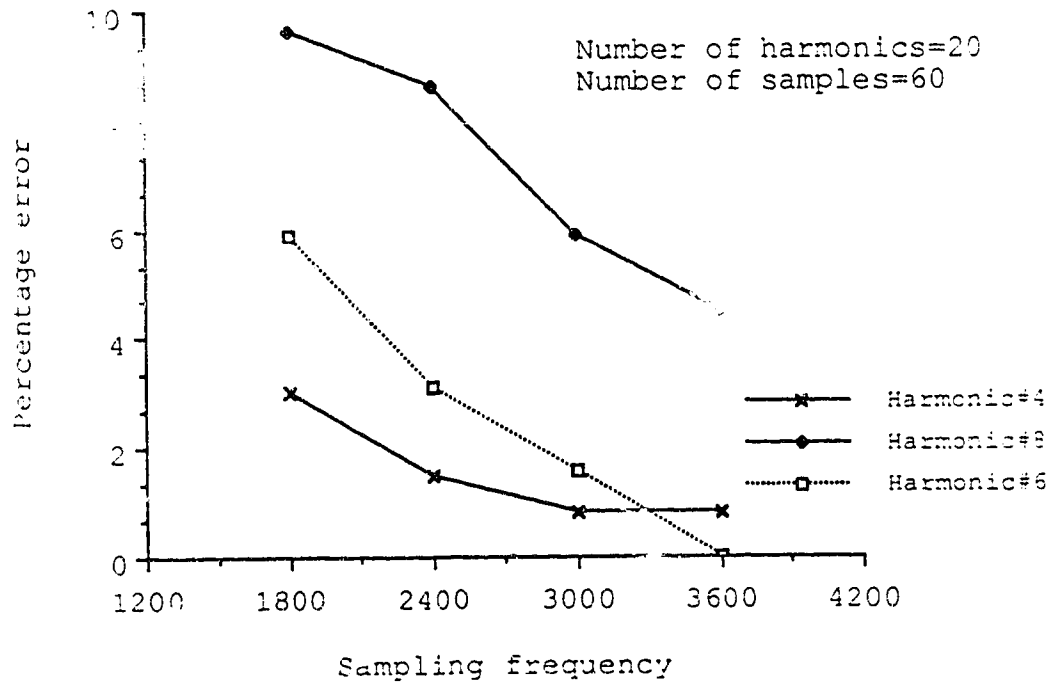


Fig. 4.16 Variations of the percentage error with the sampling frequency

For comparison with DFT see page 58

data window size will be changed consequently. The number of samples considered is varied between 48 to 96 in step of 12. Figure (4.17) shows that the percentage error is constant with the data window size. This figure implies that it is not necessary to use a window size of an integral multiple of a complete cycle after the first cycle. This was not the case when using the DFT algorithm, where an integral multiple of one complete cycle should be used.

Frequency drift

The algorithm was tested for different levels of frequency drift starting from ± 0.05 Hz up to ± 0.5 Hz. The sampling frequency was chosen to be 3600 Hz while the number of samples is 60 and the number of harmonics was 26. It has been found that the frequency drift has little effect on the estimate if the drift is small and the error starts increases with drift. This error is acceptable for the reasonable frequency drift in the power system, ± 0.05 Hz. However to reduce this error it is recommended that the fundamental frequency be updated for each set of measurements. Figure (4.18) gives the estimate when there is -0.5 Hz frequency drift compared to the estimate without any drift. The exact value is shown on the same graph as well. It is worthwhile to state here how the simulation of the frequency drift of -0.5 Hz, in this example, was made. The measurements were sampled at 59.5 Hz instead of 60 Hz, -0.5 Hz drift, at the same time the connection matrix $A(t)$, usually calculated off line, was calculated using 60 Hz.

LS

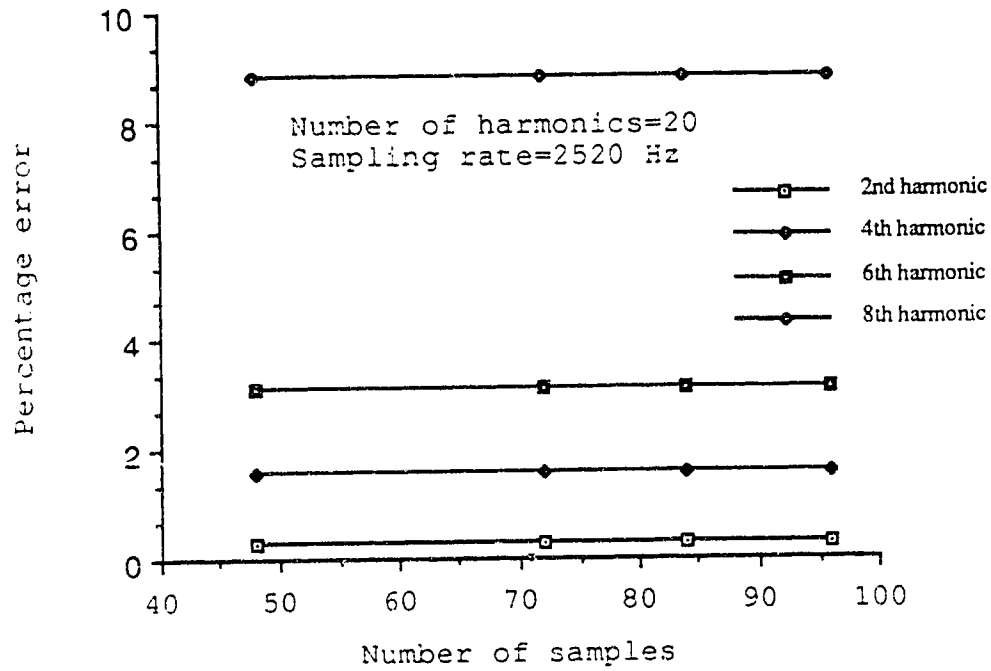


Fig. 4.17 Variation of the percentage error with the data window size

For comparison with DFT see page 60

LS

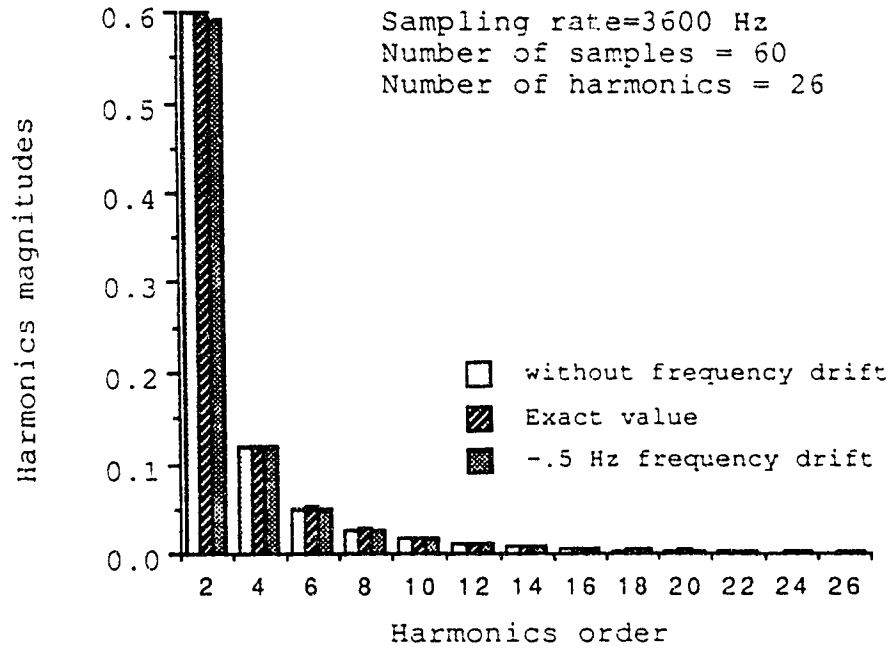


Fig. 4.18 The effect of the frequency drift on the harmonic magnitudes

For comparison with DFT see page 61

Bad data

To show the effect of bad data on the estimate the measurement set is contaminated with 2 points of bad data. These points are obtained by reversing the sign of the original points. For 26 harmonics, 180 samples and sampling frequency of 10800 Hz, the estimate of the harmonics magnitudes is compared to that obtained without any bad data in figure (4.19). It is clear that the estimate is strongly affected by the bad data. This is considered to be the main problem associated with this kind of algorithm.

Time reference ($t=0$)

The algorithm was tested when the time reference was selected to be at the middle of the window size. In this case the numerical values of the elements of each row of the left pseudo inverse matrix becomes symmetrical about the center of the row. Then the time reference was shifted from the middle of the data window and the algorithm was tested again. It was then found that the position of the time reference has no effect on the estimate of the harmonic magnitudes and phases. However, to reduce the computation burden, it is recommended that the time reference should be in the middle of the data window to obtain a symmetrical A^+ matrix.

The previous discussions showed that the LS technique can be easily applied to estimate the magnitudes and phases of the harmonics. To get good results it is recommended that the sampling rate should be higher than twice the frequency of the highest harmonic considered

LS

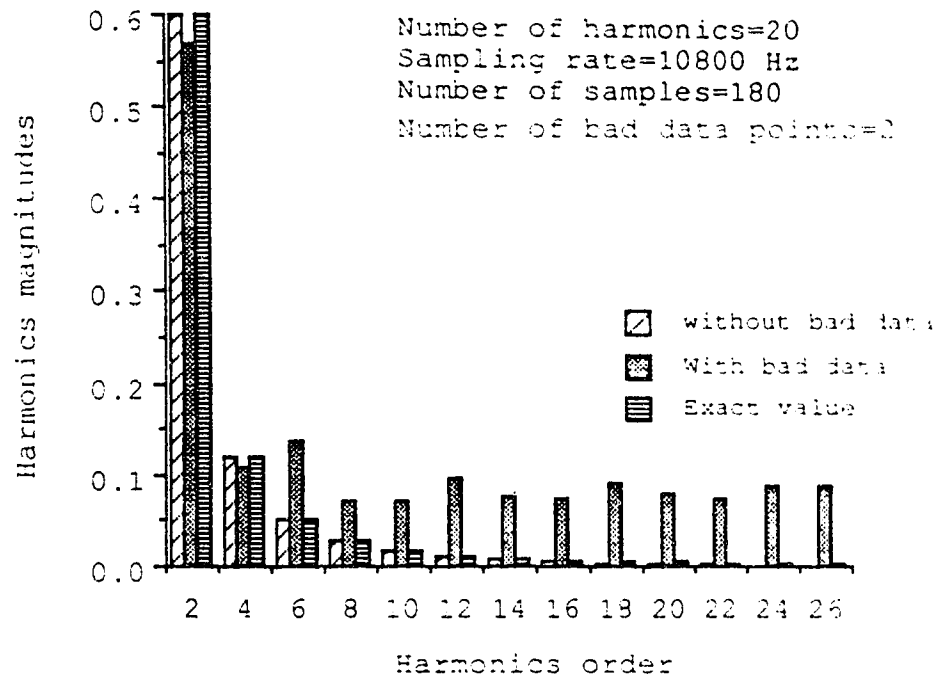


Fig. 4.19 The effects of the bad data on the harmonics magnitudes
For comparison with DFT see page 63

in the signal, to avoid aliasing. Increasing the sampling frequency further reduces the error in the estimate. However too high a sampling rate is undesirable as the elements of the matrix $(A^T A)^{-1}$ have to be multiplied by the sampled values, and any noise present in the signal would be amplified. It has been found also that to reduce the error in the estimate, more harmonics should be considered and the data window size should be at least one complete cycle. It is not necessary to have an integral multiple of one cycle after that. As mentioned before, the signal under consideration is assumed to be a stationary signal. If the above recommendations are considered then an excellent estimate would be obtained as shown in figure (4.20). In this case a sampling frequency as high as 10800 Hz is chosen and 180 samples, covering one complete cycle, are used. It is clear that the maximum error in estimating 20 harmonics is only about 3.5% .

4.2.3: The least absolute value case

Since this new approach has been developed it has been subjected to many tests [16,21,22,34,35,36,37,38]. The technique was found to behave just like the least squares technique and it gives the same results providing that there are no bad data points. Therefore the main concern, here, is to show the ability of the algorithm to reject the bad data without any prior knowledge about its presence. In this subsection two simple examples are presented in order to support this fact.

LS

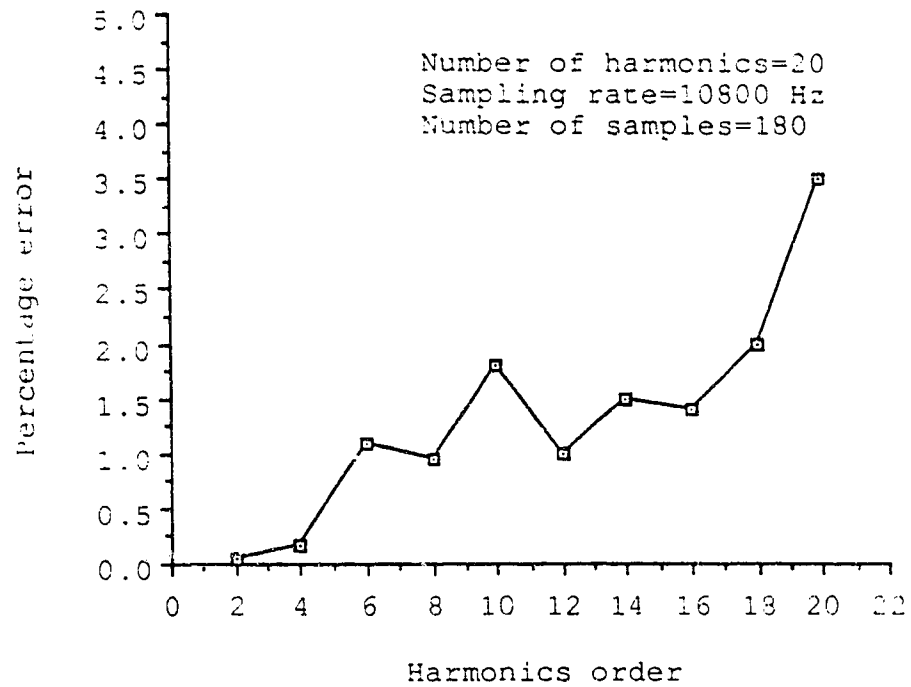


Fig. 4.20 The percentage error in the voltage magnitude

For comparison with DFT see page 64

Example 1

Here the example considered is the full wave rectified voltage. Considering the last case discussed in the least squares subsection, in which the sampling frequency was 10800 Hz, the number of samples was 180 and there were 20 harmonics considered. Figure (4.21) shows that the percentage error of both the LAV and the LS is almost the same if there are no bad data points. The effect of the bad data is shown in figure (4.22). This figure clearly indicates that while the LS algorithm is badly affected by the bad data the LAV algorithm still produces the same estimate as if there is no bad data.

Example 2 [13]

The algorithm is tested here using a voltage waveform with known harmonic contents. The waveform consists of the fundamental, the third, the fifth, the eleventh, the thirteenth and the nineteenth harmonics. The waveform is described as [13]:

$$v(t) = 1.0\cos(\omega_0 t + 10^\circ) + 0.1\cos(3\omega_0 t + 20^\circ) + 0.08\cos(5\omega_0 t + 30^\circ) + 0.08\cos(7\omega_0 t + 40^\circ) \\ + 0.06\cos(11\omega_0 t + 50^\circ) + 0.05\cos(13\omega_0 t + 60^\circ) + 0.03\cos(19\omega_0 t + 70^\circ)$$

The sampling frequency used for this simple example is 3840 Hz with the number of samples=128 (2 cycles, with 64 samples/cycle). The results obtained for harmonics magnitudes and phase angles estimates, with no bad data, are given in figures (4.23) and (4.24), while figures (4.25) and (4.26) give the same estimates with some bad data points contaminating the signal. Examining these curves, for this

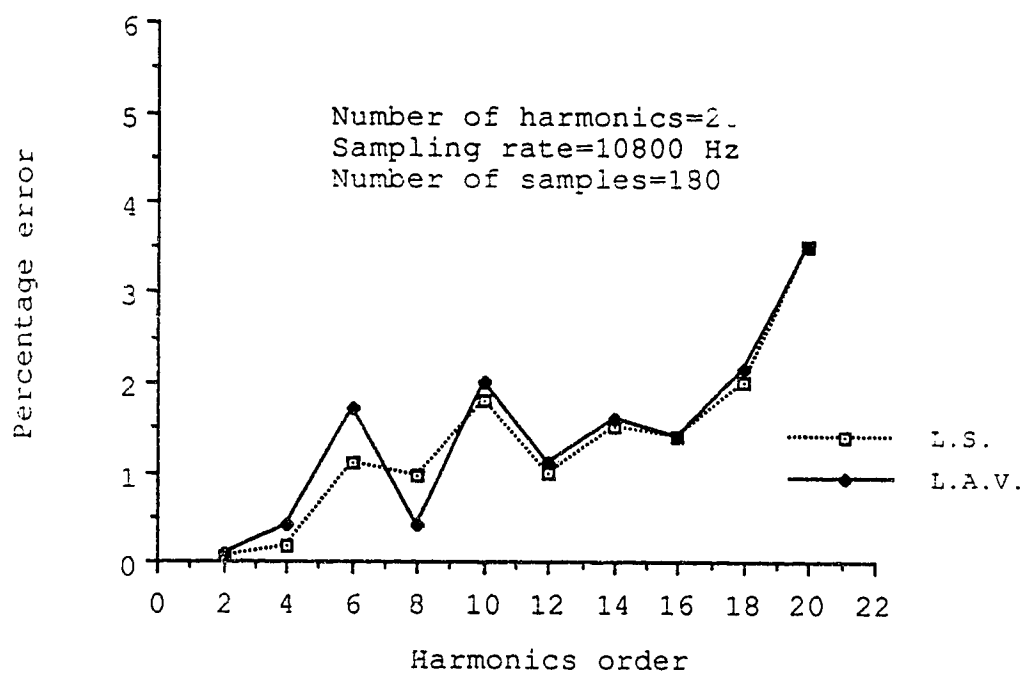


Fig. 4.21 The percentage error in the voltage magnitude

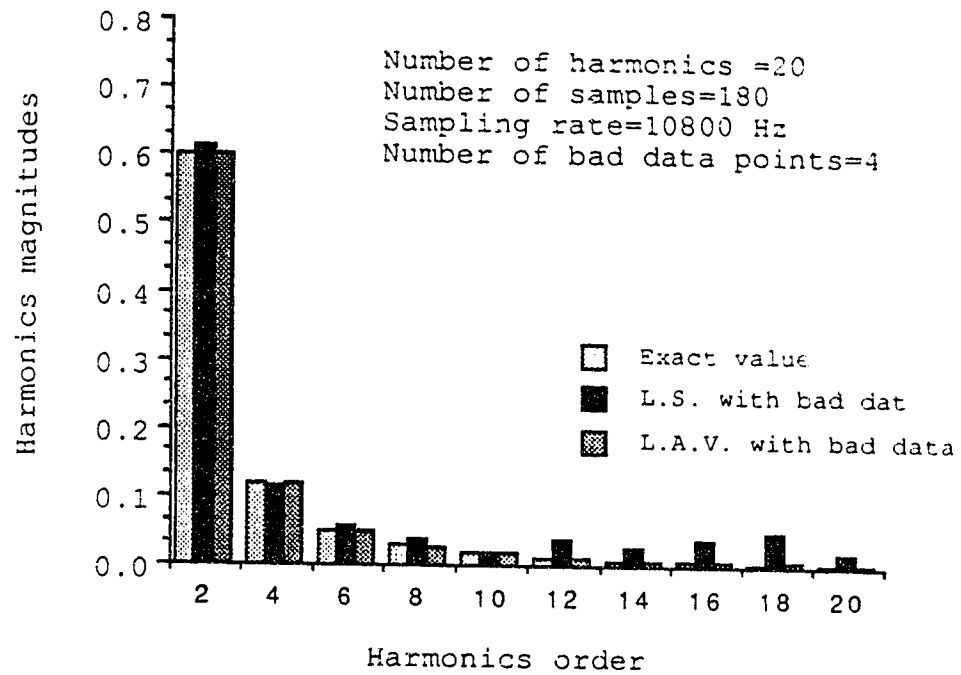


Fig. 4.22 The effect of the bad data on the harmonics magnitudes

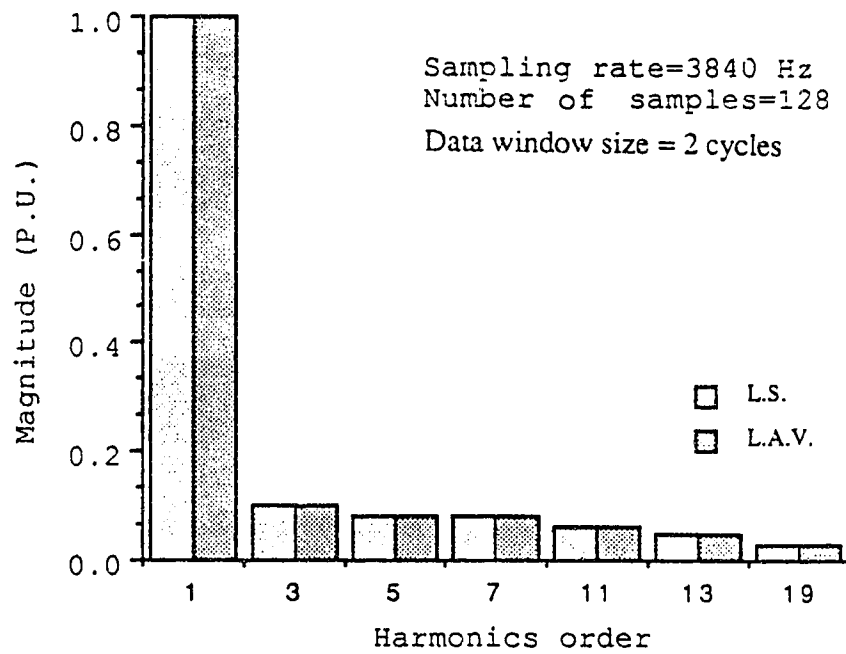


Fig. 4.23 Harmonics magnitudes

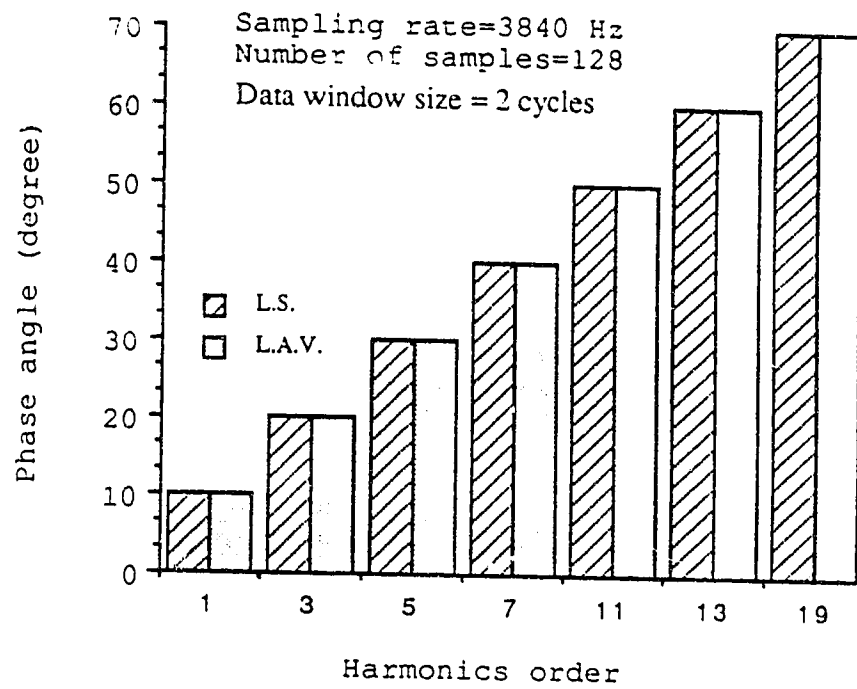


Fig. 4.24 Harmonics phase angles

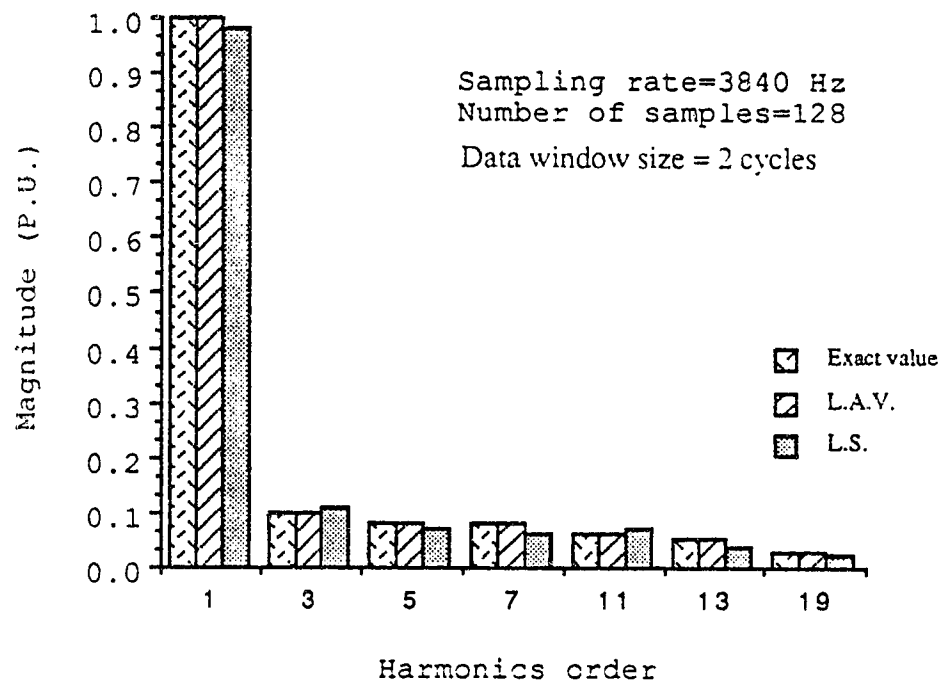


Fig. 4.25 Bad data effects on the harmonics magnitudes

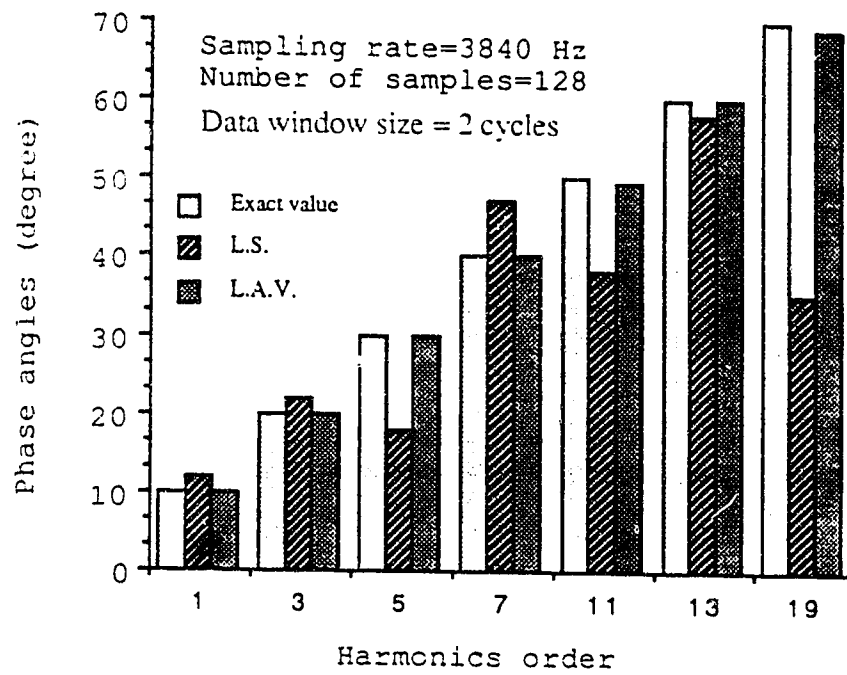


Fig. 4.26 Bad data effects on the phase angles

simple example, reveals that with no bad data, the proposed algorithm gives results as good as the least squares algorithm. With bad data contaminating the measurements, the proposed technique produces exact estimates, in contrast to the least squares which produces poor estimates, and the most affected estimate with these outliers is the phase angle of each harmonic.

Effects of the frequency drift on the estimates of the harmonics magnitude and phase angle are also investigated for this example. Figures (4.27) and (4.28) give the results obtained for harmonics magnitudes as well as the phase angles, when the frequency drift is -0.5 Hz and -2.0 Hz. Examining these two curves reveals that for a small drift, -0.5 Hz, the harmonics magnitudes estimate do not change appreciably, but for large frequency drift, -2.0 Hz, the magnitudes change by small amount. The phase angles are the estimates most affected by the frequency drift. These change appreciably as the frequency changes, and the proposed algorithm produces a poor estimate for them.

4.3: Test of the algorithms: Actual recorded data

The three algorithms are tested again in this section using actual recorded data. Here the considered waveforms are nonstationary. A complete description of the system under consideration is given in Appendix II. This system consists of a variable speed drive controlling a 3000 HP, 25 KV induction motor, connected to an oil pipeline compressor. A sample of the voltage and current signals is shown in figures (4.29) and (4.30). Figure (4.29) shows the voltage

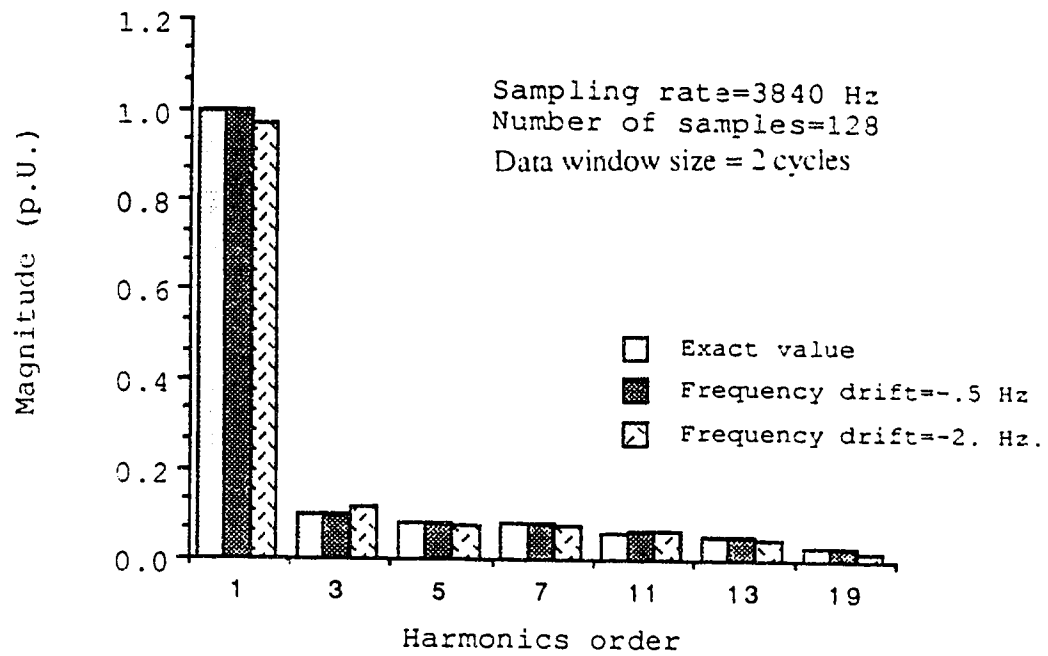


Fig. 4.27 Harmonics magnitudes with frequency drift

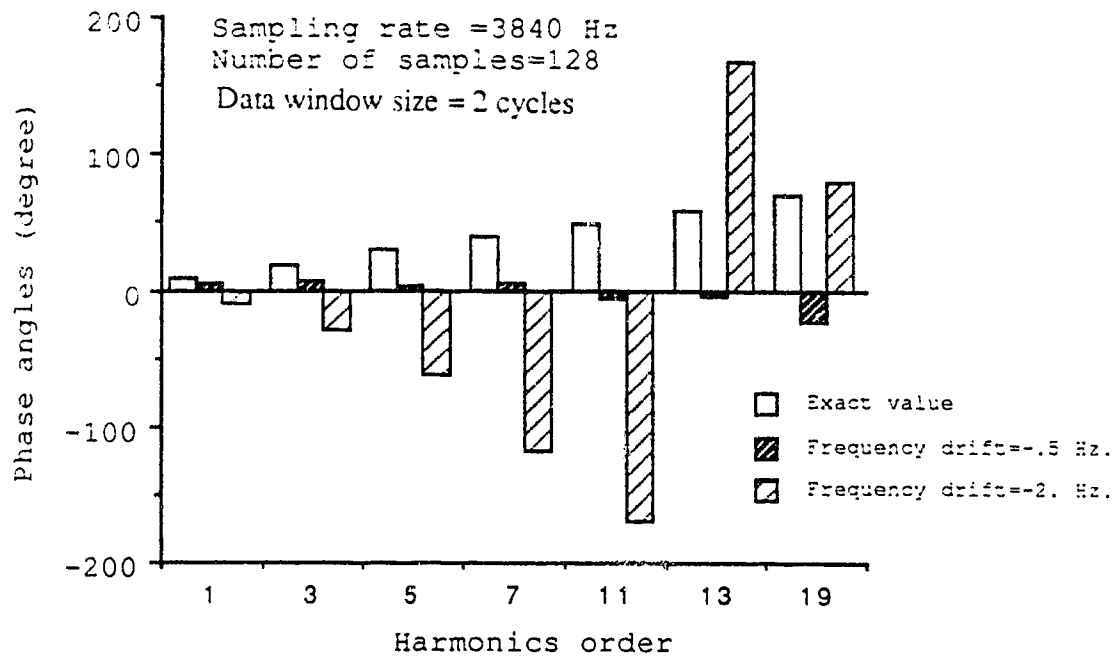


Fig. 4.28 Harmonics phase angles with frequency drift

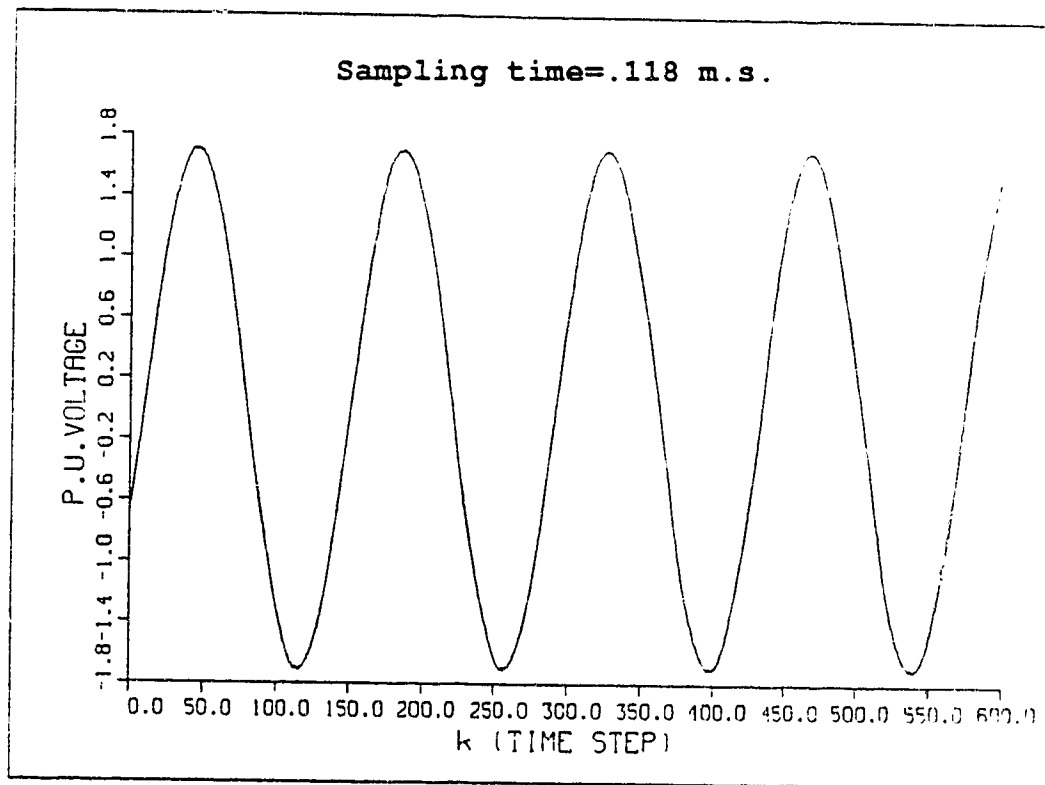


Fig. 4.29 Actual recorded voltage for phase A

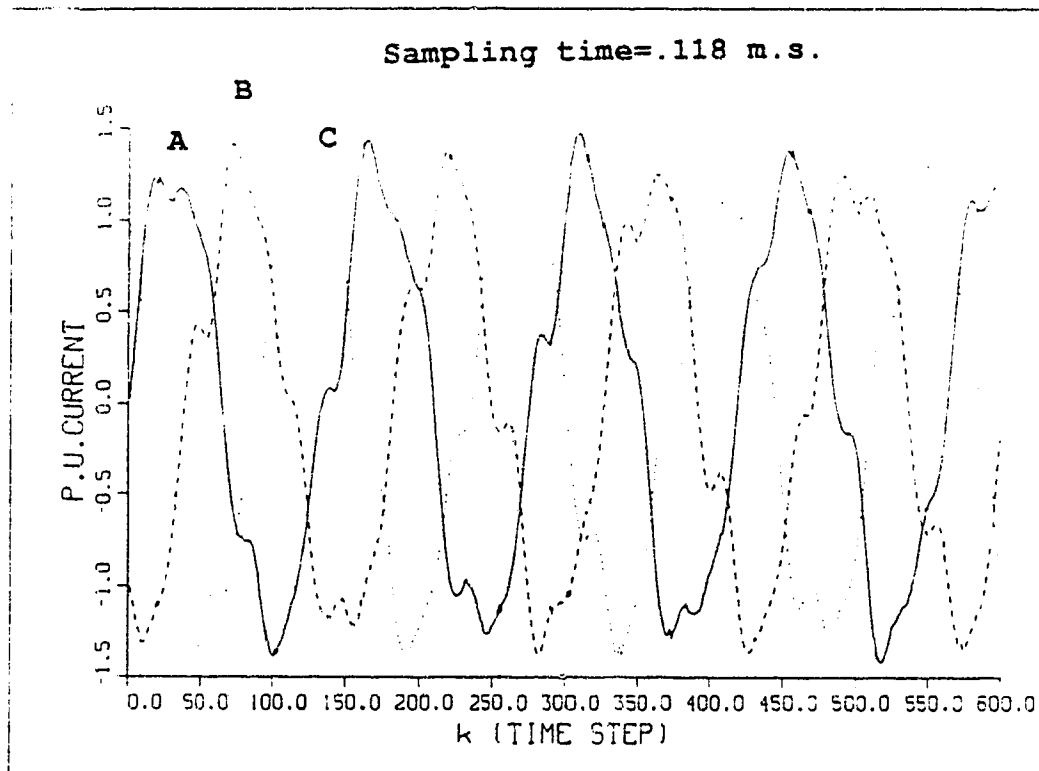


Fig. 4.30 Actual recorded phase currents

waveform of phase A. It is almost sinusoidal, and hence it contains nearly no harmonics. The three phase currents in figure (4.30) show a high harmonics level in each. It is clear that the currents have variable magnitudes from one cycle to another (nonstationary waveforms).

In this section a comparison between the three algorithms is made as they deal with nonstationary waveforms, first between the DFT and the LS, and then between the LAV and the LS.

4.3.1: Comparison between the DFT and the LS

Here the two algorithms are compared to each other when estimating the harmonic content of the waveforms in figures (4.29) and (4.30). The effects of the data window size, the sampling frequency, the number of harmonics considered and the bad data presence are examined.

First with the sampling rate = 8474.57 Hz and for one complete cycle the harmonic content, up to 23 harmonics, of the voltage and the currents is obtained. The line spectrum for the voltage V_A is shown in figure (4.31) while the phase angles of these harmonics voltages are given in figure (4.32). It is clear that the voltage waveform is almost sinusoidal where the total harmonic distortion factor was found to be about 1.9 % with the fundamental voltage of 1.707 per unit. Figure (4.33) gives the harmonic content of the current I_A while figure (4.34) shows the corresponding phase angles of these harmonics. The distortion factor for I_A was found to be about 13.66 % and 13.53 % while the fundamental current was 1.27 and 1.33 per unit using the LS

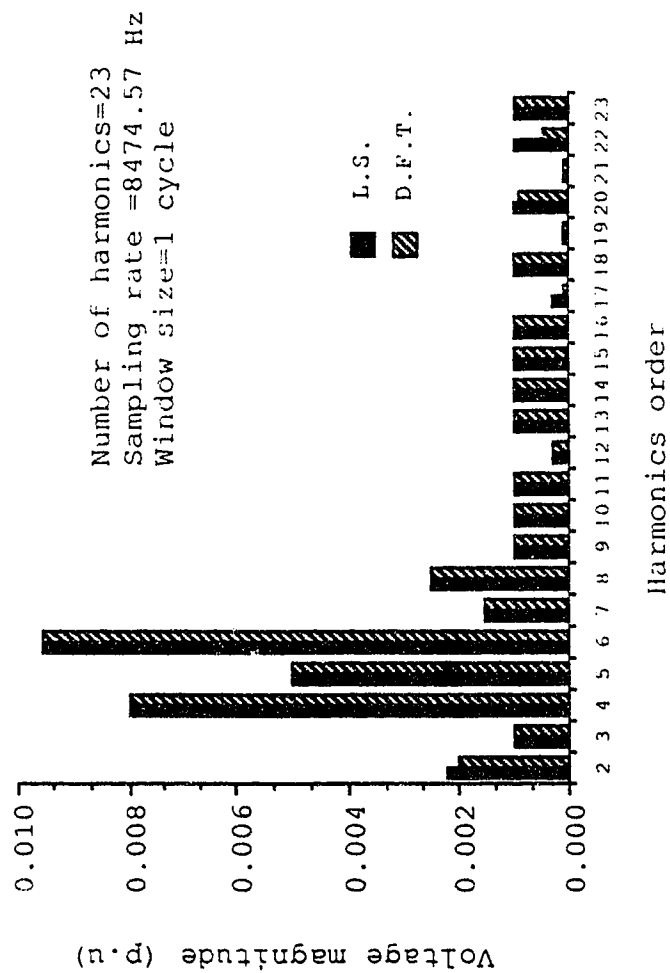


Fig. 4.31 Line spectrum for the voltage V_A

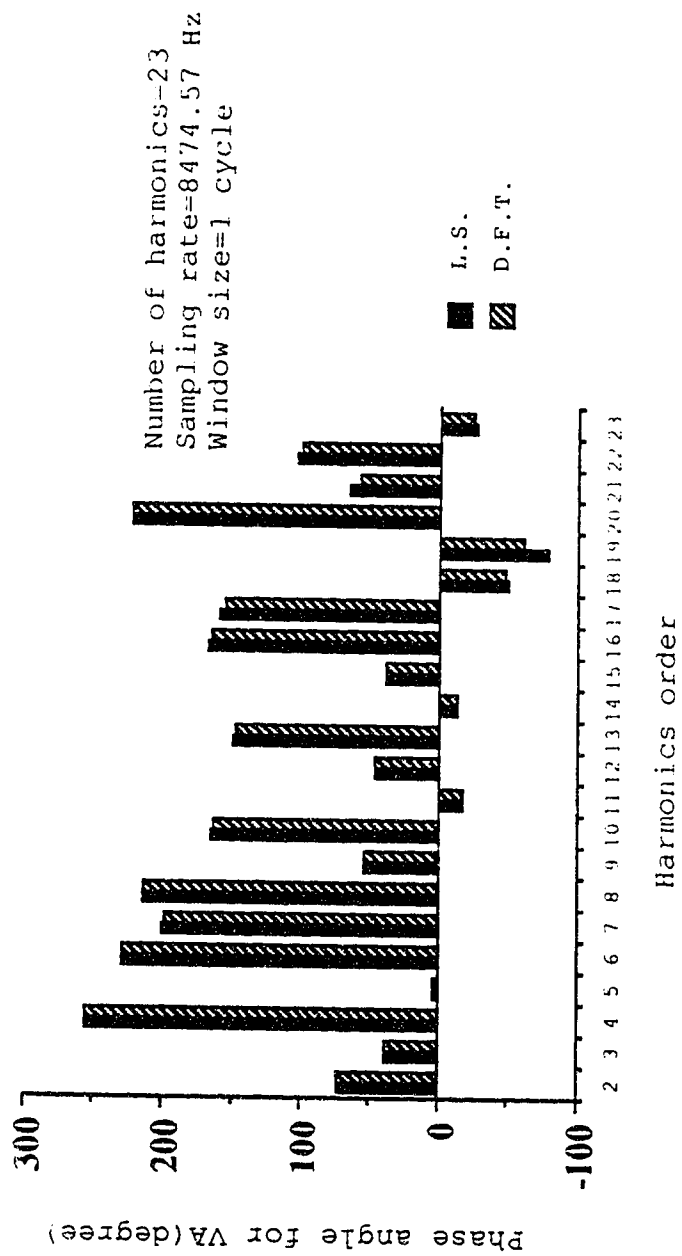


Fig. 4.32 Phase angles for V_A

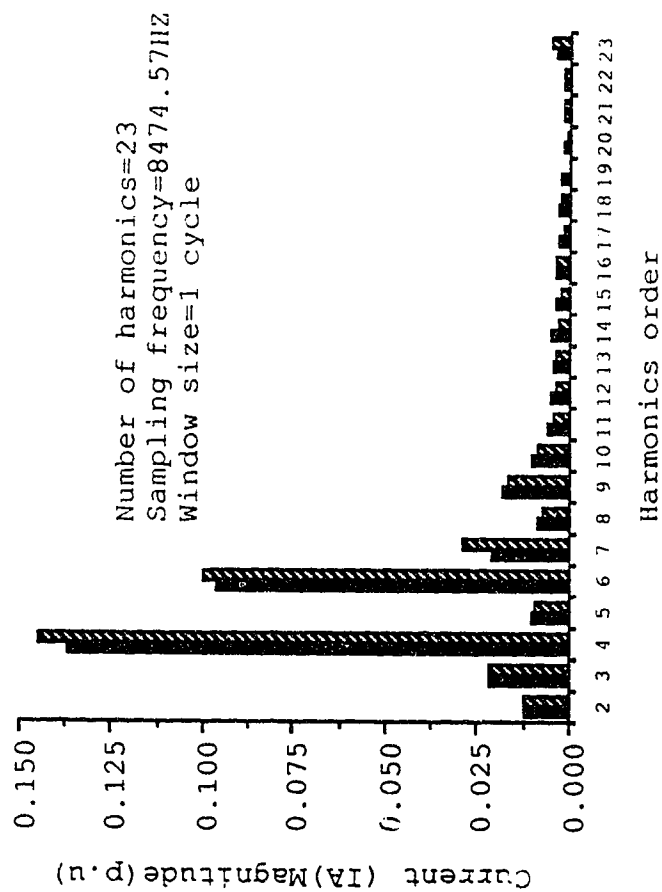


Fig. 4.33 Line spectrum for I_A

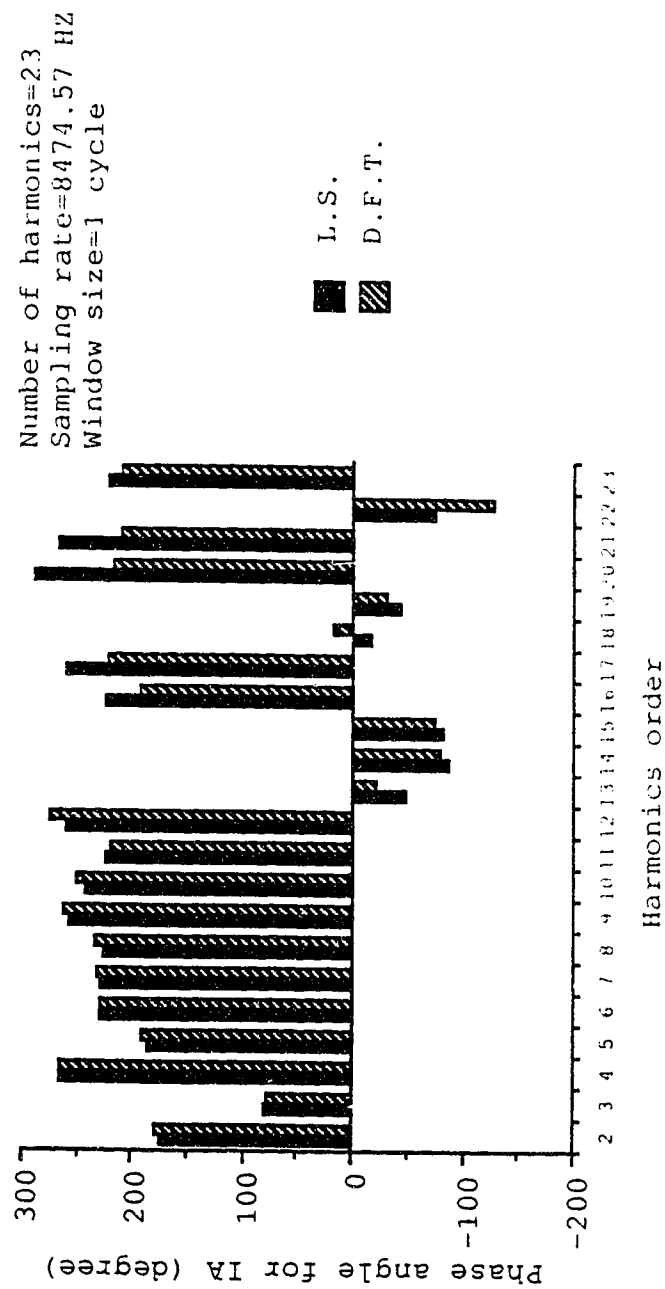


Fig. 4.34 Phase angles for I A

and the DFT techniques respectively. The harmonic power for phase A is shown in figure (4.35). Figures (4.30) to (4.35) indicate that both the DFT and the LS techniques give, almost, the same results with a small difference some times.

Effects of number of harmonics

The algorithms were tested for a different number of harmonics considered in the voltage and the currents waveforms, the number of harmonics is chosen to be 7, 15, 23 and 30 harmonics. The test was performed for a sampling frequency of 8474.57 Hz and a data window size of 2 cycles. Figures (4.36), (4.37) and (4.38) give samples of the results obtained. Examining those curves reveals that both the DFT and the LS algorithms produce a constant estimate with a variable number of harmonics considered. The magnitudes and the phase angles of the most significant harmonics in I_A are shown in figures (4.36) and (4.37) while figure (4.38) gives the harmonic power of those harmonics which is also constant independent on the number of harmonics considered.

Effects of sampling frequency

The algorithms were tested at different sampling frequencies of 2118.644, 2824.86, 4237.2881 and 8474.57 Hz. The test was performed for 23 harmonics and data window size of 2 cycles. As a sample of the results obtained, figures (4.39) and (4.40) are given to show the variations of the harmonics magnitudes and phase angles of the current I_A with the sampling frequency. Figure (4.41) gives the

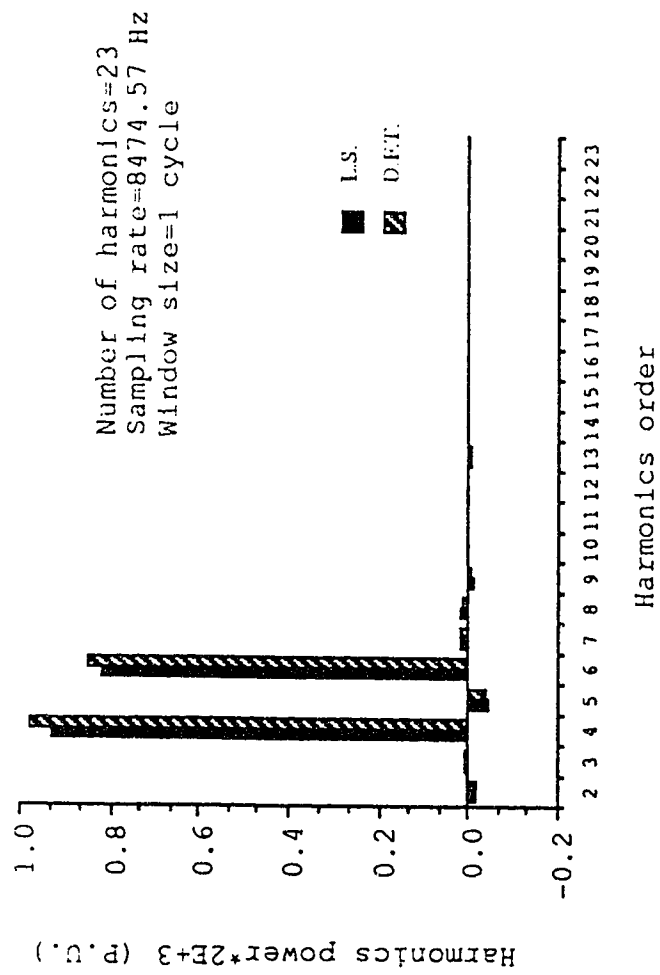


Fig. 4.35 Harmonics power for phase A

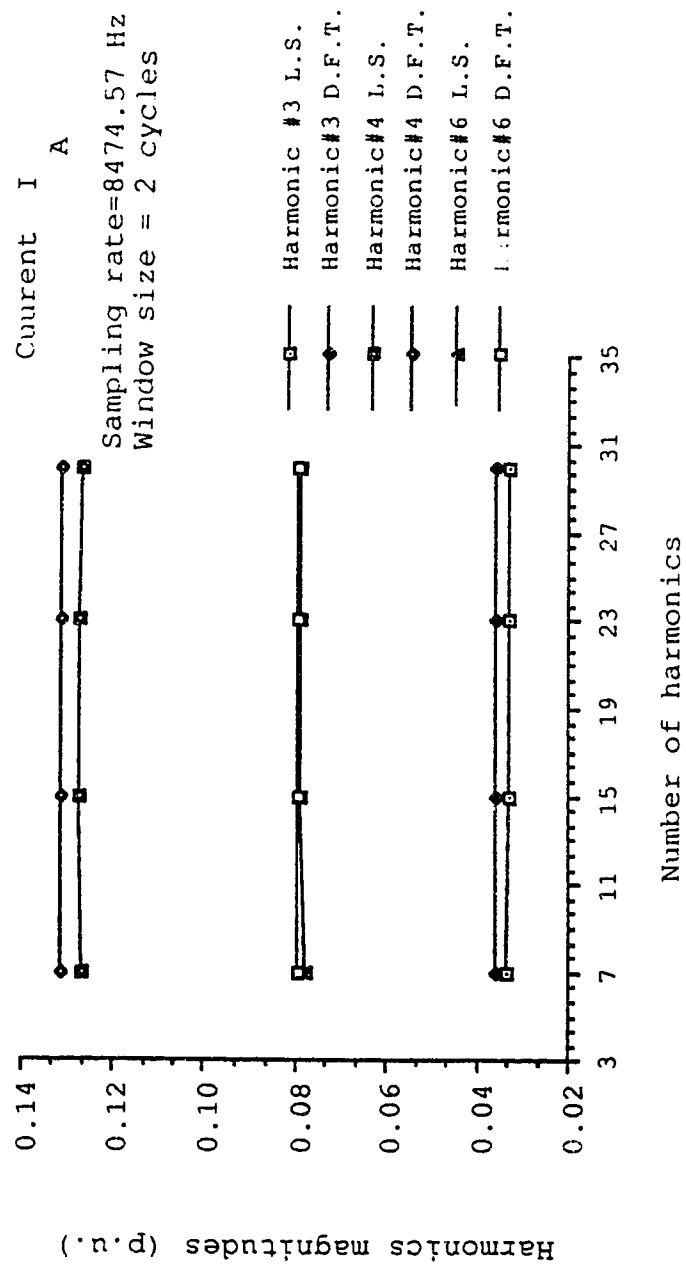


Fig. 4.36 Variations of harmonics magnitudes with the number of harmonics

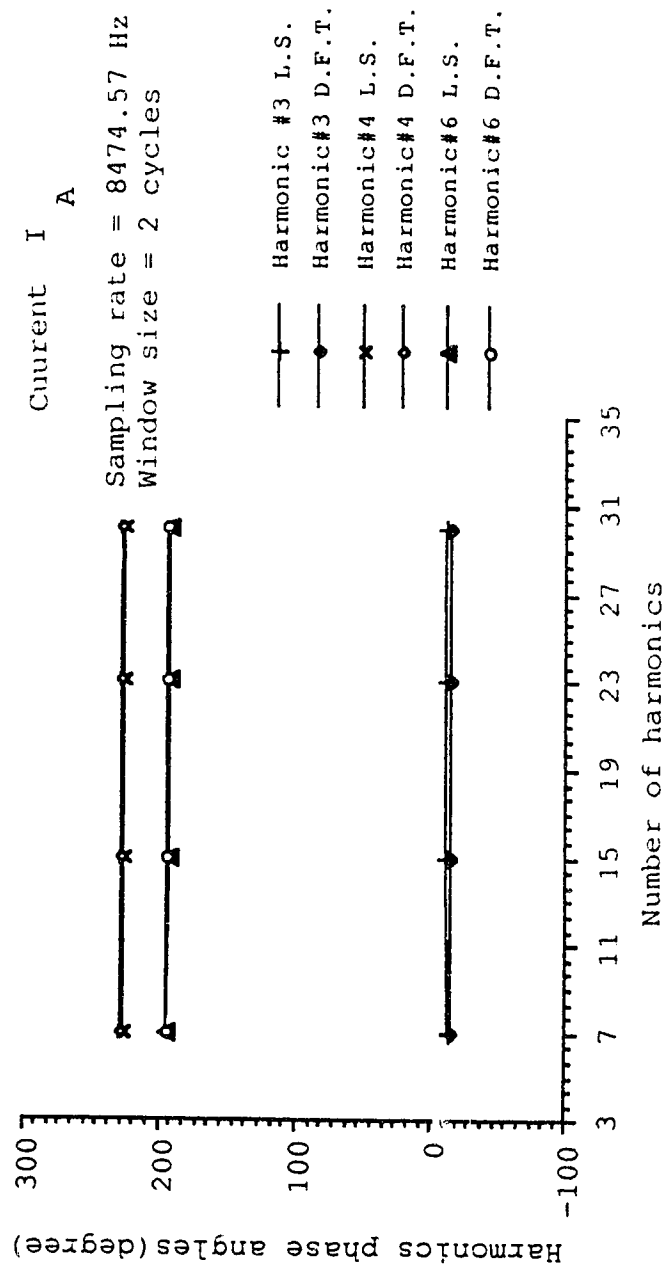


Fig. 4.37 Variations of harmonics phase angles with the number of harmonics

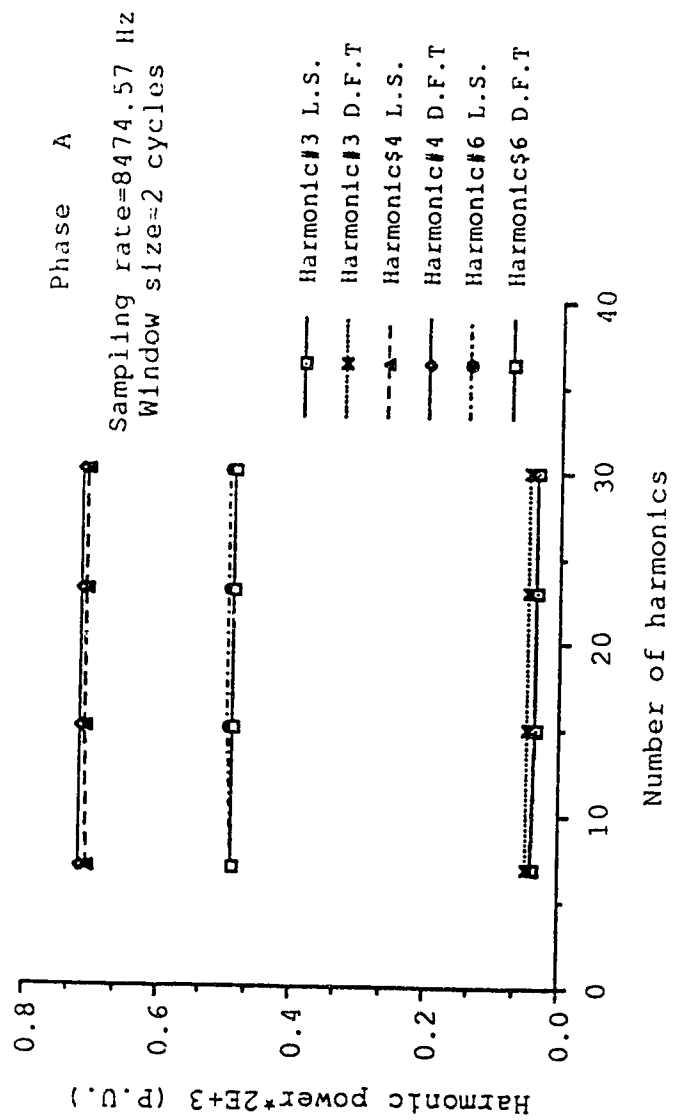


Fig. 4.38 Variations of harmonics power with the number of harmonics

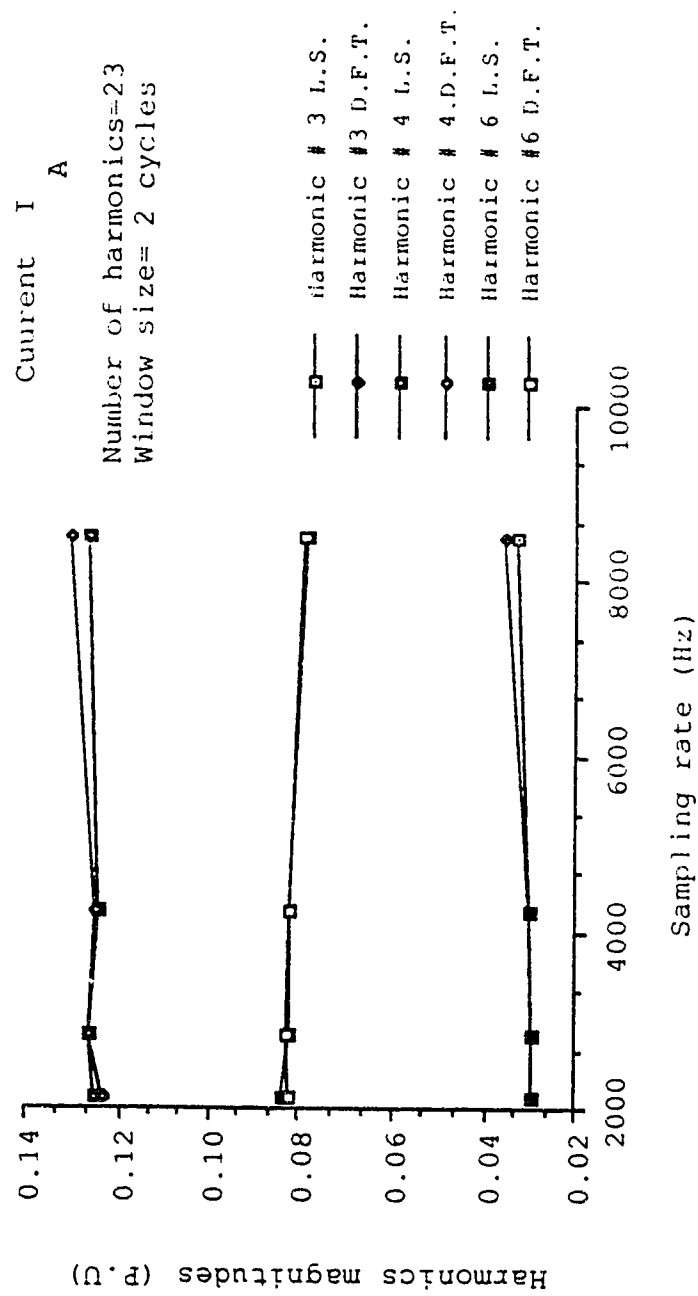


Fig. 4.39 Variations of harmonics magnitudes with sampling rate

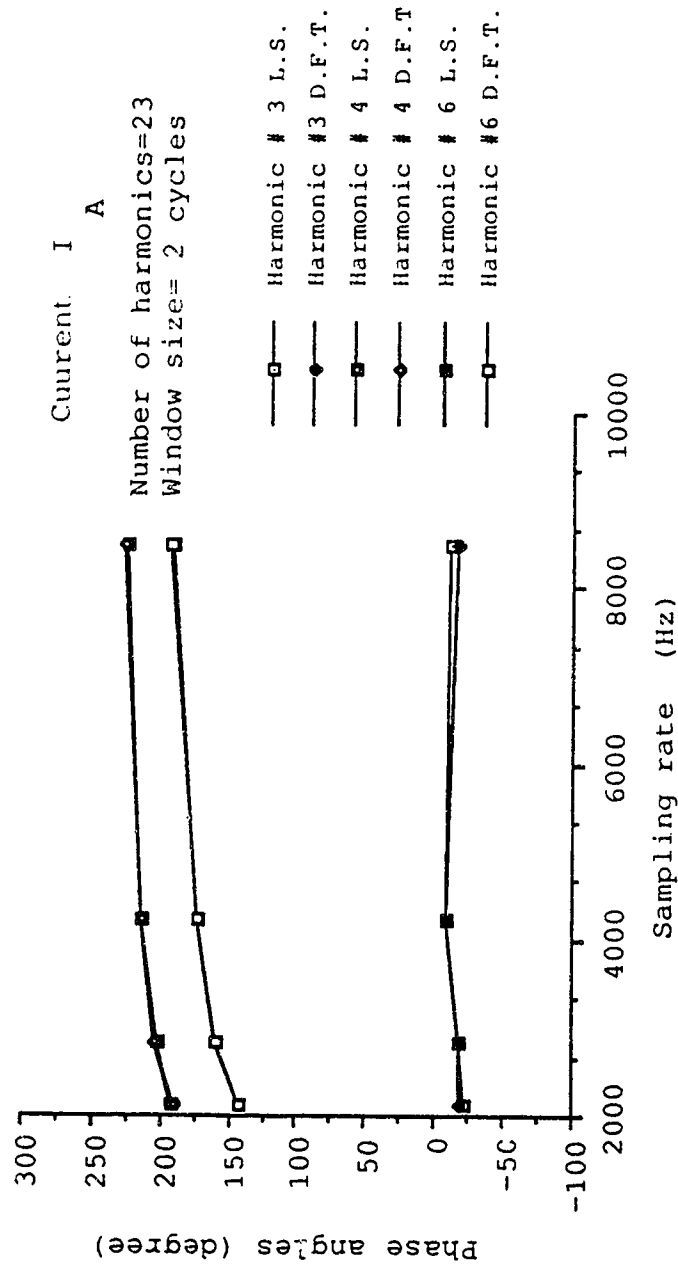


Fig. 4.40 Variations of harmonics phase angles with Sampling rate

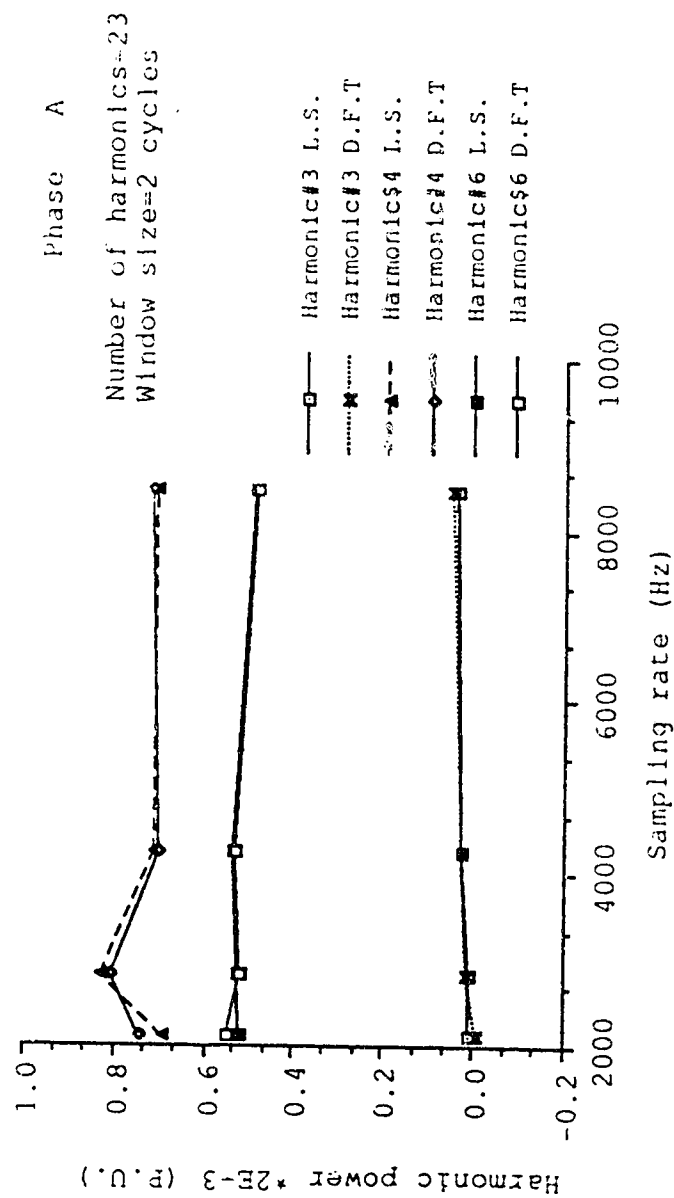


Fig. 4.41 Variations of harmonics power with sampling rate

harmonics power variations with the sampling frequency as well. Examining those figures reveals that the DFT as well as the LS algorithm produces the same estimate for the harmonics magnitude, phase angle and harmonics power regardless of what the sampling frequency is. Of course increasing the sampling frequency gives more accurate results and it was found that after about 4000 Hz the estimates, for both techniques, are nearly constant.

Effects of data window size

The effects of varying the data window size was examined and a sample of the results obtained is given here when the sampling frequency is 8474.57 Hz and 23 harmonics are considered. The data window size is chosen to be 1, 2, 3 and 4 cycles. Figures (4.42) and (4.43) give the harmonic magnitudes and the phase angles for the current I_A . The harmonic power variations with the data window size are shown in figure (4.44). These curves show that both algorithms produce the same estimate but, the harmonics magnitudes, phase angles and the harmonic power are not constant, they vary from one cycle to another. Indeed, this is due to the nature of the waveforms considered (nonstationary).

Effects of bad data

Both algorithms were tested when the measurement set was contaminated with bad data points. Two bad data points were chosen randomly, where the signs of the two measurements were inverted. Figures (4.45) and (4.46) give the results obtained for the magnitude

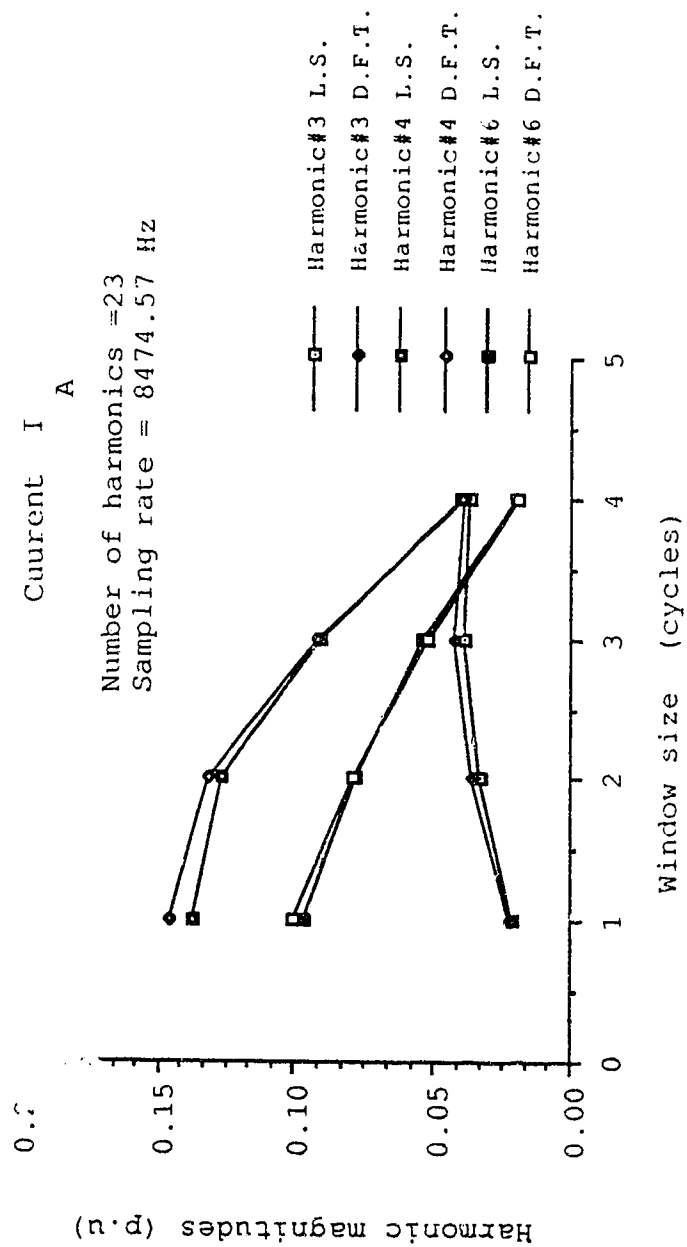


Fig. 4.42 Variations of harmonics magnitudes with the data window size

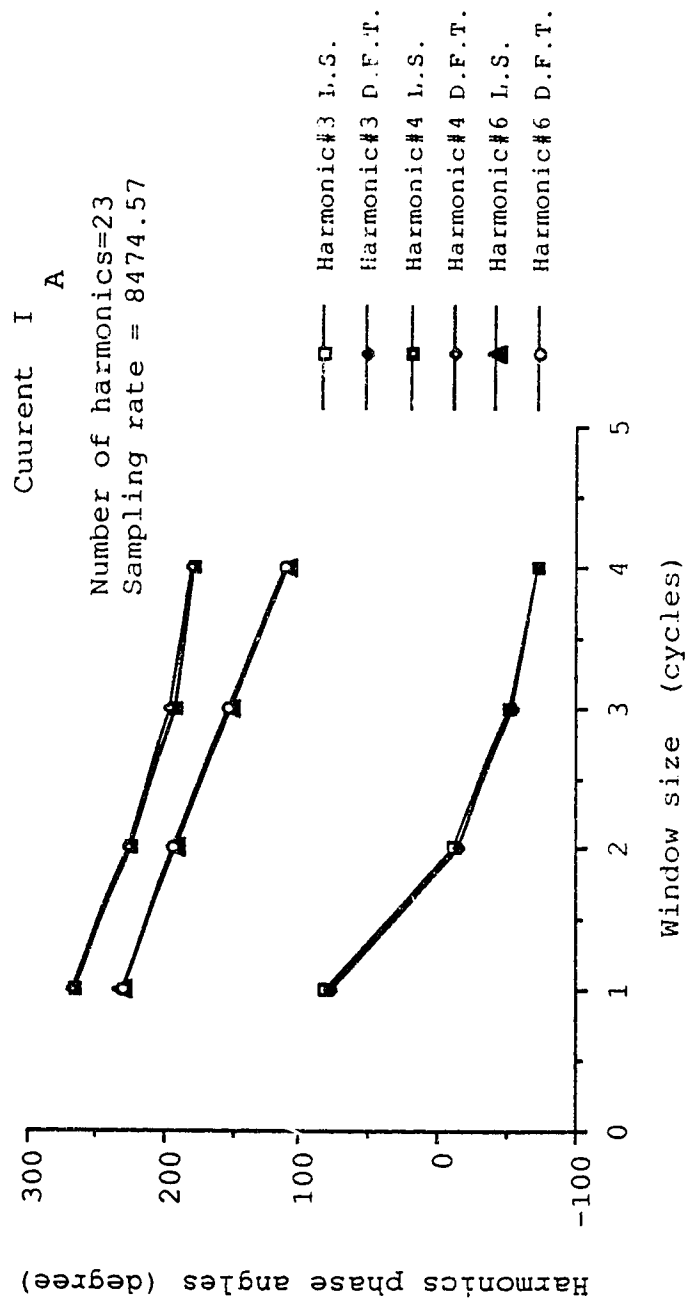


Fig. 4.43 Variations of harmonics magnitudes with the data window size

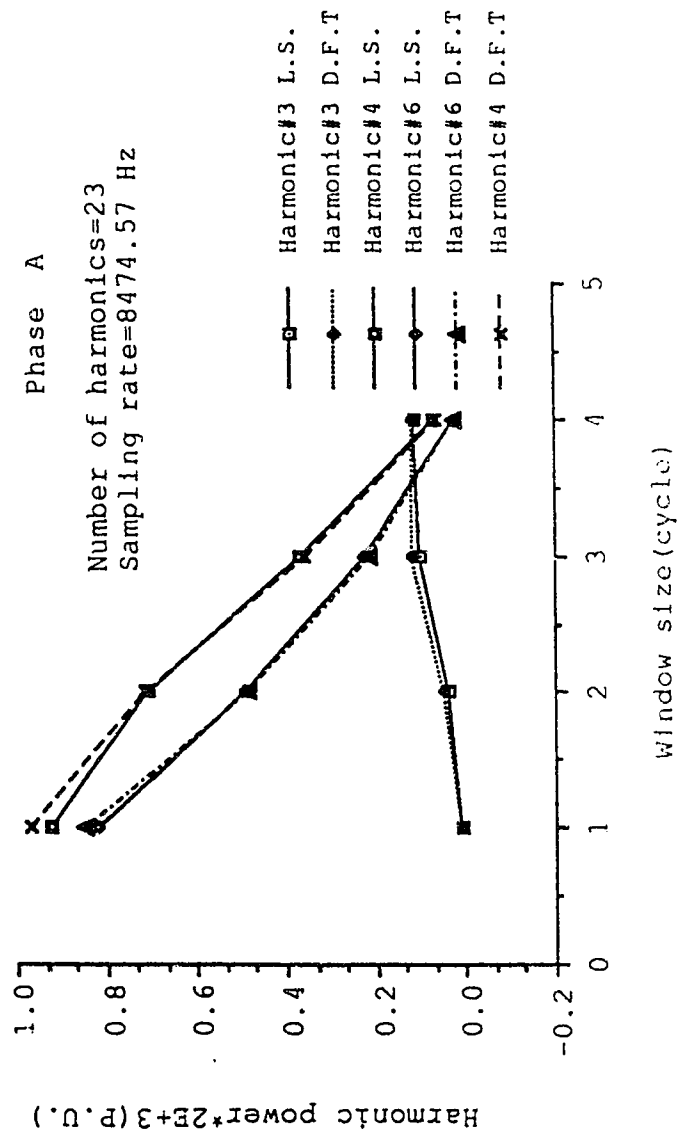


Fig. 4.44 Variation of harmonics power with the data window size

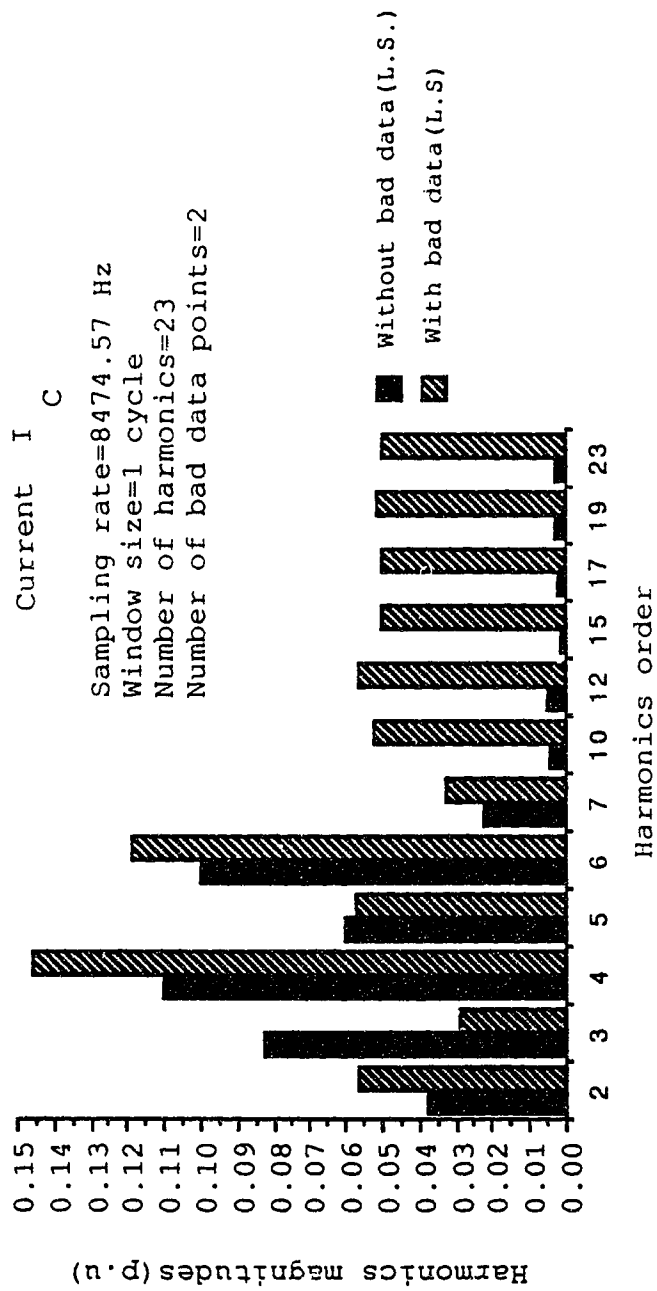


Fig. 4.45 The effects of the bad data on the harmonics magnitudes

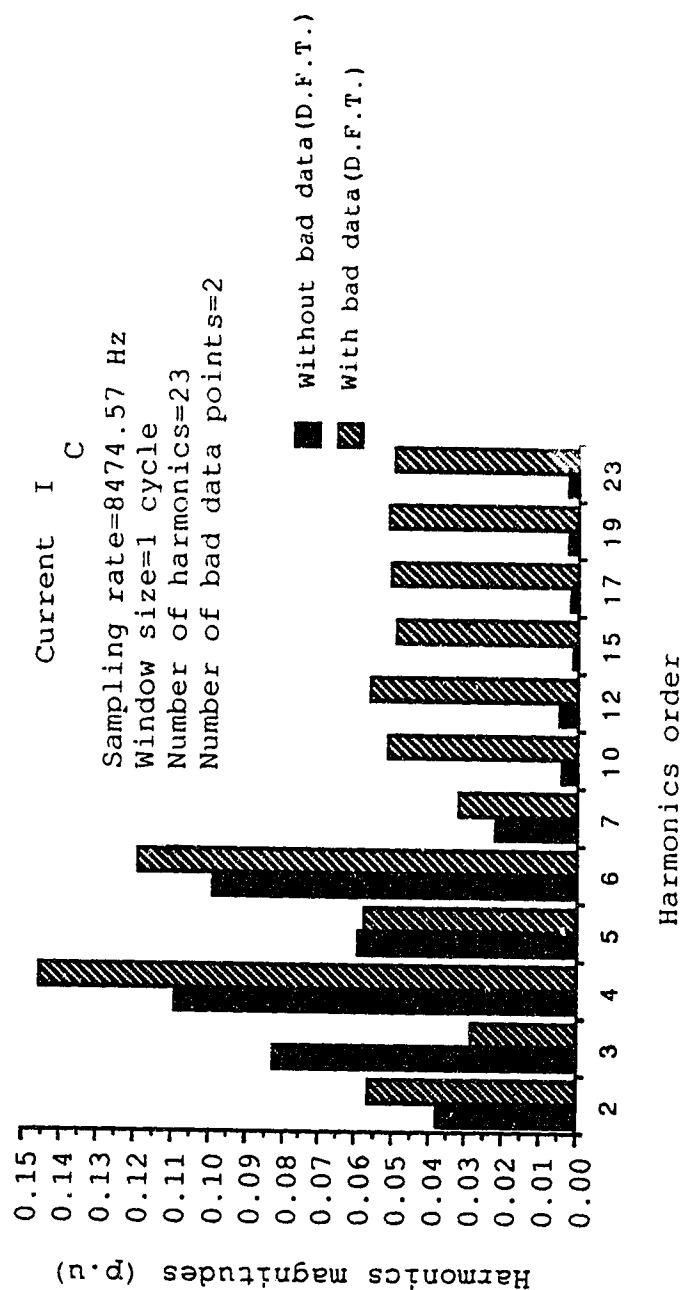


Fig. 4.46 The effects of the bad data on the harmonics magnitudes

of the current I_c when the LS and the DFT techniques are used, it can be noticed, from these figures, that both techniques produce the same poor estimates.

At the end of this comparison some important points should be mentioned here. These points can be summarized as:

1. The DFT and the LS techniques produce a good estimate when used with a reasonable sampling frequency and number of harmonics.
2. The effect of the data window size is important when dealing with nonstationary waveforms, extensive runs showed that increasing the data window size, in this case, gives a poor estimate and both algorithms started to act as smoothing filters and ended up with a false harmonics estimate as the data window size increases. Figure (4.47) shows that if only one cycle is considered, as a window size, the reconstructed current is very close to the given one for the first cycle but, after that the reconstructed, estimated, wave stays the same while the actual current is changing from cycle to another. If 4 cycles are considered, as a window size, a large error occurs and the reconstructed wave becomes nearly sinusoidal as shown in figure (4.48). The only way to overcome this problem is to solve for each set of measurements, corresponding to each cycle, separately. In this way the harmonics content of each cycle can be correctly estimated. This is shown in figure (4.49), a very good estimate is obtained when each cycle is considered separately.

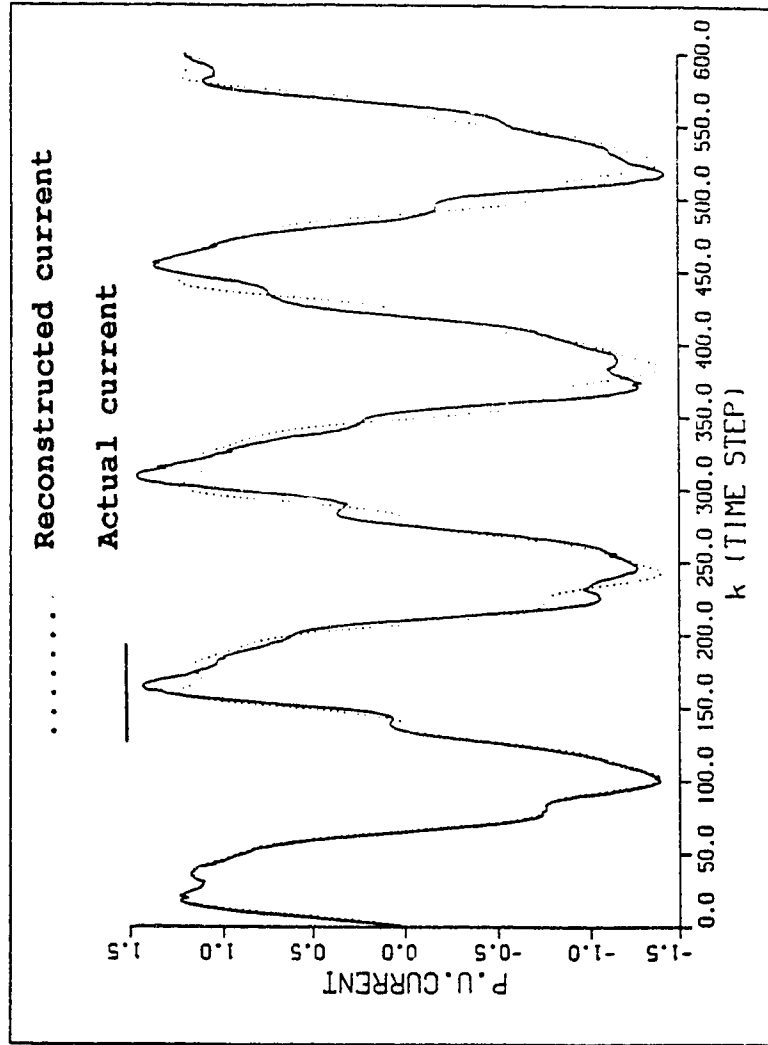


Fig. 4.47 Actual and reconstructed current for phase A
Window size=1 cycle

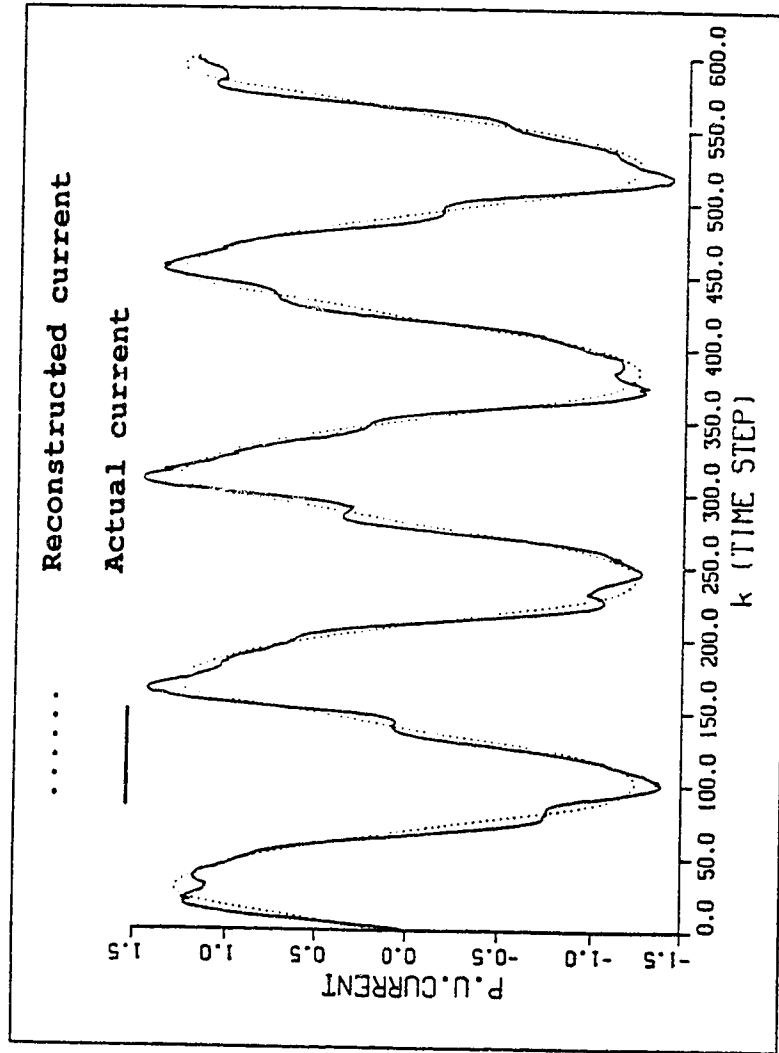


Fig. 4.48 Actual and reconstructed current for phase A

Window size=4 cycles

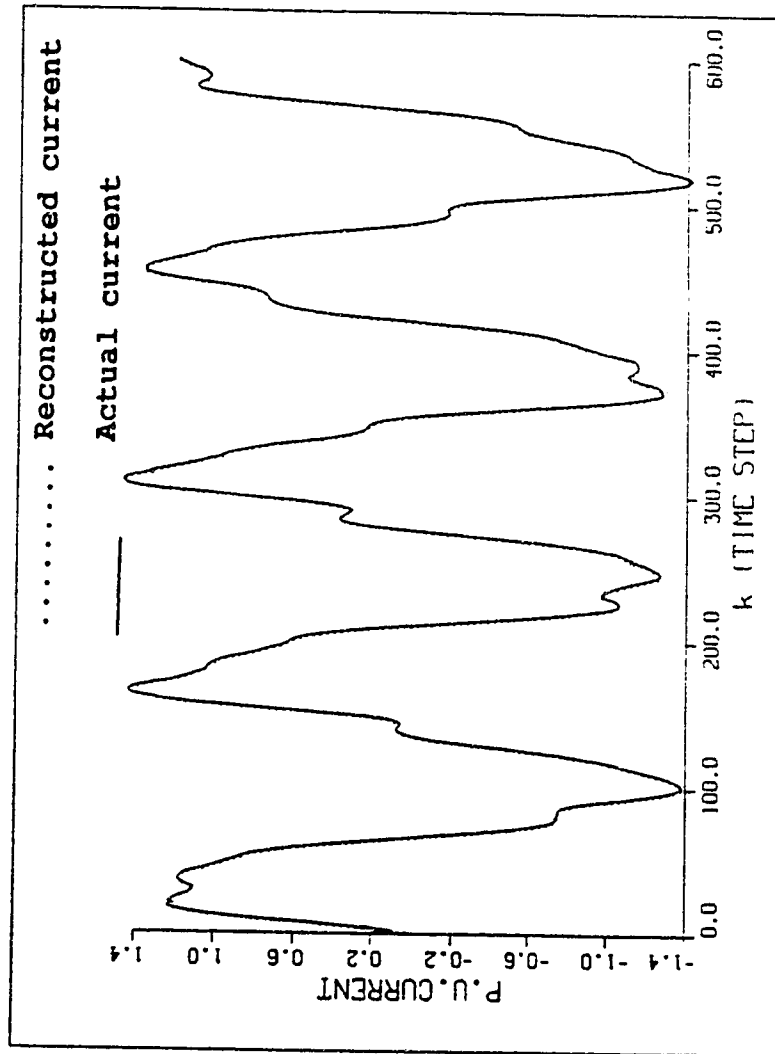


Fig. 4.49 Actual and reconstructed current considering each cycle separately

3. The DFT algorithm is much faster in producing the estimate than the LS algorithm.

4. Both algorithms are sensitive to the presence of the bad data points in the set of the measurements.

4.3.2: Comparison between the LAV and the LS techniques

The main objective of this comparison is to show that both algorithms produce, nearly, the same estimation if the set of measurement is free of bad data, but if the set of measurement is contaminated with bad data then, the LAV algorithm will reject those points automatically and produces a better estimate than that produced by the LS. In this part samples of the results obtained are presented.

At this stage the LAV algorithm, together with the LS, are used for identifying the harmonic content of the voltage and current waveforms. Once this has been done the harmonics power can be calculated and hence, the harmonic sources can be identified. In this test 15 harmonics are considered and a data window size of one cycle is used with sampling frequency of 8474.57 Hz. Figures (4.50), (4.51), (4.52) and (4.53) give a sample of the results obtained for phase B. Figure (4.50) gives the line spectrum of harmonic magnitude of the current of phase B, while figure (4.51) gives the phase angles of these harmonics. The total distortion factor for the current was found to be about 15.9% and 16.2% with the fundamental current of 1.243 and 1.238 per unit using the LS and the LAV techniques

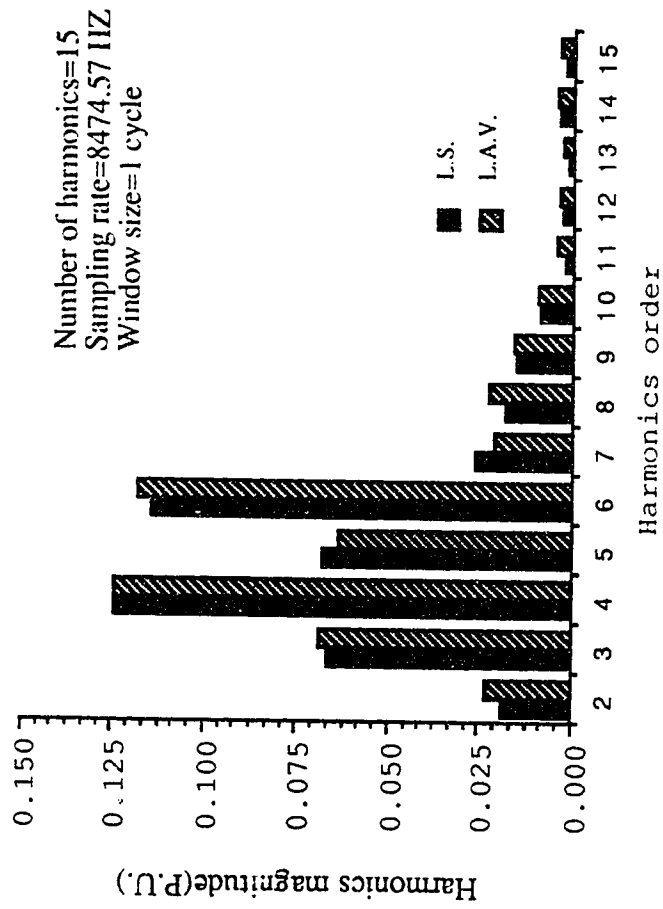


Fig. 4.50 Line spectrum for I B

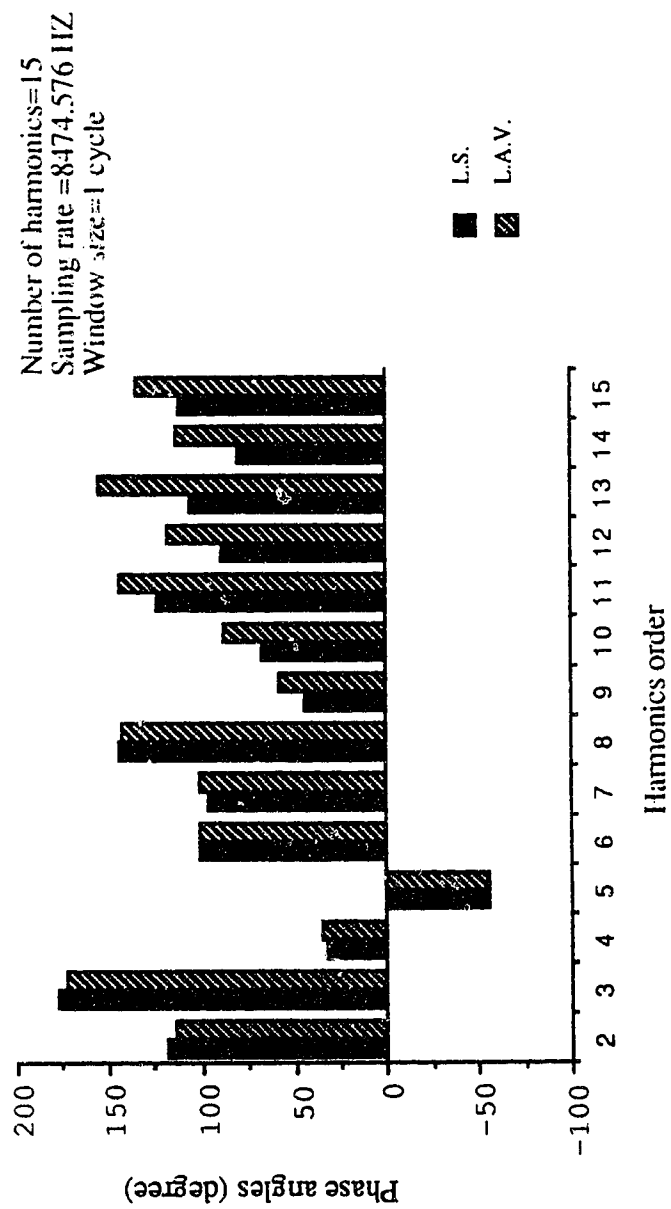


Fig. 4.51 Phase angles for I B

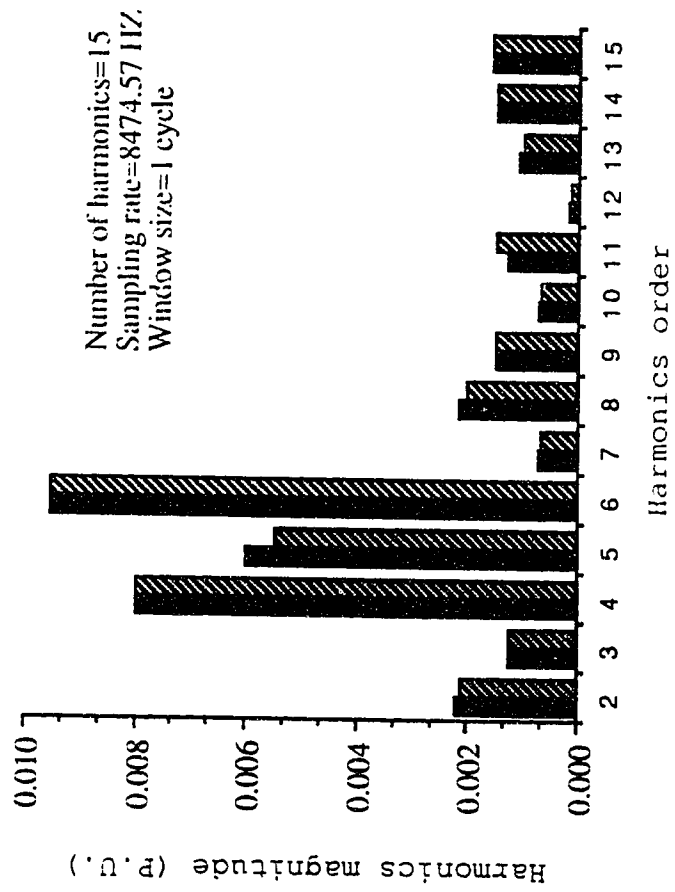


Fig. 4.52 Line spectrum for V B

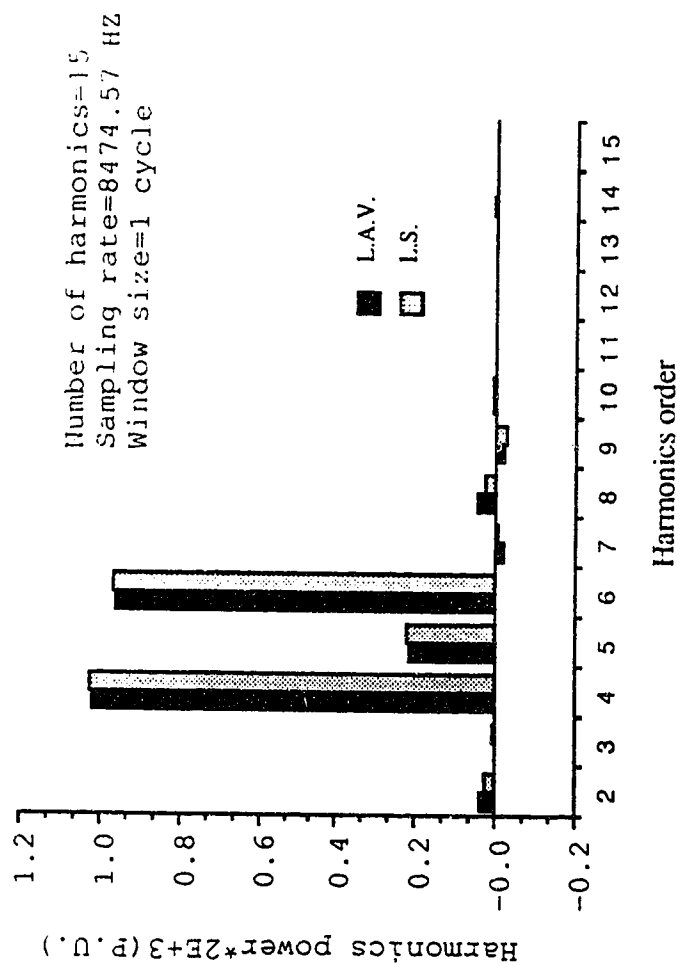


Fig. 4.53 Harmonics power for phase B B

respectively. Figure (4.52) gives the line spectrum of the harmonic magnitude in the voltage of phase B. The distortion factor was found to be about 1.9% with the fundamental voltage of 1.706 per unit using both techniques. Furthermore figure (4.53) gives the harmonics power of phase B. Examining these curves reveals that the current of phase B contains, besides the fundamental, the second, the third,...and the tenth harmonics, and after the tenth harmonic the magnitudes of the harmonics become very small and can be neglected. It is clear that the most effective harmonics in the current I_B are harmonics number 4, 6, 3 and 5 respectively. The proposed algorithm gives results as good as the least squares algorithm for harmonics magnitudes estimates, while it gives different results than the least squares for the phase angles estimates starting from the ninth harmonic. The voltage of phase B contains harmonics of the same order as the current, but the magnitudes are very small except for the fourth and the sixth, which have considerable magnitudes. Finally for this case harmonics number 4 and 6 can be considered as harmonic sources, since they produce positive power. Indeed, this bus can now be considered as a harmonics bus.

In the next part, we discuss different factors that have great influence on the performance of the LAV algorithm, namely the data window size, the sampling frequency and the number of harmonics considered.

Number of harmonics

The LAV algorithm is tested, together with the LS, with a

different number of harmonics, starting from 11 up to 23 , with a data window size of 1 cycle and a sampling frequency of 8474.57 Hz. Figures (4.54), (4.55) and (4.56) give the harmonics magnitudes, the phase angles and the power estimate variations of the third, fourth and sixth harmonic with the number of harmonics for phase B when both LAV and LS techniques are applied. Examining these curves shows that the variation of the number of harmonics considered has a slight effect on the estimate, it can be noticed also that both the LAV and the LS algorithms give the same results.

Sampling frequency

Effects of sampling frequency on the behavior of the LAV algorithm are studied here. One cycle is considered to estimate 15 harmonics while the sampling frequency is chosen to be 2118.64, 2824.86, 4237.28 and 8474.56 Hz. Figures (4.57) and (4.58) show a sample of the results obtained for phase B. In figure (4.57) the harmonics magnitudes have a constant value for the third and fourth harmonics, but for the sixth harmonic the magnitude changed slightly with the sampling frequency. Figure (4.58) shows the harmonics power variations with the sampling frequency. These curves indicate that the sampling frequency has a slight effect on the estimates, providing that the sampling frequency satisfies the sampling theorem. It is obvious that increasing the sampling rate gives better results since, most estimates started to reach a constant value after about 4237 Hz.

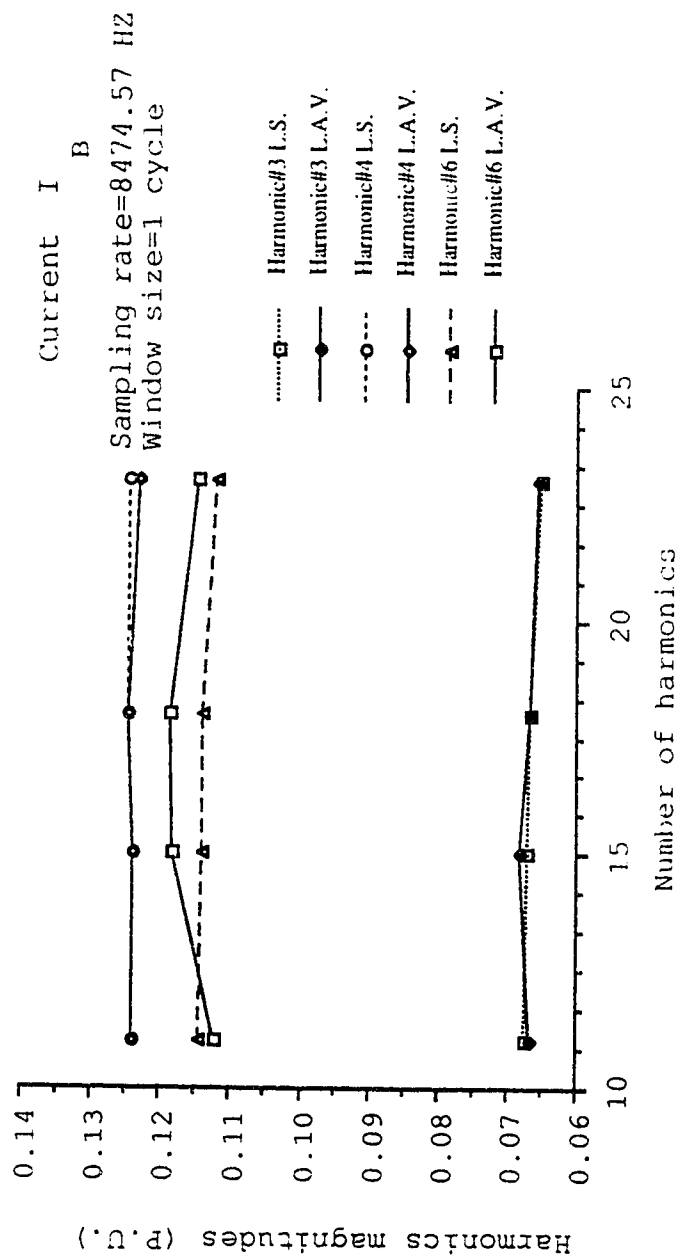


Fig. 4.54 Variations of harmonics magnitudes with the number of harmonics

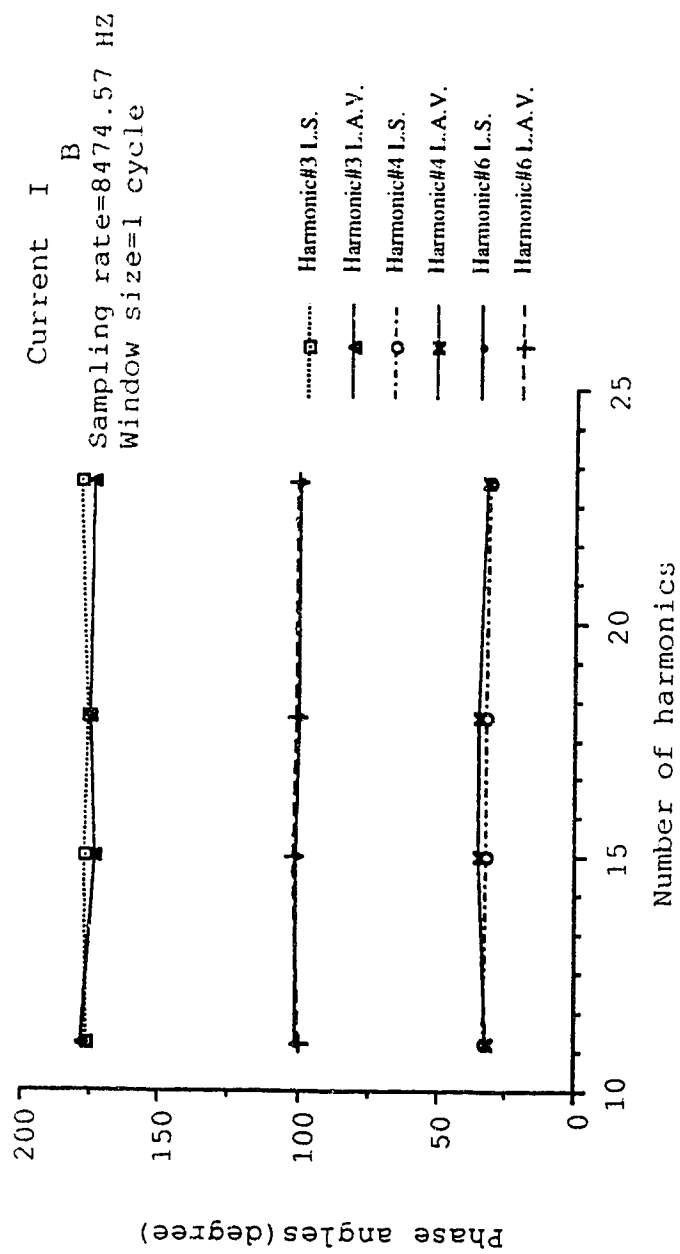


Fig. 4.55 Variation of harmonics phase angles with the number of harmonics

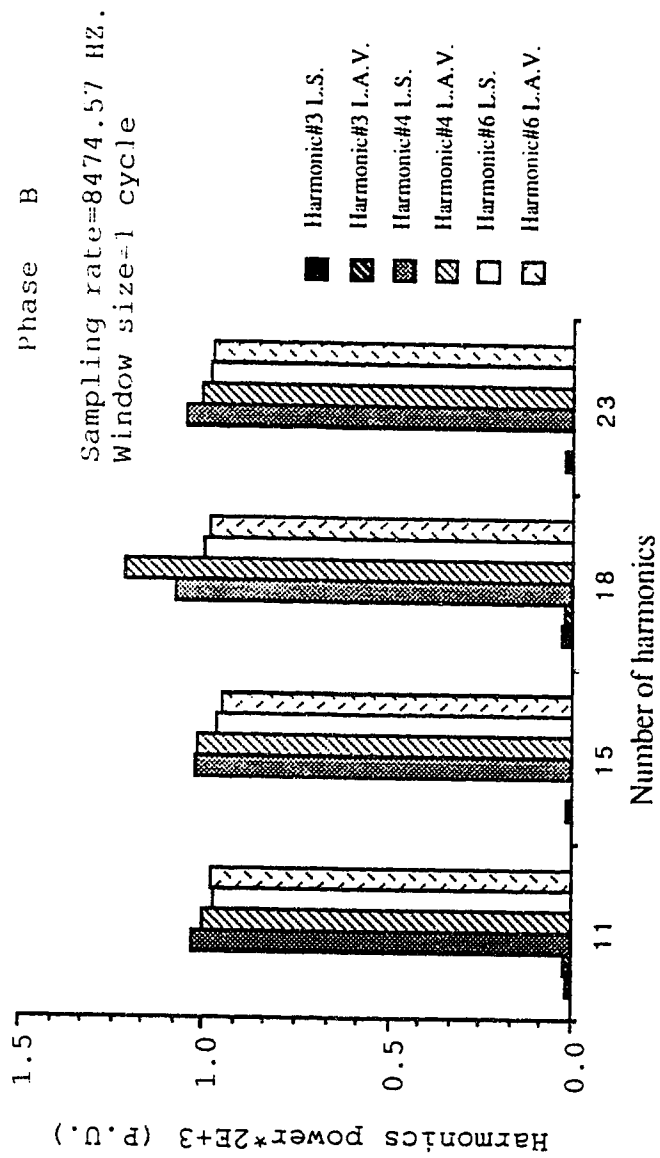


Fig. 4.56 Variations of harmonics power with the number of harmonics

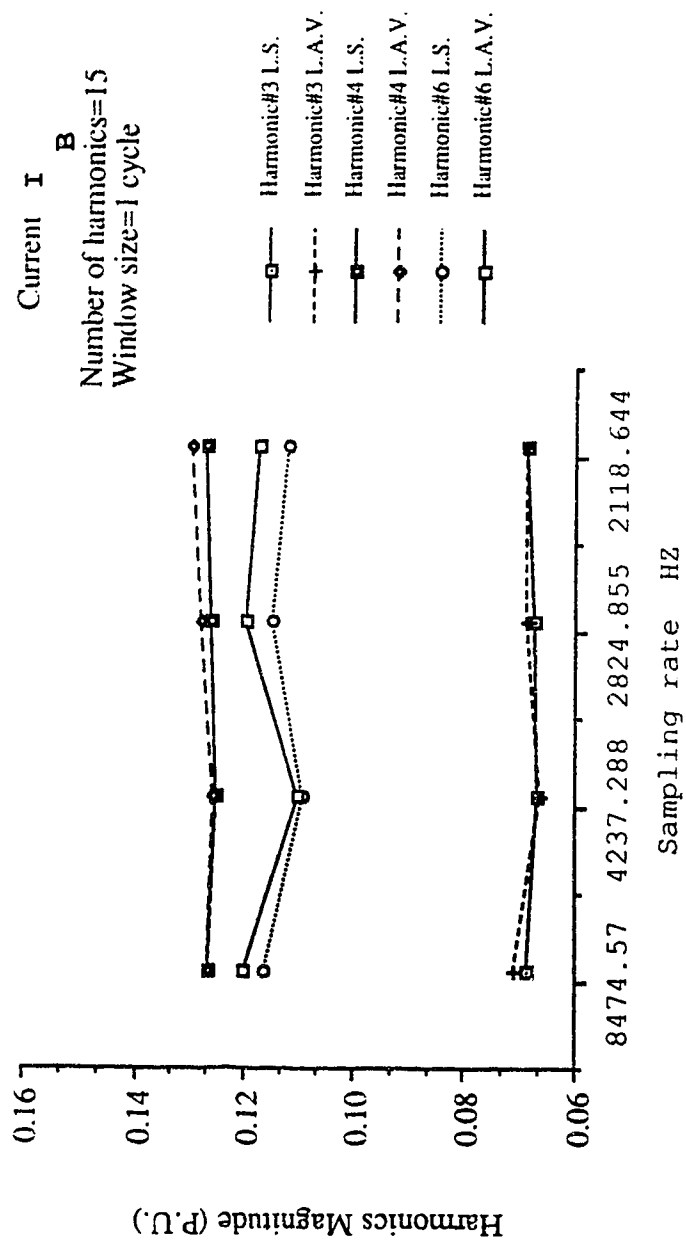


Fig. 4.57 Variations of harmonics magnitudes with the sampling rate

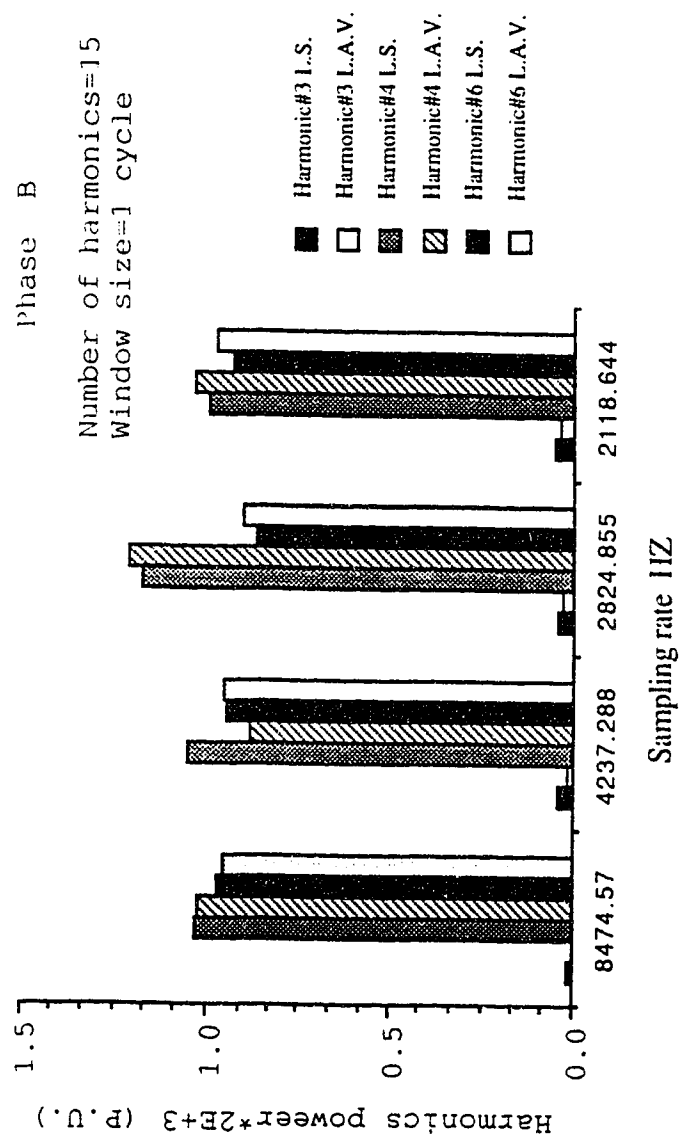


Fig. 4.58 Variations of harmonics power with the sampling rate

Data window size

The LAV algorithm is tested, together with the LS algorithm, for different window sizes between 1 and 4 cycles in steps of 1 cycle. The sampling frequency is chosen to be 8474.57 Hz and the number of harmonics considered is 15. Under this combination of parameters, the LAV algorithm is implemented to estimate the harmonics content of the three phase currents as well as the harmonics content of the three phase voltages and hence the harmonics power. Samples of the results for phase B are shown in figures (4.59) and (4.60). It can be noticed, from figures (4.59) and (4.60), that the harmonics magnitudes and the harmonics power vary as the data window size varies. This is due to the fact that the waveform of the phase current varies from cycle to the other, but as mentioned earlier the estimate is accurate only when each cycle is used separately to find the estimate for the harmonics content in that cycle. Again it is clear that the LAV algorithm gives results very close to those obtained using the LS algorithm specially for the one cycle case which is the most accurate case.

Bad data effects

The LAV algorithm is tested, together with the LS algorithm, to estimate the harmonics magnitudes and their phase angles when the data set is contaminated with bad data, the bad data points are chosen randomly. Figure (4.61) gives the effect of the bad data on the estimates of the harmonics magnitudes, when the number of harmonics considered is 23 and the data window size is 1 cycle, while the sampling rate is 8474.57 Hz. It can be noticed that the LAV produced

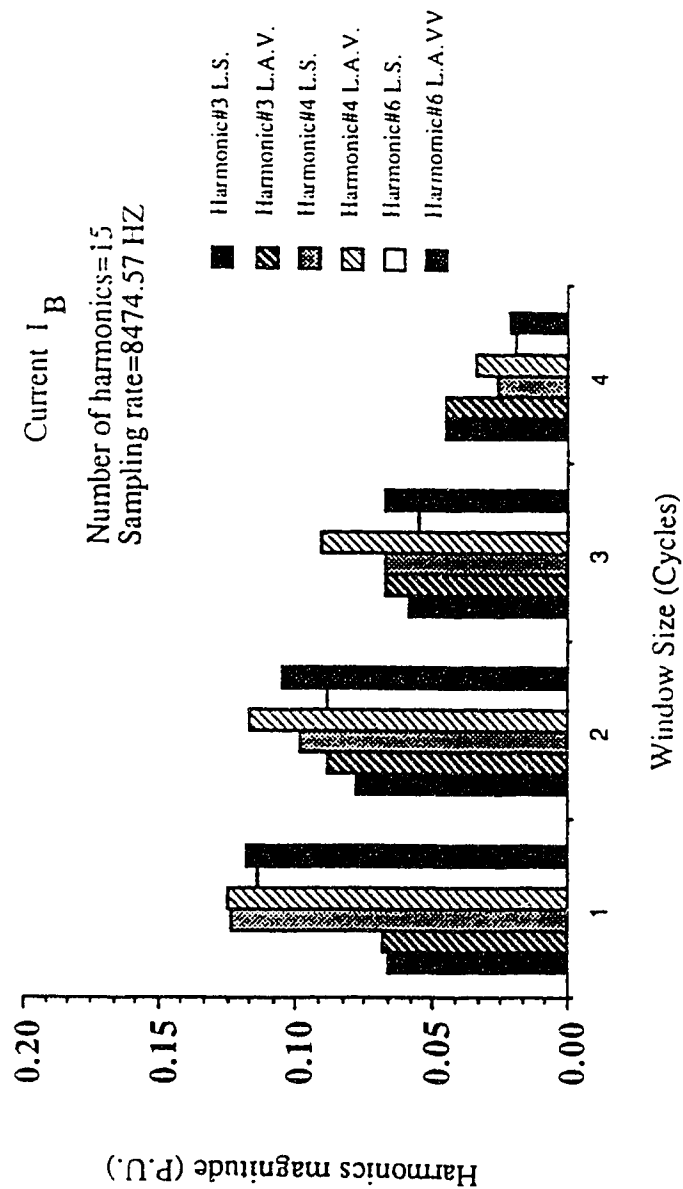


Fig. 4.59 Variations of harmonics Magnitude with the data window size

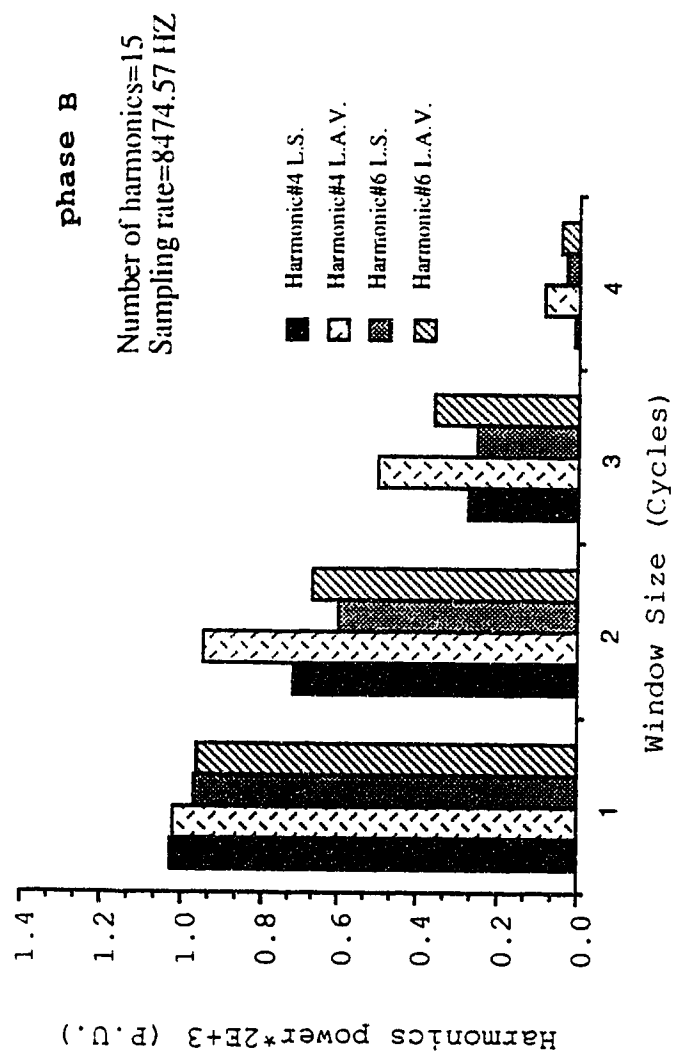


Fig. 60 Variations of harmonics power with the data window size

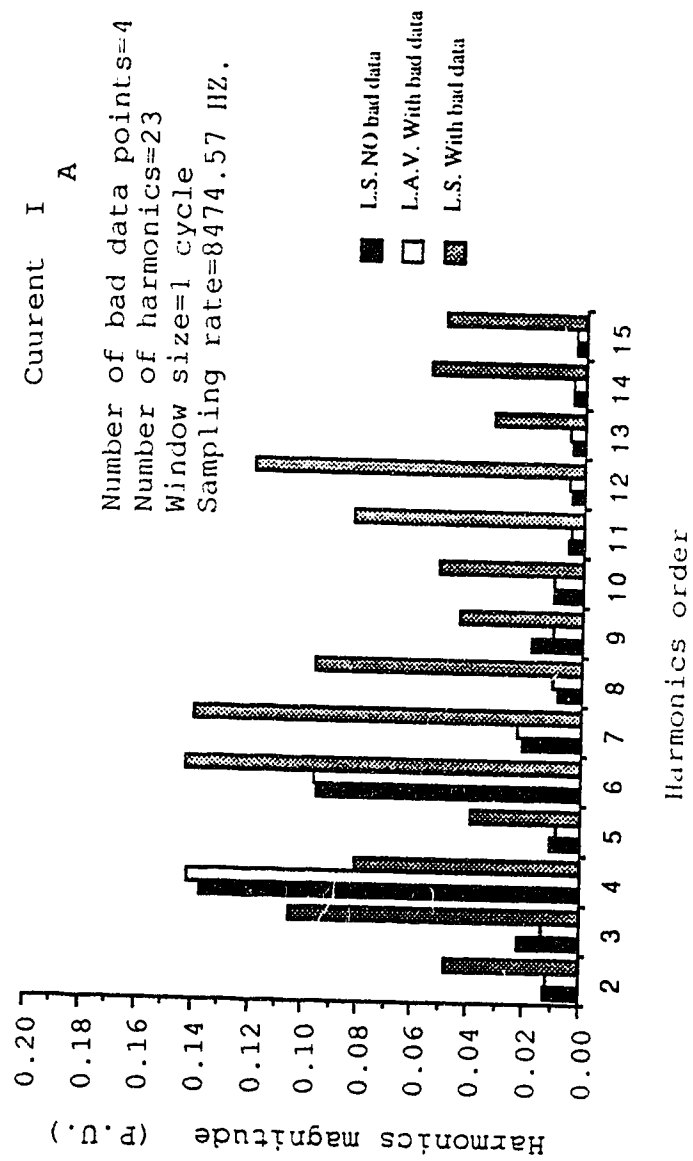


Fig. 4.61 Effect of bad data on harmonics magnitudes

good estimates, in contrast to the LS algorithm which produced poor estimates. Indeed, that is true, since the LS algorithm uses the entire set of measurements, while the LAV algorithm uses a number of measurements equal to the number of parameters to be estimated.

Conclusions

In this chapter the DFT, the LS and the LAV techniques were presented with applications in estimating the harmonics content of stationary and nonstationary waveforms. In the stationary case it was found that the three algorithms produce very close estimates if there is no bad data, but with bad data points the LAV algorithm has produced the best estimate by rejecting those bad points. In the nonstationary waveform case it has been found that in order to get a good estimates, each cycle of the data should be used by the algorithm separately.

CHAPTER V

PARAMETER ESTIMATION : THE DYNAMIC CASE

In this chapter, the parameter estimation techniques applicable to on-line harmonics identification are considered. The dynamic parameter estimation problem is first introduced followed by the theory and development of the Kalman and a newly developed least absolute value based filter.

The algorithms are tested, first, using a simulated example, then practical data is used. A comparison between the two algorithms will be provided as well.

5.1: Stochastic estimation

When a dynamic system is subjected to parameter variations that can not be specified ahead of time, then deterministic cost function of the type considered in chapter IV can not be minimized by the estimate. If, however, the statistics of these uncertain quantities are known, a similar cost function can be used. The literature indicates, that for a process where the error distribution is Gaussian, the expected value of the least error squares cost function results in optimal estimation. This is the well known Kalman filter [39,40]. In the case where the error distribution is non-Gaussian researchers have theorized that the least absolute value based filter would be better, but the inherent iterative nature of this technique has prevented the realization of such an estimator, the recent

development of a noniterative LAV static estimator lead to the formulation of a LAV based dynamic filter [41].

5.2: Dynamic estimation problem [39,40,42,43,44]

Given the discrete system described by the set of equations (3.49) as:

$$\Theta(k+1) = \Phi(k) \Theta(k) + \varepsilon(k) \quad (5.1)$$

$$z(k) = H(k) \Theta(k) + w(k) \quad (5.2)$$

It is assumed, at this point, that we have an initial estimate of the process at some point k , and that this estimate is based on all of our knowledge about the process prior to this instant. This estimate will be denoted as $\bar{\Theta}$ where the symbol $\bar{\cdot}$ means that this is the best estimate at this point, prior to assimilating the measurement at instant k . Then the error in this estimate can be written as:

$$\bar{e}(k) = \Theta(k) - \bar{\Theta}(k) \quad (5.3)$$

and the associated error covariance matrix will be

$$\bar{P}(k) = E \{ \bar{e}(k) \bar{e}^T(k) \} = E \{ [\Theta(k) - \bar{\Theta}(k)] [\Theta(k) - \bar{\Theta}(k)]^T \} \quad (5.4)$$

Next the estimate $\bar{\Theta}$ will be improved after considering the measurement $z(k)$ according to the following equation

$$\hat{\Theta}(k) = \bar{\Theta}(k) + K(k) [z(k) - H(k)\bar{\Theta}(k)] \quad (5.5)$$

where $\hat{\Theta}(k)$ is the updated estimate and $K(k)$ is the gain to be determined.

The error covariance matrix associated with this updated estimate can then be expressed as

$$P(k) = E\{e(k) e(k)^T\} = E\{[\Theta(k) - \hat{\Theta}(k)] [\Theta(k) - \hat{\Theta}(k)]^T\} \quad (5.6)$$

Substituting from (5.2) into (5.5) and then the resultant expression for $\hat{\Theta}(k)$ into equation (5.6), equation (5.7) can be written as

$$P(k) = E\{ [(\Theta(k) - \bar{\Theta}(k)) - K(k)(H(k)\Theta(k) + w(k) - H(k)\bar{\Theta}(k))] \\ [(\Theta(k) - \bar{\Theta}(k)) - K(k)(H(k)\Theta(k) + w(k) - H(k)\bar{\Theta}(k))]^T \} . \quad (5.7)$$

Performing this expectation gives

$$P(k) = (I - K(k)H(k)) \bar{P}(k) (I - K(k)H(k))^T + K(k)R(k)K(k)^T. \quad (5.8)$$

Now, before starting the next step, we need to project ahead both $\Theta(k)$ and $P(k)$ to use them as initial values for the next step, $(k+1)$.

The updated estimated $\hat{\Theta}(k)$ is easily projected ahead via the state transition matrix, $\Phi(k)$, according to the following relation

$$\bar{\Theta}(k+1) = \Phi(k) \hat{\Theta}(k) \quad (5.9)$$

The error associated with $\bar{\Theta}(k+1)$ will be

$$\begin{aligned} \bar{e}(k+1) &= \Theta(k+1) - \bar{\Theta}(k+1) \\ &= [\Phi(k)\Theta(k) + \varepsilon(k)] - \Phi(k)\hat{\Theta}(k) \\ &= \Phi(k)e(k) + \varepsilon(k) \end{aligned} \quad (5.10)$$

Providing that $\varepsilon(k)$ and $e(k)$ are uncorrelated, the error covariance matrix can be expressed as:

$$\begin{aligned} \bar{P}(k+1) &= E \{ \bar{e}(k+1) \bar{e}(k+1)^T \} \\ &= E \{ [\Phi(k)e(k) + \varepsilon(k)] [\Phi(k)e(k) + \varepsilon(k)]^T \} \\ &= \Phi(k) P(k) \Phi(k)^T + Q(k) \end{aligned} \quad (5.11)$$

Now, using equations (5.9) and (5.11) we can find the initial values for Θ and P to start the estimation process for step $K+1$.

Equations (5.5), (5.8), (5.9) and (5.11) together describe the recursive chain that allows for sequential data processing; the only missing equation here is the equation which describes the gain K .

Calculation of the gain is usually done in such away to satisfy a certain cost function. If the cost function is based on the stochastic least squares minimization criteria the resulting filter is the Kalman filter (KF) [40], but if the cost function is based on the least absolute value criteria, the filter will be the weighted least

absolute value filter (WLAVF) [41].

5.2.1: Kalman filtering

The problem here is to find the gain vector K that minimizes the stochastic least squares cost function given by [40,42,44]

$$J_2 = E \left\{ \sum_{k=1}^m e(k)^T e(k) \right\} \quad (5.12)$$

where m is the total number of measurements. It is clear that the cost function will be a minimum when each individual cost element is an absolute minimum.

The cost function at the k^{th} instant can be written as:

$$J_2(k) = E \left\{ e(k)^T e(k) \right\} \quad (5.13)$$

Now, the problem is to find the particular vector $K(k)$ that minimizes the individual terms along the major diagonal of $P(k)$, because these terms represent the estimation error variances for the elements of the state vector being estimated. We now, temporarily drop the symbol (k) , which refers to the instant k , in order to avoid unnecessary clutter in the derivation [42]. Equation (5.8) then becomes

$$P = (I - KH) \bar{P} (I - KH)^T + KRK^T \quad (5.14)$$

Equation (5.14) can be rewritten as

$$P = \bar{P} - [K\bar{H}\bar{P} - \bar{P}\bar{H}^T K^T] + K(\bar{H}\bar{P}\bar{H}^T + R)K^T \quad (5.15)$$

Assuming that $[\bar{H}\bar{P}\bar{H}^T + R]$ is symmetric and positive definite we can write

$$S S^T = \bar{H}\bar{P}\bar{H}^T + R \quad (5.16)$$

Using this factorised form, equation (5.15) can be rewritten as

$$P = \bar{P} - K\bar{H}\bar{P} - \bar{P}\bar{H}^T K^T + K S S^T K^T \quad (5.17)$$

Equation (5.18) can then be obtained by completing the square in equation (5.17).

$$P = \bar{P} + (KS - A)(KS - A)^T - A A^T \quad (5.18)$$

Expanding equation (5.18) and comparing it to equation (5.17) gives

$$K S A^T + A S^T K^T = K\bar{H}\bar{P} + \bar{P}\bar{H}^T K^T \quad (5.19)$$

If A is chosen to be equal to $[\bar{P}\bar{H}^T(S^T)^{-1}]$ then equation (5.19) is satisfied and hence equations (5.17) and (5.18) will be equivalent.

Now refer back to equation (5.18), it is clear that the only term involving K is the second term, and it is the product of a matrix and its transpose, and that guarantee nonnegative diagonal elements. Therefore to minimize the diagonal elements of P the term $(KS-A)$

should be zero. Then we can write

$$K S = A \quad (5.20)$$

Substituting for A in equation (5.20) gives

$$\begin{aligned} K &= \bar{P} H^T (S^T)^{-1} S^{-1} \\ &= \bar{P} H^T (SS^T)^{-1} \end{aligned} \quad (5.21)$$

Substitute from equation (5.16) into equation (5.21) and reintroduce the time step symbol, k, the Kalman filter gain can be expressed as

$$K(k) = \bar{P}(k) H(k)^T [H(k) \bar{P}(k) H(k)^T + R(k)]^{-1} \quad (5.22)$$

Equation (5.22) can now implemented along with equations (5.5), (5.8), (5.9) and (5.11) to complete the discrete Kalman filter.

5.2.2: Least absolute value filtering

The weighted least absolute value cost function to be minimized is given by [41,43,44,46]

$$J_1 = \sum_{i=1}^m | N (\Theta - \bar{\Theta}) - r_i^{-1} (z_i - H_i \Theta) | \quad (5.23)$$

where Θ = Ux1 actual state vector

$\bar{\Theta}$ = Ux1 mean value vector

r_i = weighting element of i^{th} measurement

z_i = i^{th} measurement

H_i = the i^{th} row of the measurement matrix

$N = e^T \bar{P}^{-1}$, and

$\bar{P} = UxU$ error covariance matrix before the measurement

$e = Ux1$ column (1,1,1,...,1) vector

Using minimum norm theorem, the cost function of equation (5.23) is minimum when

$$J_1 = \sum_{i=1}^m |\varepsilon_i| = 0 \quad (5.24)$$

$$\text{and hence, } |\varepsilon_i| = 0 \quad , \text{with } i=1,2,\dots,m \quad (5.25)$$

where ε_i , the i^{th} element of the cost function, is given by

$$\varepsilon_i = N(\Theta - \bar{\Theta}) - r_i^{-1} (z_i - H_i \Theta) \quad (5.26)$$

Equation (5.26) can be written in a compact form as

$$\varepsilon = C(\Theta - \bar{\Theta}) - R^{-1} (Z - H\Theta) = 0 \quad (5.27)$$

where the following matrices are defined as

ε = column $(\varepsilon_1, \varepsilon_2, \dots, \varepsilon_m)$,

R^{-1} = diagonal $(r_1^{-1}, r_2^{-1}, \dots, r_m^{-1})$ is an $m \times m$ weighting matrix ,

H = matrix of $m \times U$,

$C = LN$, of dimensions $m \times U$,

where $L = m \times 1$ column (1,1, ...,1) vector .

Equation (5.27) gives the best estimation for Θ as

$$(C + R^{-1}H) \hat{\Theta} = C\bar{\Theta} + R^{-1}Z . \quad (5.28)$$

If $R^{-1}H\bar{\Theta}$ is added and subtracted to and from the R.H.S. of equation (5.28) then this equation can be rewritten as

$$(C+R^{-1}H)\hat{\Theta} = (C+R^{-1}H)\bar{\Theta} + R^{-1}(Z-H\bar{\Theta}) . \quad (5.29)$$

Now, define the $m \times U$ matrix A as

$$A = (C+R^{-1}H) . \quad (5.30)$$

Then equation (5.29) becomes

$$A\hat{\Theta} = A\bar{\Theta} + R^{-1}(Z-H\bar{\Theta}) . \quad (5.31)$$

Equation (5.31) describes an over determined system of equations, which can be solved using the new LAV technique explained earlier in chapter IV. Following the same steps, equation (5.32) can be rewritten as

$$\dot{A} \hat{\Theta} = \dot{A} \bar{\Theta} + \dot{R}^{-1}(\dot{Z} - \dot{H} \bar{\Theta}) \quad (5.32)$$

Where the symbol $\dot{\cdot}$ refers to the reduced set corresponding to the best, smallest, residuals. Now the LAV solution can be reached as

$$\hat{\Theta} = \bar{\Theta} + \dot{A}^{-1} \dot{R}^{-1} (\dot{Z} - \dot{H} \bar{\Theta}) \quad (5.33)$$

define K as

$$\begin{aligned} K &= \dot{A}^{-1} \dot{R}^{-1} \\ &= (\dot{R} \dot{A})^{-1} . \end{aligned} \quad (5.34)$$

In the dynamic case, there is only one measurement at a time, then of course we can drop $\dot{\cdot}$ from the equations.

Now, we can find an expression for the discrete gain at step K as

$$\begin{aligned} K(k) &= (R(k) A(k))^{-1} \\ &= [R(k) L e^T \bar{P}(k) + H(k)]^{-1} . \end{aligned} \quad (5.35)$$

Now, equation (5.35) together with equations (5.5), (5.8), (5.9) and (5.11) completely describe the weighted least absolute value filter algorithm.

At the end of this section is a summary of the steps to be followed to perform the dynamic estimation process using either the KF or the WLAVF [42,43,44,45,46].

1. Start with initial $\bar{P} = P(0)$, and $\bar{\Theta} = \Theta(0)$ to calculate the filter gain

$$K(k)_{KF} = \bar{P}(k)H(k)^T [H(k)\bar{P}(k)H(k)^T + R(k)]^{-1}$$

$$K(k)_{WLAVF} = [H(k) + R(k)Lc^T \bar{P}^{-1}(k)]^{-1}.$$

2. Compute the error covariance for update estimate

$$P(k) = [I - K(k)H(k)] \bar{P}(k) [I - K(k)H(k)]^T + K(k)R(k)K(k)^T.$$

3. Update estimate with measurement $z(k)$

$$\hat{\Theta}(k) = \bar{\Theta}(k) + K(k)[z(k) - H(k)\bar{\Theta}(k)].$$

4. Project ahead error covariance and estimate

$$\bar{P}(k+1) = \Phi(k)P(k)\Phi(k)^T + Q(k), \text{ and}$$

$$\bar{\Theta}(k+1) = \Phi(k) \hat{\Theta}(k).$$

It is clear that the only difference between the KF and the WLAVF lies in the gain matrix $K(k)$.

5.3: Test of the algorithms: simulated example

In this section, the two algorithms mentioned above are tested using a simple simulated example. Here the waveform is considered to have a constant magnitude during the window size (stationary

waveform). Later in section 5.4 the algorithms will be tested for nonstationary waveforms.

The KF and the WLAVF algorithms are tested here using a voltage signal waveform of known harmonic content [13]. The waveform is described as:

$$v(t) = 1.0\cos(\omega_0 t + 10^\circ) + 0.1\cos(3\omega_0 t + 20^\circ) + 0.08\cos(5\omega_0 t + 30^\circ) + 0.08\cos(7\omega_0 t + 40^\circ) \\ + 0.06\cos(11\omega_0 t + 50^\circ) + 0.05\cos(13\omega_0 t + 60^\circ) + 0.03\cos(19\omega_0 t + 70^\circ)$$

The data window size for this example is chosen to be 2 cycles, with sampling frequency of 3840 Hz and 64 samples per cycle.

The two algorithms were tested using both models 1 and 2 developed earlier in chapter IV. It is worth while to mention here that the static least squares estimate was used to provide the algorithms with the initial values for the state vector $\bar{\Theta}(0)$ and its covariance matrix $\bar{P}(0)$ [47].

It was found that both KF and WLAVF give the same estimate for the magnitudes and the phase angles when either model 1 or model 2 used, but the only difference was in the gain matrix K.

Figures (5.1) and (5.2) give the estimated magnitudes of the fundamental, 3rd, 7th, 11th and the 13th respectively while Figure (5.3) gives the estimated phase angles for the same harmonics when KF or WLAVF are used with either model 1 or model 2. Figure (5.4) gives KF gain for the 60 Hz states x_1 and y_1 when model 1 is used while figure (5.5) gives the WLAVF gain for the same components when the same model is used. Figures (5.6) and (5.7) give the KF gain and the

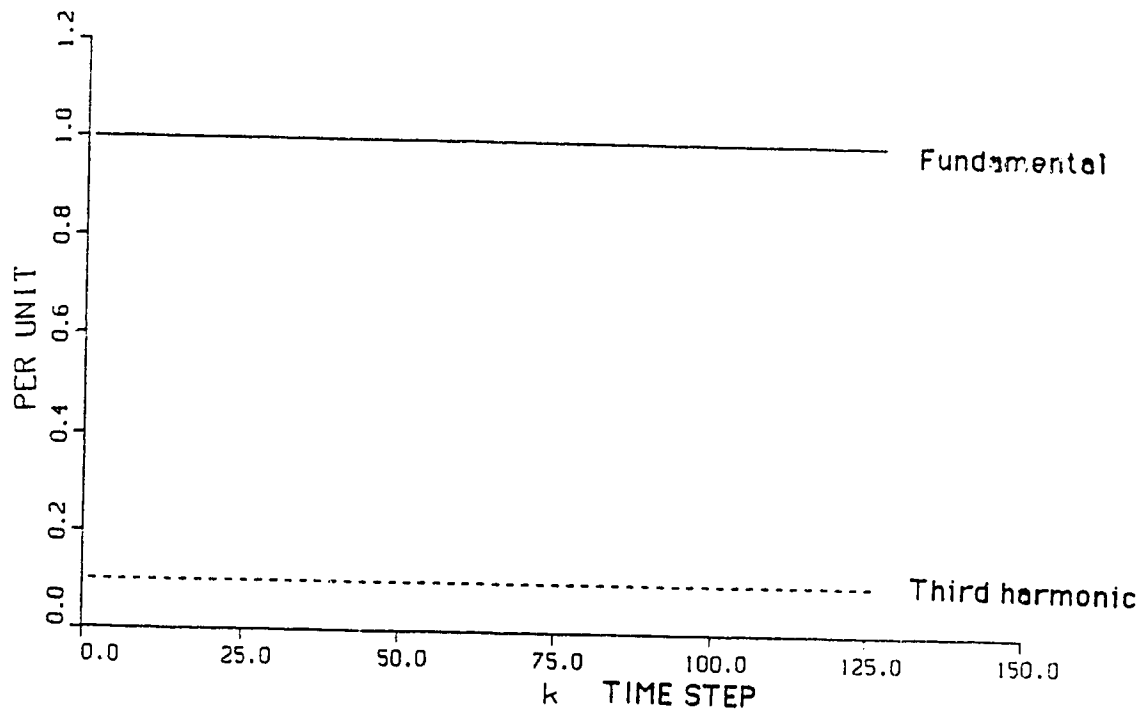


Fig. 5.1 Estimated magnitude of 60 Hz and third harmonic
using KF and WLAVF (Models 1 and 2)

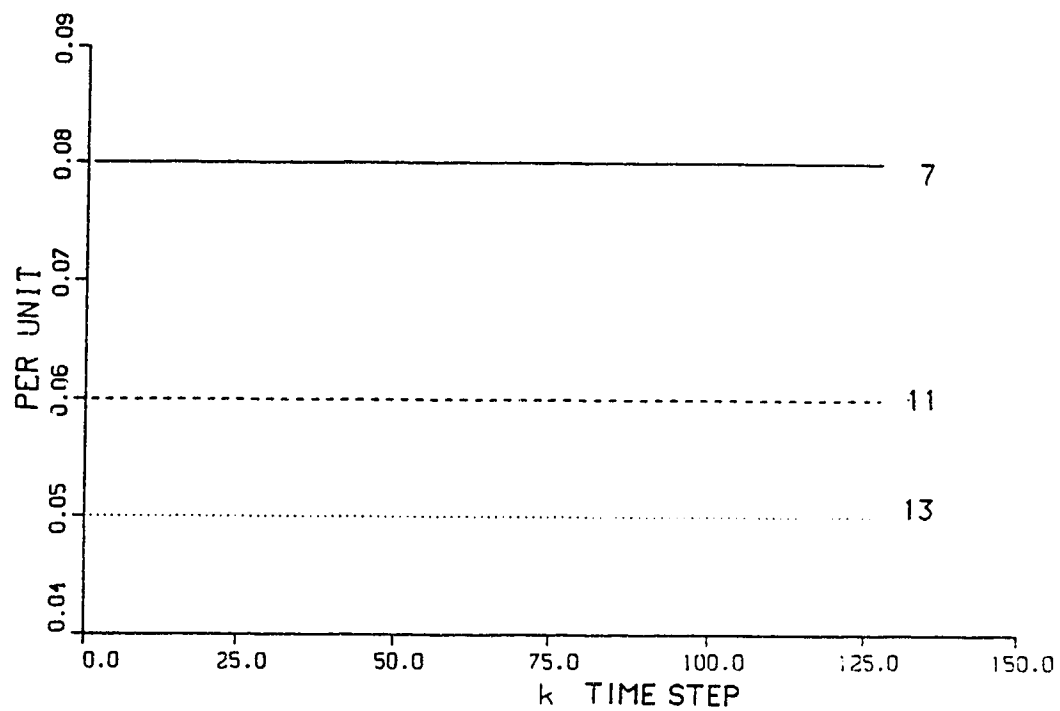


Fig. 5.2 Estimated magnitude of seventh,eleventh and
thirteenth harmonic using models 1 and 2
(KF and WLAVF)

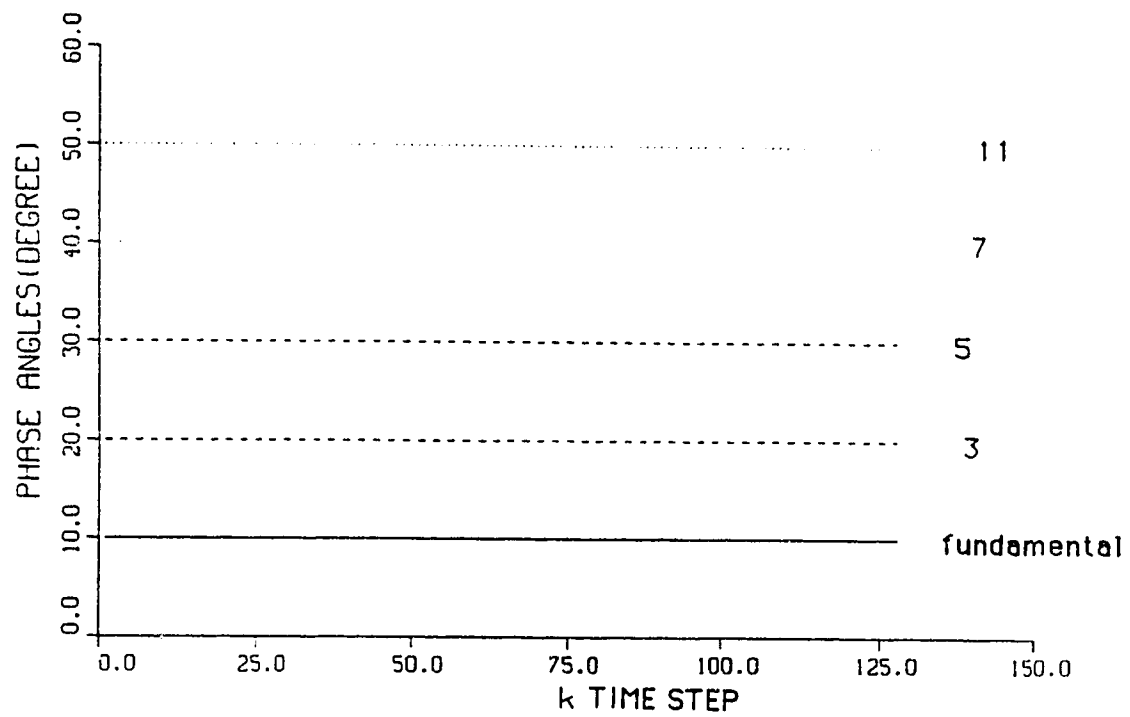


Fig. 5.3 Estimated phase angles using models 1 and 2
(KF and WLAVF)

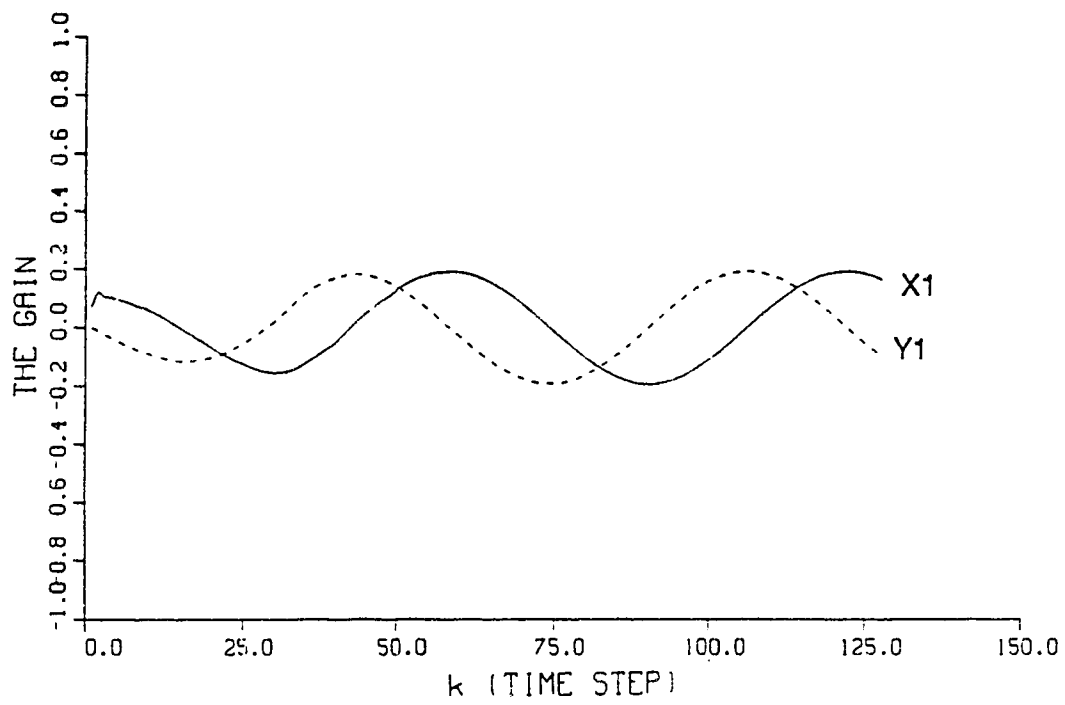


Fig. 5.4 Kalman filter gain for X1 and Y1 (Model 1)

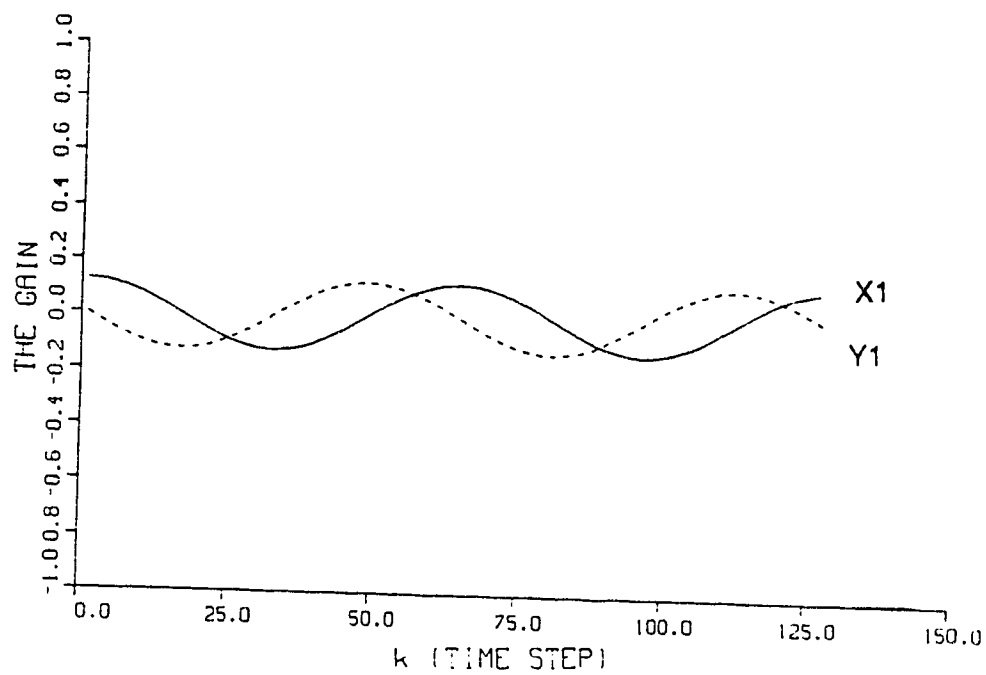


Fig. 5.5 The WLAVF gain for X1 and Y1 (Model 1)

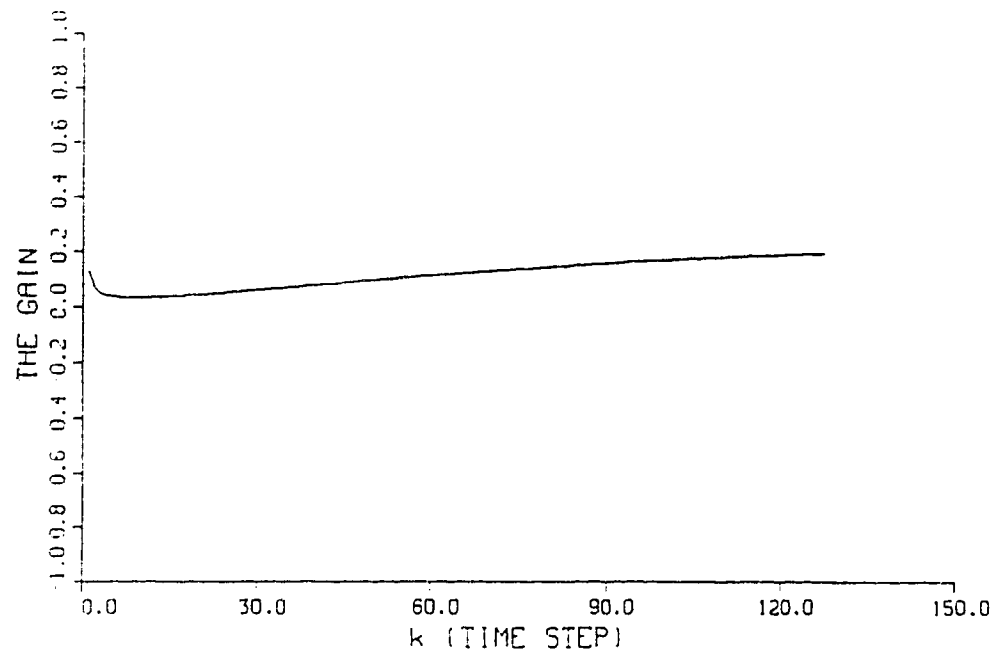


Fig. 5.6 Kalman filter gain for X1 (Model 2)

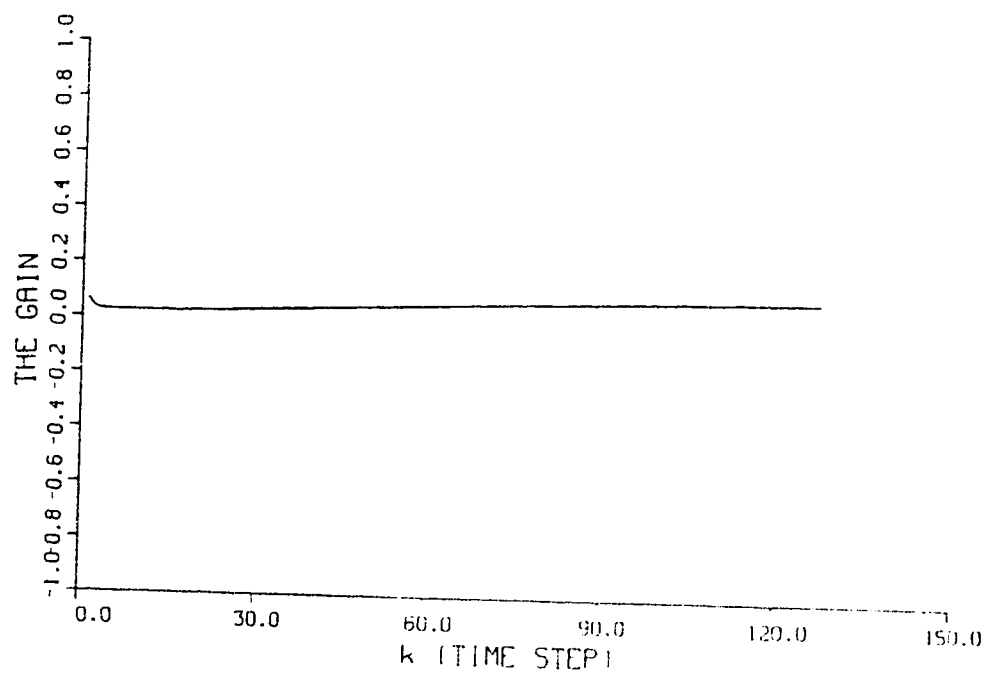


Fig. 5.7 The WLAVF gain For X1 (Model 2)

WLAVF gain for the component x_1 when model 2 is used. Examining curves from (5.1) to (5.7) reveals

1. The two algorithms, for both models, estimate exactly the harmonic contents of the waveform, and the two models produce the same results with the two algorithms.
2. When model 1 was used the gain values were oscillating with the fundamental frequency, but when model 2 was used the gain elements start to change without oscillations. In both cases the gain values reach steady state after a short time. Indeed, this was because of the good initialization of the filters.
3. Extensive runs show that model 1 reduced the computation time, therefore this model will be used in the next sections.

Effects of the frequency drift on the estimates are also investigated for this simulated example, where the drift was assumed to change between -0.05 and -0.1 Hz. A sample of the results is shown in figure (5.8) which indicates that for a frequency drift up to about -0.1 Hz the estimates of the harmonic magnitudes do not change appreciable. Of course there is an error, about 2%, but it is acceptable for a small drift. However the error in estimating the phase angles could reach about 20% . To overcome this drawback, it is important to always update the frequency by measuring it before each measurement is used.

5.4: Test of the algorithms: Actual recorded data

The two algorithms are tested again in this section using the

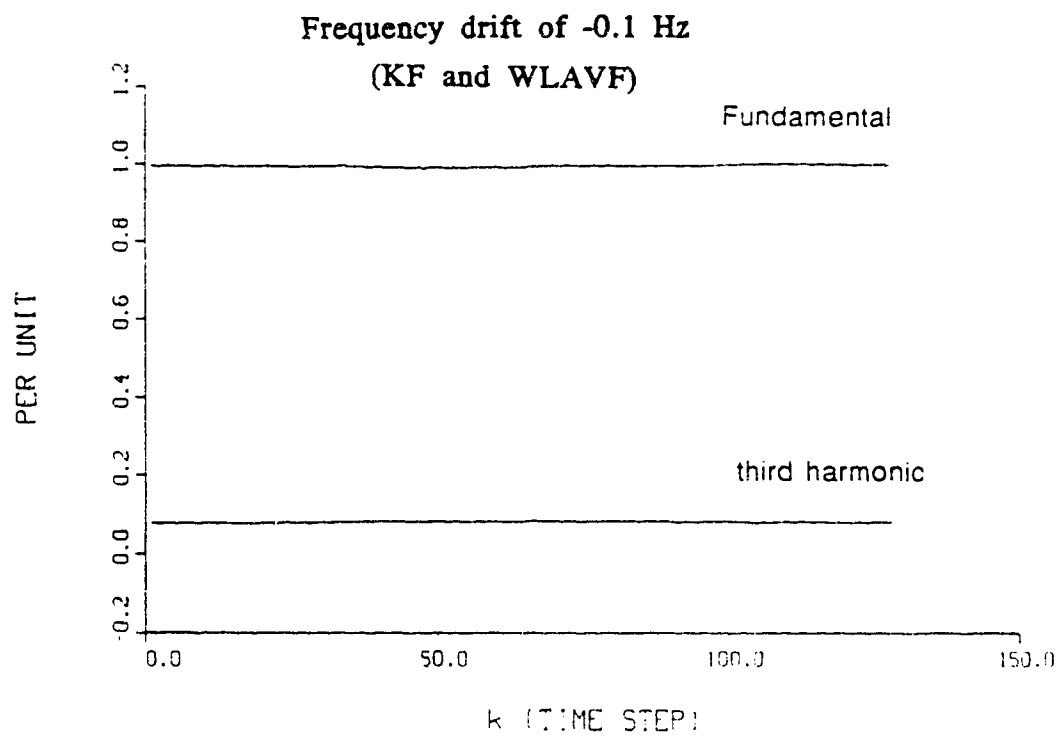


Fig. 5.8 Estimated magnitudes of the fundamental and third harmonic components

actual recorded data of Appendix II. Here the considered waveforms are nonstationary. The section starts with using the KF algorithm and then the WLAVF algorithm and finally at the end of this section a comparison between the two algorithms is provided.

5.4.1: Kalman filter case

The Kalman filtering algorithm is implemented for identifying and measuring the harmonic contents for the practical system of Appendix II. The voltage and currents waveforms are given in figures (4.29) and (4.30). The algorithm is tested to observe the effects of window size, sampling frequency and number of harmonics considered.

Effects of Data window size

The algorithm is tested for different window sizes starting from 0.5 cycles up to 2 cycles. In this study 15 harmonics are considered and the sampling frequency is kept constant at 8474.57 Hz, which is the sampling frequency supplied and it is satisfying the sampling theorem. Under this combination of parameters, the Kalman filtering algorithm is implemented to estimate the harmonic contents of the three phase voltages as well as the harmonic contents of the three phase currents and hence the power generated from each harmonic component. Figures (5.9) to (5.14) give samples of the results obtained for the estimated magnitude of the harmonics content of the voltage and the current of phase A together with the power generated from each phase. Examining these curves reveals the following:

1. The phase voltage V_A contains nearly no harmonics, since the

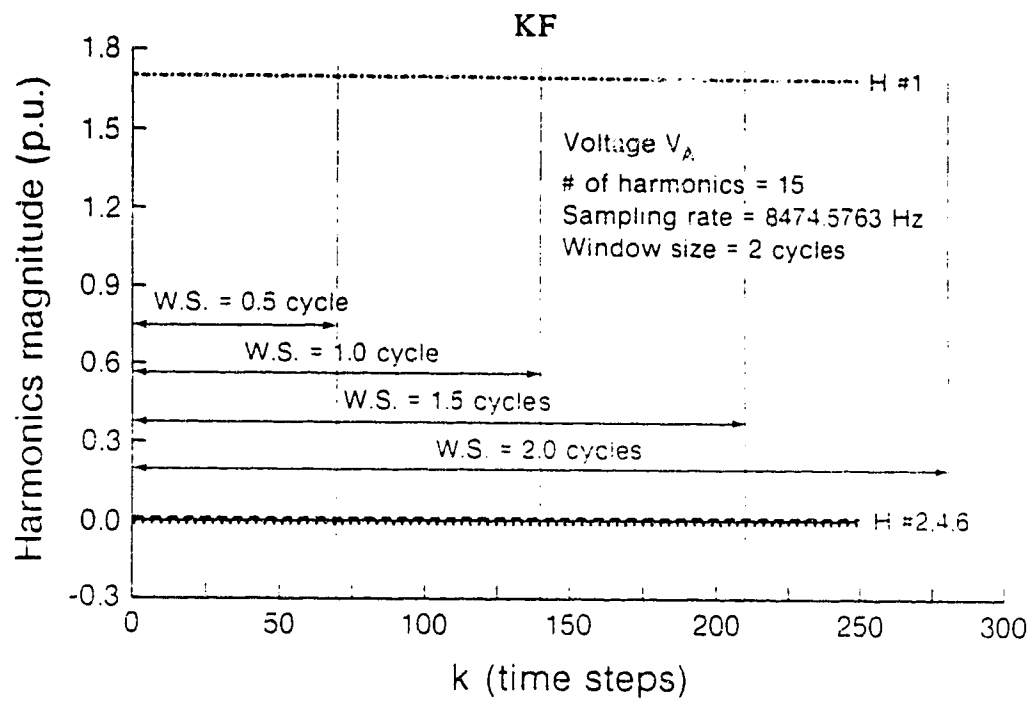


Fig. 5.9 Harmonics magnitude of V_A versus time steps at different window sizes.

KF

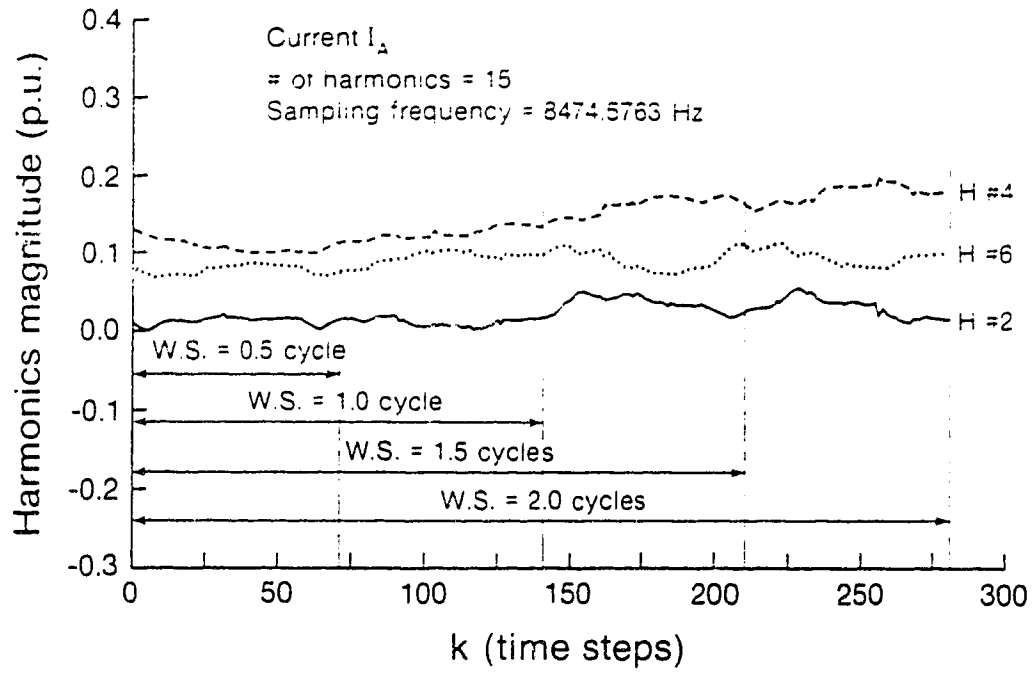


Fig. 5.10 Harmonics magnitude of I_A versus time steps at different window sizes.

KF

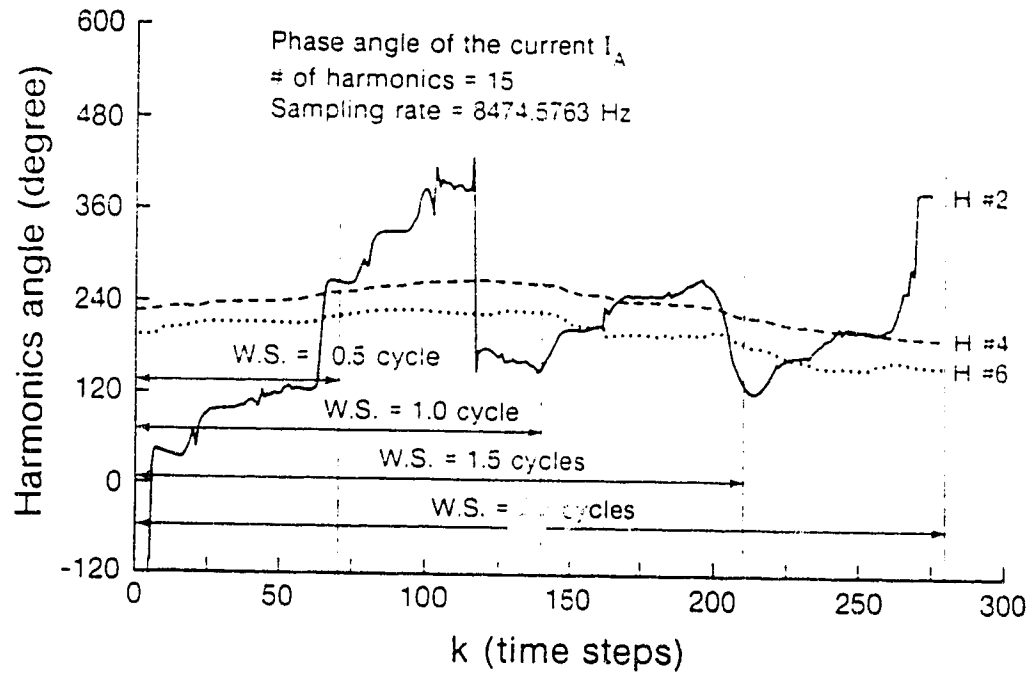


Fig. 5.11 Harmonics phase angles of I_A versus time steps at different window sizes.

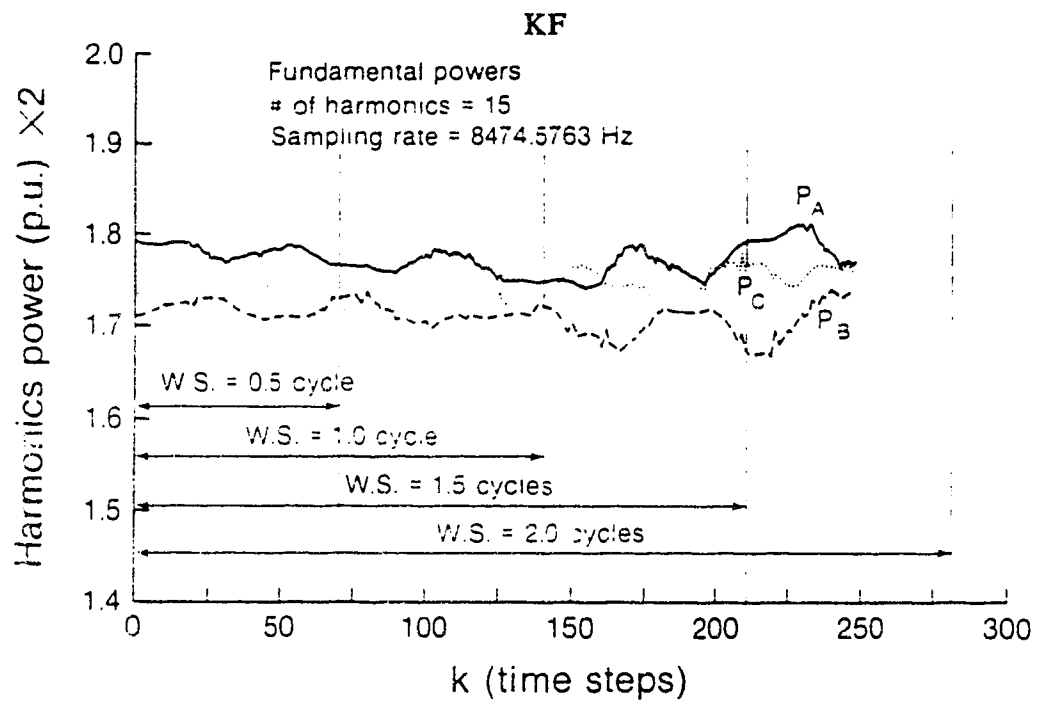


Fig. 5. 12 Fundamental powers versus time steps.

KF

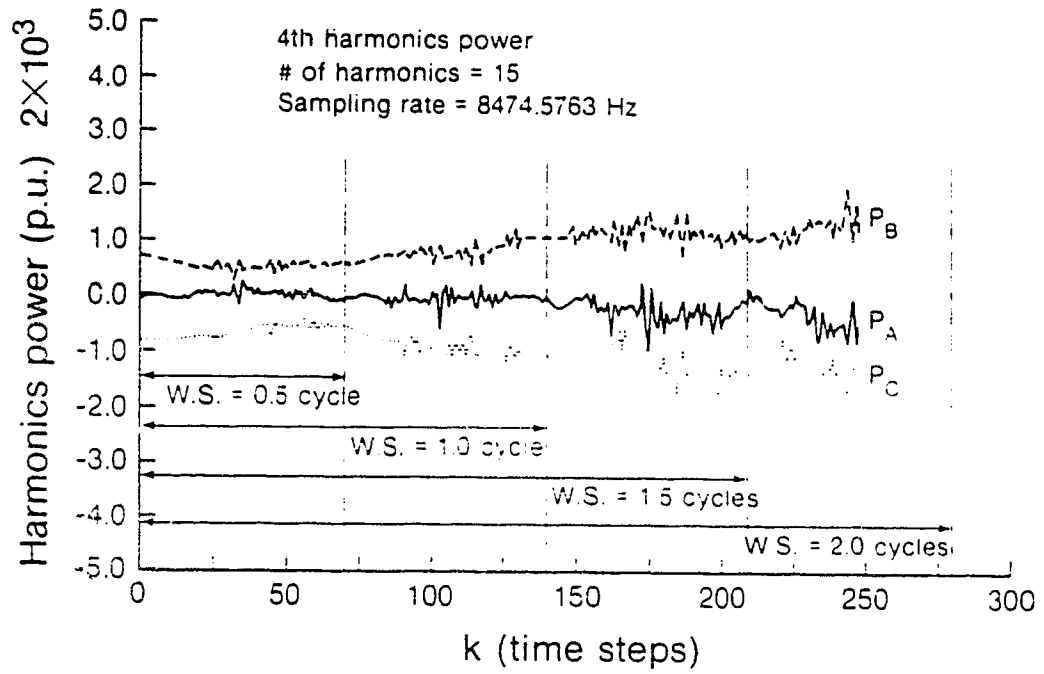


Fig. 5.13 4th harmonic power in the three phases versus time steps at different window size.

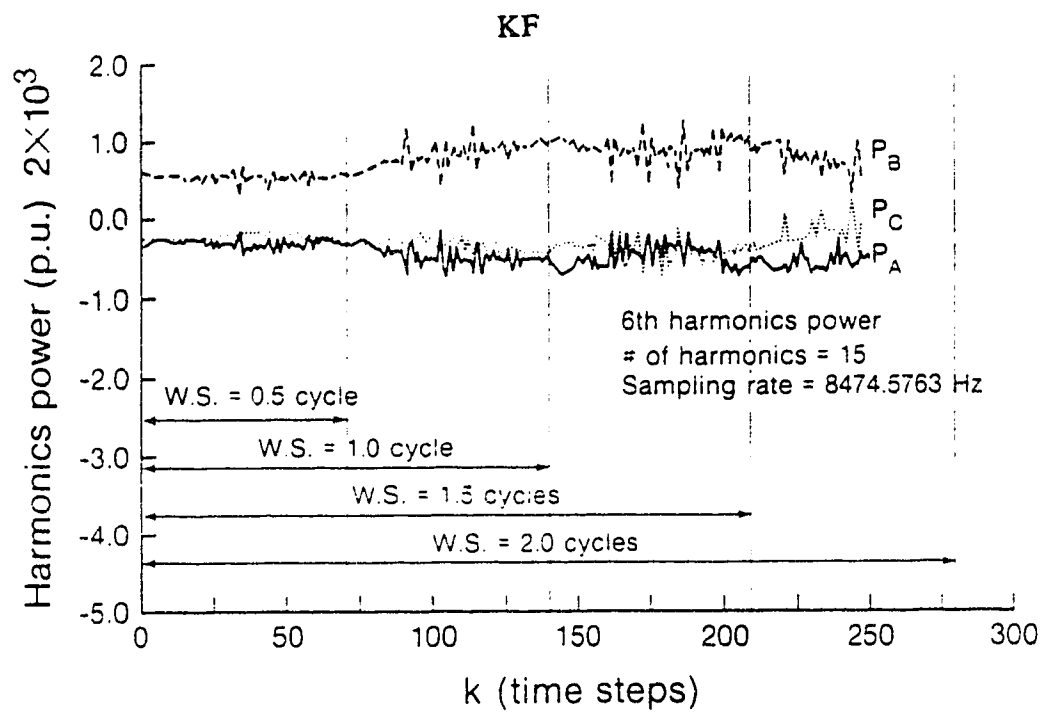


Fig. 5.14 6th harmonic power in the three phases versus time steps at different window sizes.

magnitudes of the second, fourth and the sixth harmonics are almost zero.

2. The harmonic contents of the current of phase A as well as their phase angles are given in figures (5.10) and (5.11); it can be noticed that this current contains the second, fourth and sixth harmonics. As seen from these figures the harmonic magnitudes as well as the phase angles vary as the data window size varies. Indeed this is due to the fact that the waveforms are nonstationary.
3. Figure (5.12) gives the fundamental power for each phase namely, A, B, and C in per unit; it can be noticed from this figure that the three phase powers are not the same and they vary from instant to instant during the estimation process, this is due to the fact that the waveforms are unsymmetrical as well as nonstationary.
4. Figures (5.13) and (5.14) give the 4th and the 6th harmonics power for the three phases, it can be noticed from figure (5.13) that the 4th harmonic in phase B is positive while in phase A and C are most of the time negative. It can be also noticed from figure (5.14) that the 6th power generated from phase B is positive while for phase A and C it is negative. However, the values of these powers are small compared to the fundamental power.

Effects of sampling frequency

Effects of sampling frequency on the behavior of Kalman filtering algorithm are studied when the sampling frequency varies as 2118.64, 2824.85, 4237.28 and 8474.57 Hz. while the data window size is kept constant at 2 cycles. To avoid aliasing effect, the sampling

frequency was always kept greater than twice the frequency of the highest harmonic considered. Figures (5.15) to (5.20) give a sample of the results obtained for the harmonic magnitudes of the current as well as the three phase power generated from these harmonics. Examining these curves reveals the following:

1. Provided that the sampling frequency used satisfies the sampling theorem, it can be noticed that the sampling frequency, in this case, has slight effects on the estimated harmonic magnitudes as seen in figure (5.15), (5.16) and (5.17). Figure (5.18) shows the variation of the fourth harmonic magnitude with the sampling frequency. The harmonics power, as well are mostly constant or have a slight variation from one sampling frequency to another as is seen in figures (5.19) and (5.20).
2. The fourth harmonic is still the most effective one; it has the higher magnitude in the current of phase A, with the second, third, fifth and the sixth having the smaller magnitudes.
3. The sixth harmonic power in phase B, as shown in figures (5.18) and (5.20), is still positive and in phase A and C is negative, even if the sampling rate changes.

Effects of number of harmonics

To study the effect of the number of harmonics considered on the behavior of the algorithm, a constant data window size of 1 cycle is chosen with a sampling frequency of 8474.57 Hz. The number of harmonics is changed from 7 to 23 and a sample of the results obtained is shown in figures (5.21) to (5.23). These figures show the

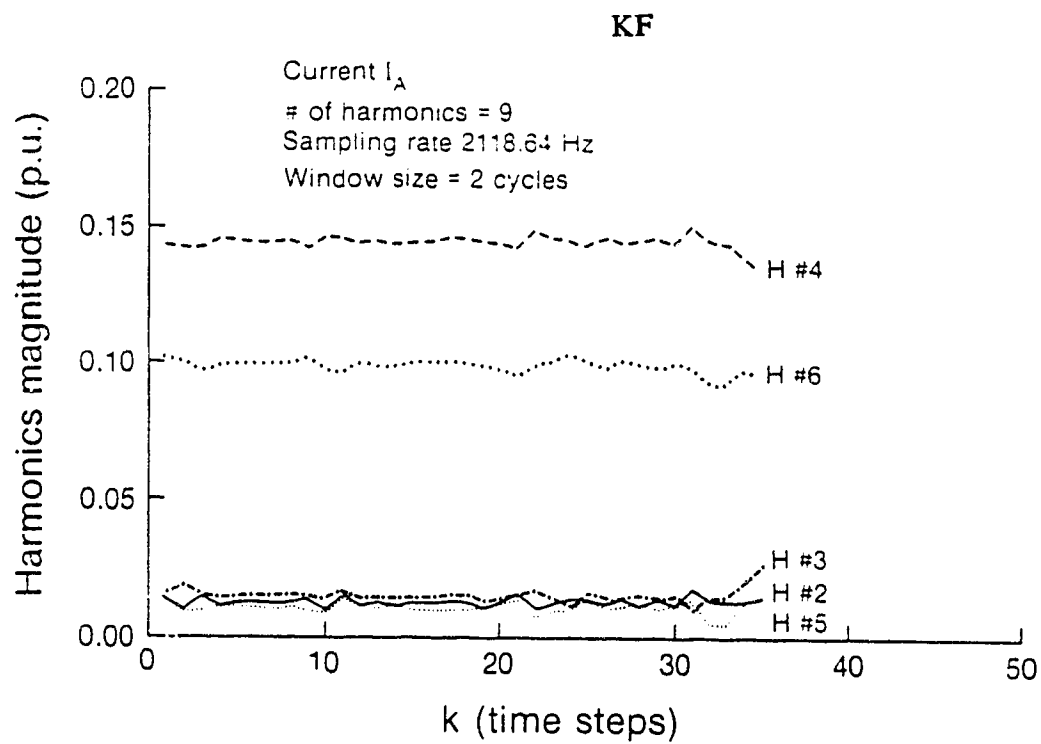


Fig. 5.15 Variation of harmonics magnitude with the time steps.

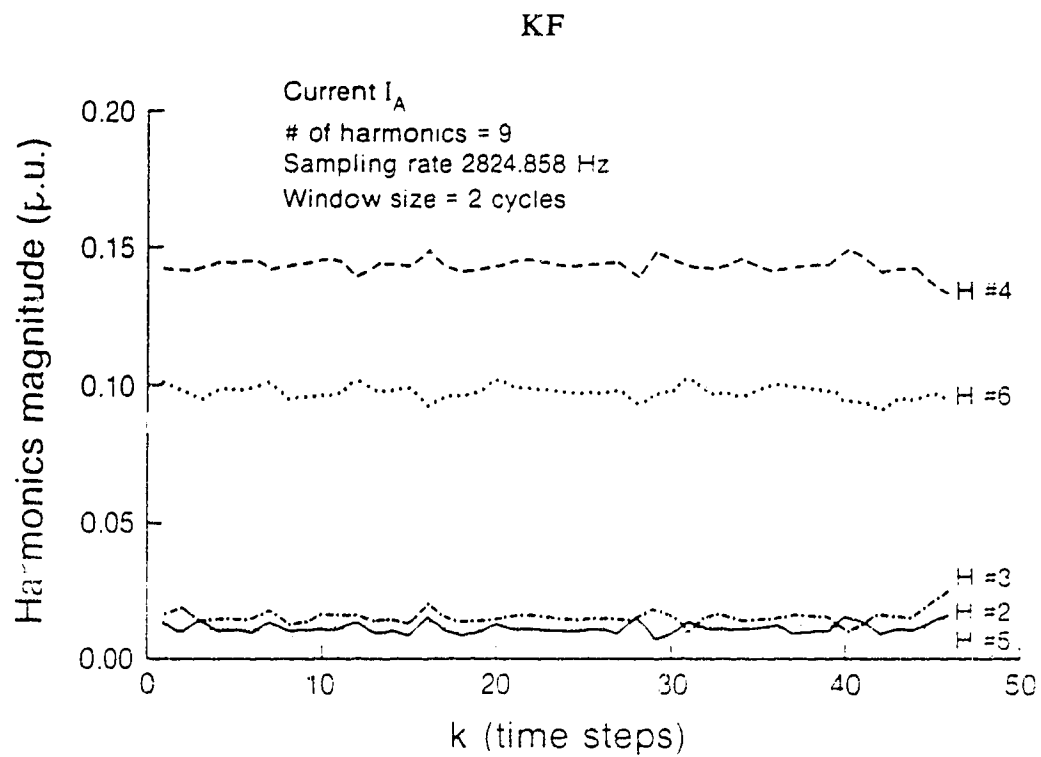


Fig. 5.16 Variation of harmonics magnitude with the time steps

KF

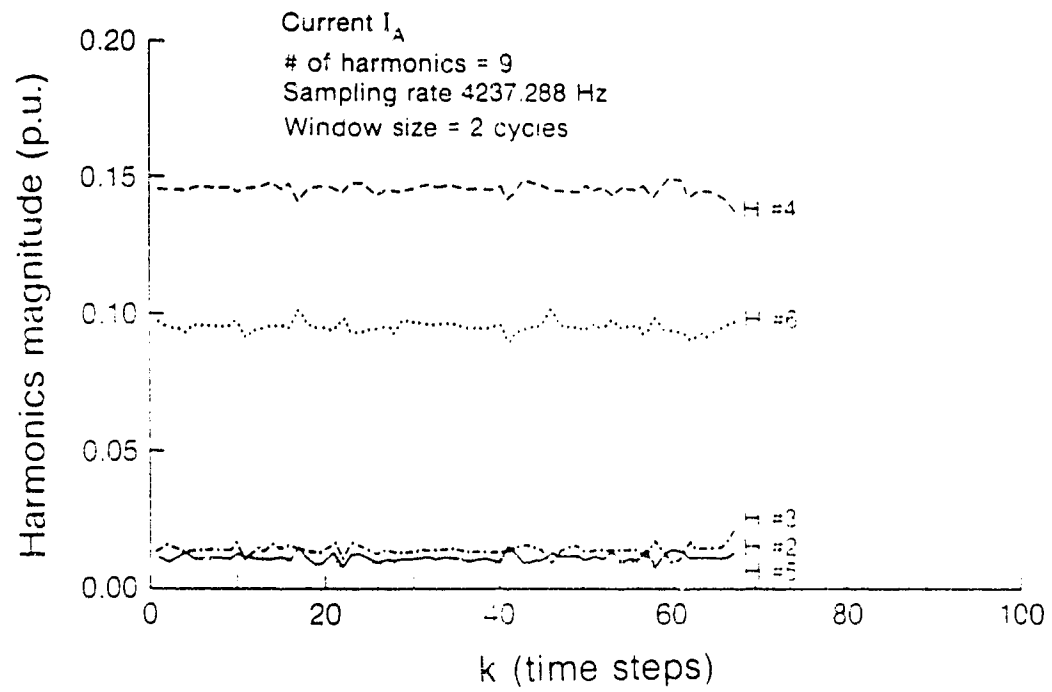


Fig. 5.17 Variation of harmonics magnitude with the time steps

KF

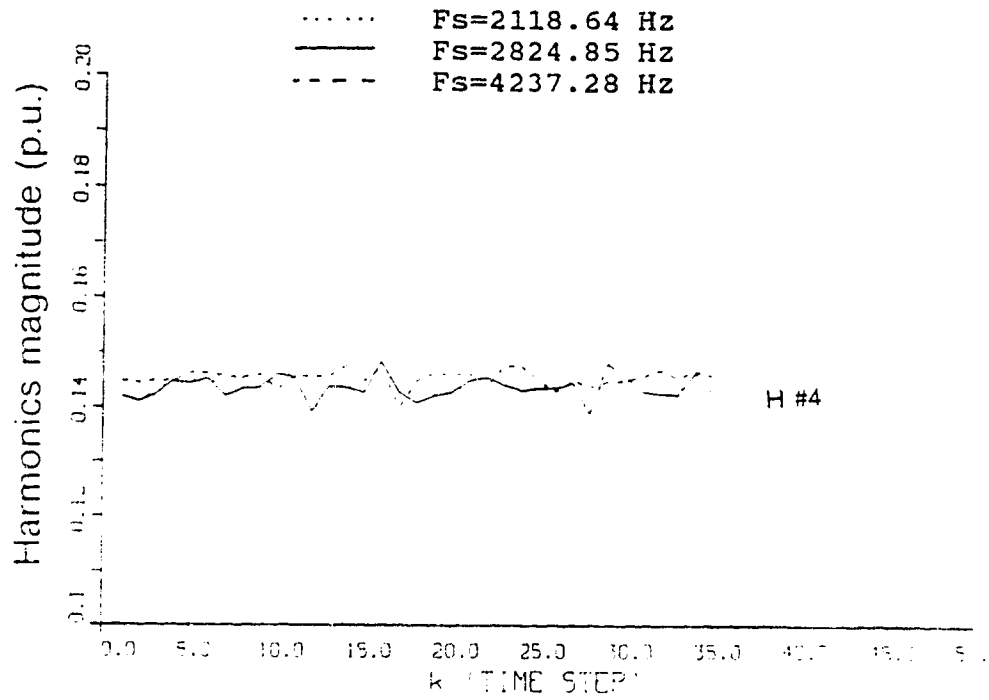


Fig. 5.18 Variations of the harmonic magnitudes with the sampling frequency

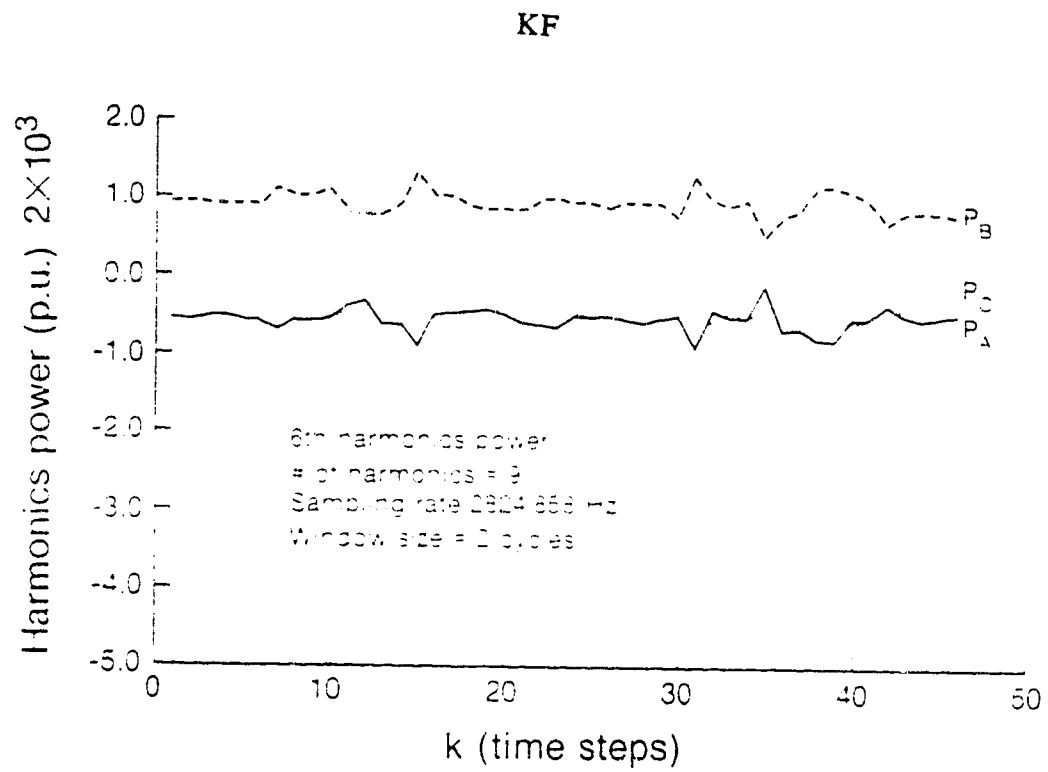


Fig. 5.19 Variation of harmonics power with the time steps

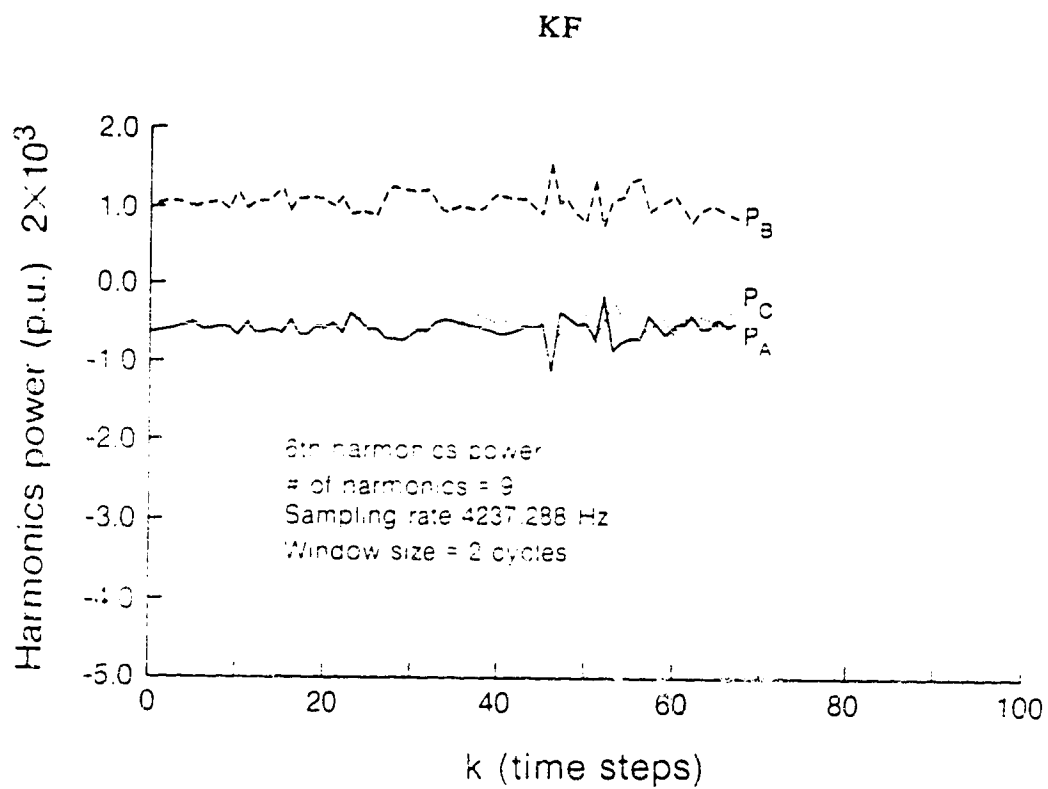


Fig. 5.20 Variation of harmonics power with the time steps.

KF

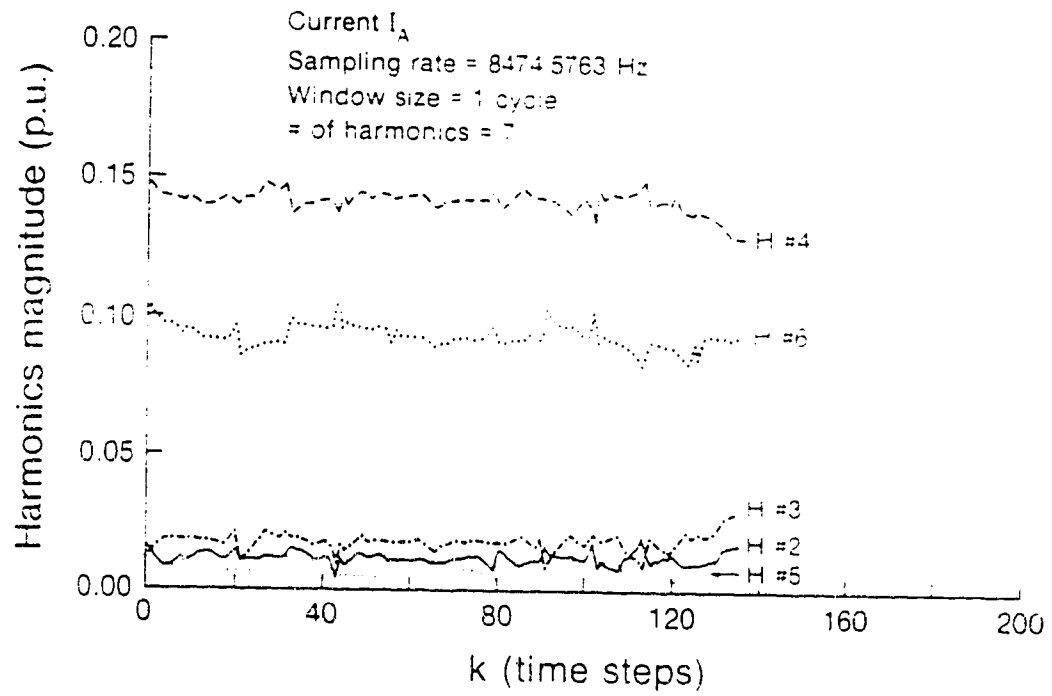


Fig. 5.21 Variation of harmonics magnitude with the time steps

KF

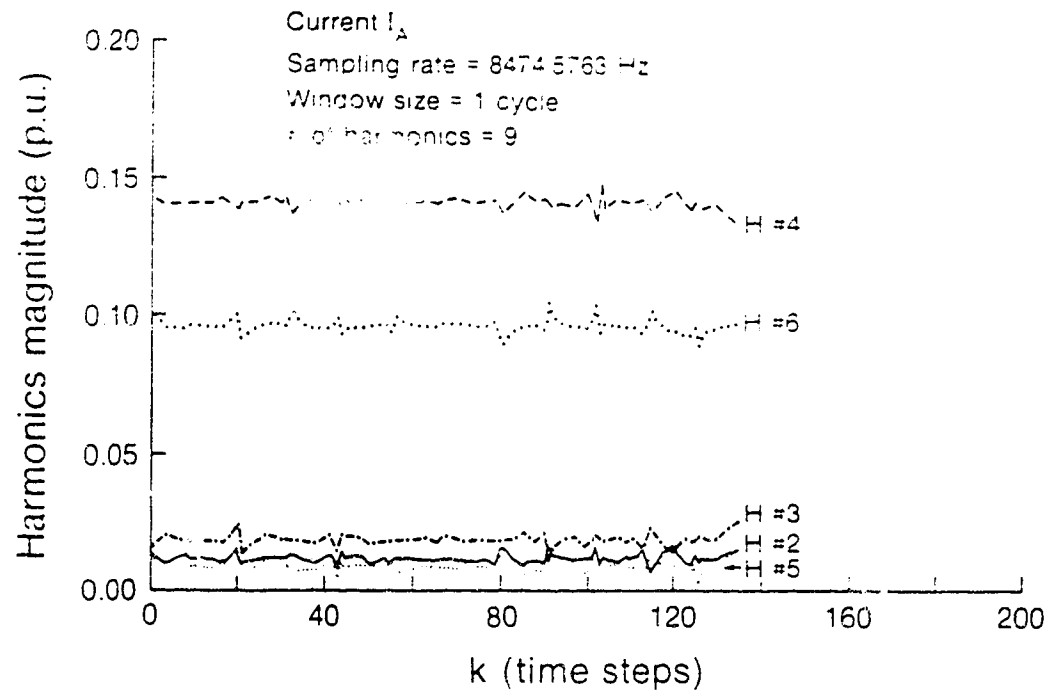


Fig. 5.22 Variation of harmonics magnitude with the time steps.

KF

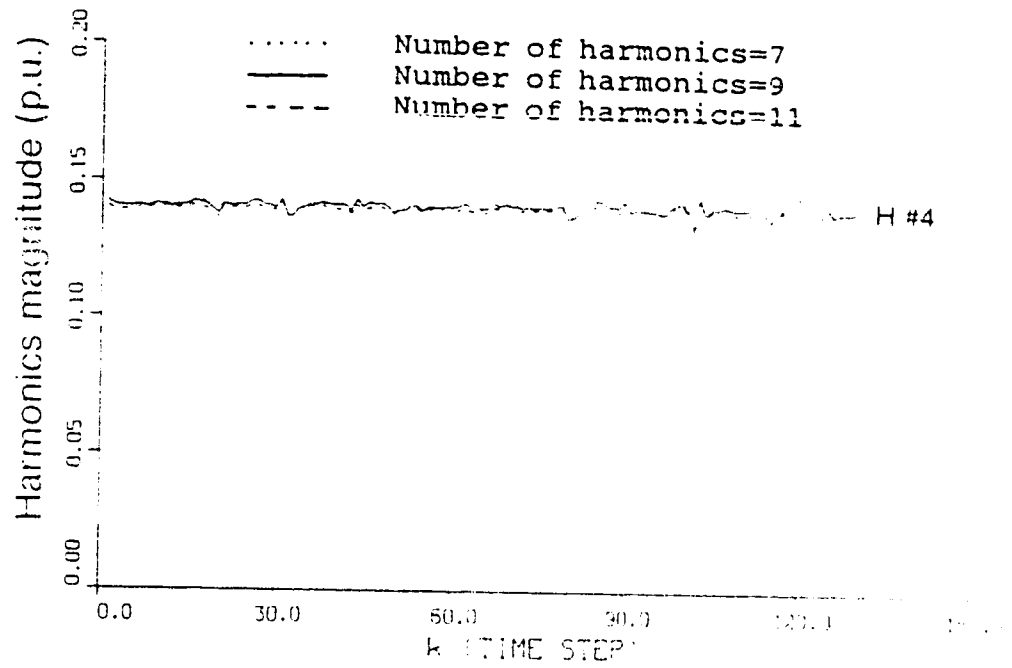


Fig. 5.23 Variations of the harmonic magnitudes with the number of harmonics considered

variation of the harmonic magnitudes when the number of harmonics is changing. Although the estimate does not change much, it is obvious that the number of harmonics considered should be kept as high as possible to get better estimate.

Subharmonics estimation

After the harmonic contents of the waveforms had been estimated, the waveform was reconstructed to get the error in this estimation. Figure (5.24) gives the real current and the reconstructed current for phase A as well as the error in this estimation. It has been found that the error has a maximum value of about 10%. The error signal is analyzed again to find if there are any subharmonics in this signal. The Kalman filtering algorithm is used here to find the amplitude and the phase angle of each subharmonic frequency. It was found that the signal has subharmonic frequencies of 15 and 30 Hz. The subharmonic amplitudes are given in figure (5.25) while the phase angle of the 30 Hz component is given in figure (5.26). The subharmonic magnitudes were found to be time varying, without any exponential decay, as seen clearly in figure (5.25).

Once the subharmonic parameters are estimated, the total reconstructed current can be obtained by adding the harmonic contents to the subharmonic contents. Figure (5.27) gives the total resultant error which now is very small, less than 3%.

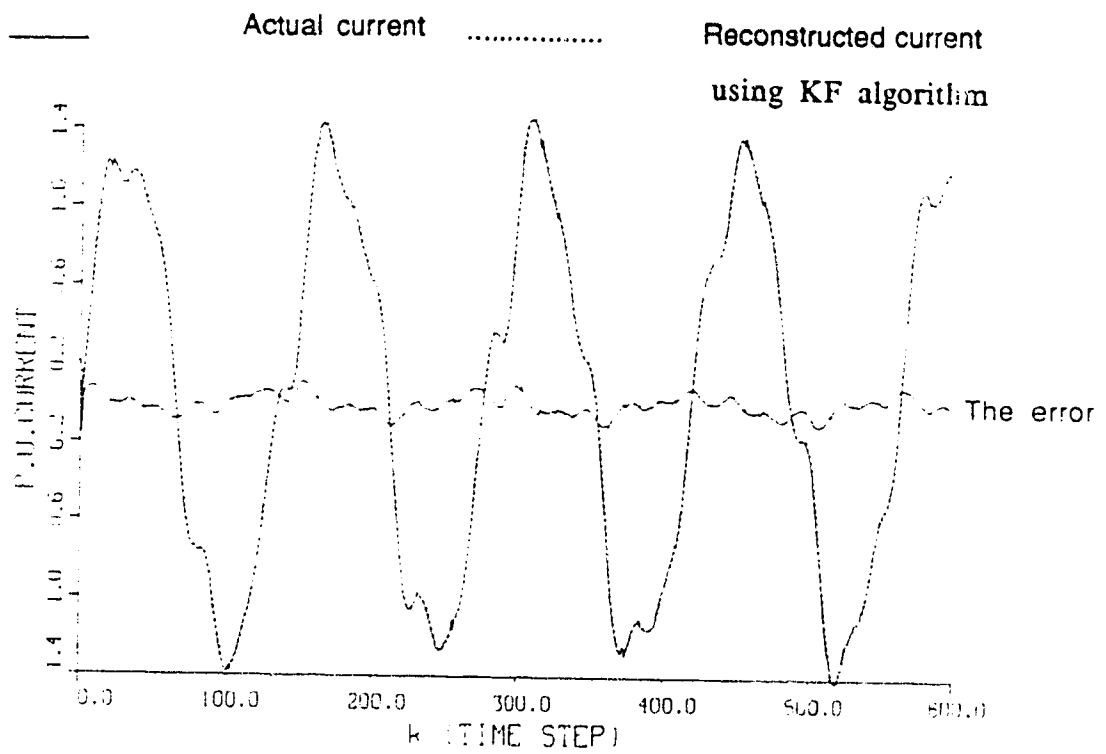


Fig. 5.24 Actual and reconstructed current for phase A

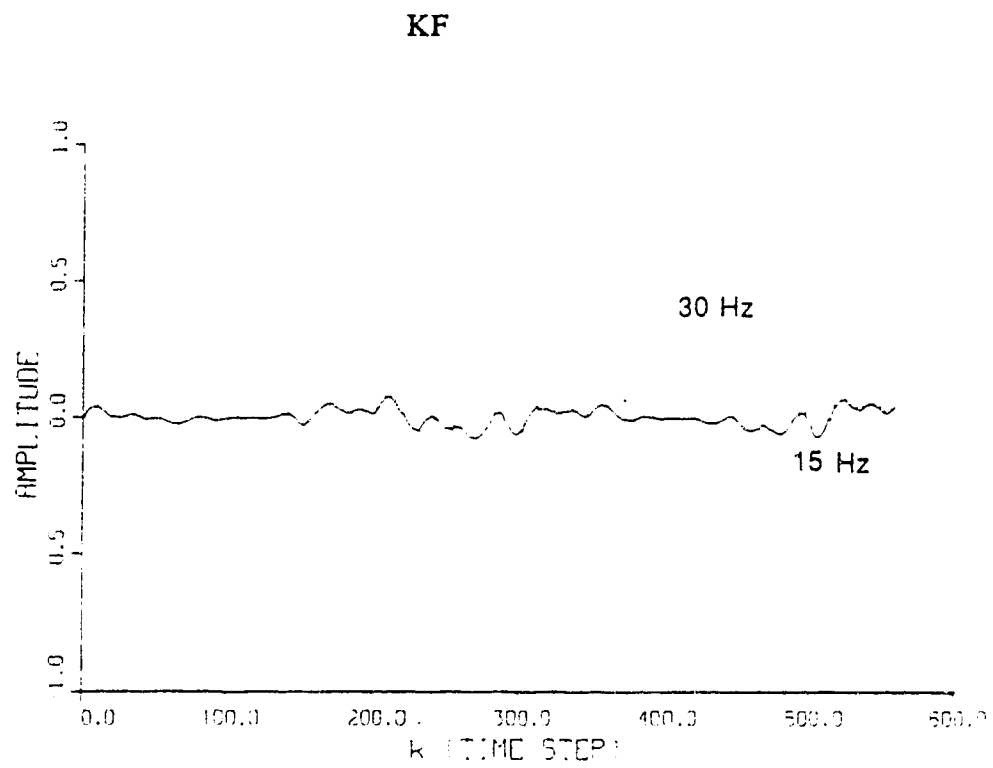


Fig. 5.25 The subharmonic amplitudes

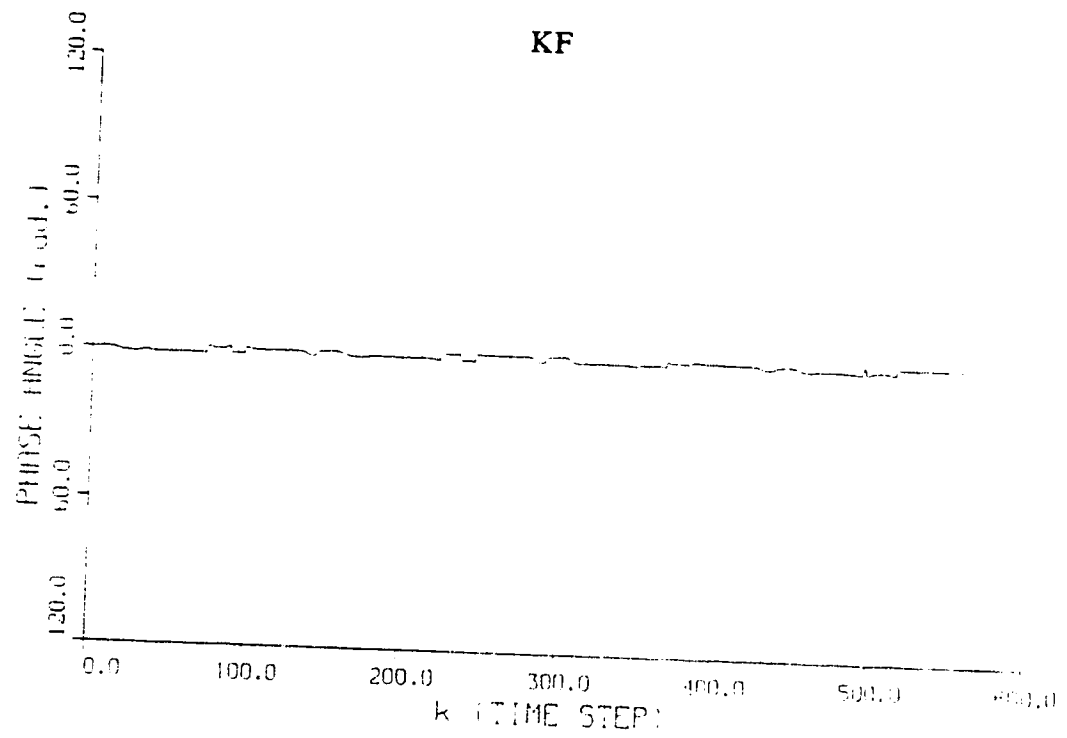


Fig. 5.26 The phase angle of the 30 Hz component

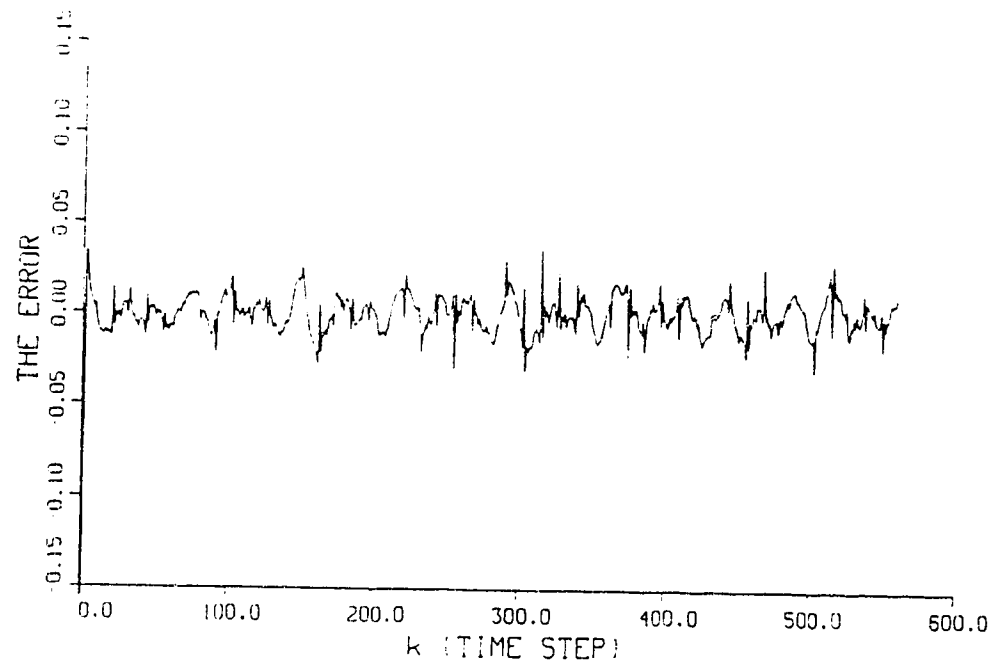


Fig. 5.27 The final error in the estimate using KF algorithm

5.4.2: Weighted least absolute value filter case

The WLAVF algorithm is implemented for identifying and measuring the harmonic content for the system of Appendix II. The effects of varying the data window size, sampling frequency and the number of harmonics is examined. The subharmonic content is identified as well in this subsection.

Effects of data window size

The algorithm is tested for different data window size, starting from 0.5 up to 2 cycles. The sampling frequency is constant at 8474.57 Hz and 15 harmonics are considered in this study. Figure (5.28) gives the harmonic magnitudes of the voltage V_A . It is clear that the voltage waveform is nearly sinusoidal. Figure (5.29) gives the harmonic magnitudes for the current I_A while figure (5.30) gives the estimation of the second harmonic magnitude using both KF and the WLAVF algorithms. Examining those two curves reveals that the magnitudes of the harmonics are time-varying, as expected, and that the most effective harmonics magnitudes are the fourth, sixth and the second. Figure (5.30) shows, as well, that this estimation is very close to that obtained using KF. Figures (5.31) gives the fundamental power of the three phases while figure (5.32) gives the sixth harmonic power. From those two figures the harmonic sources can be identified.

Effects of sampling frequency

Effects of the sampling frequency on the behavior of the algorithm are tested here. To perform this study the data window size

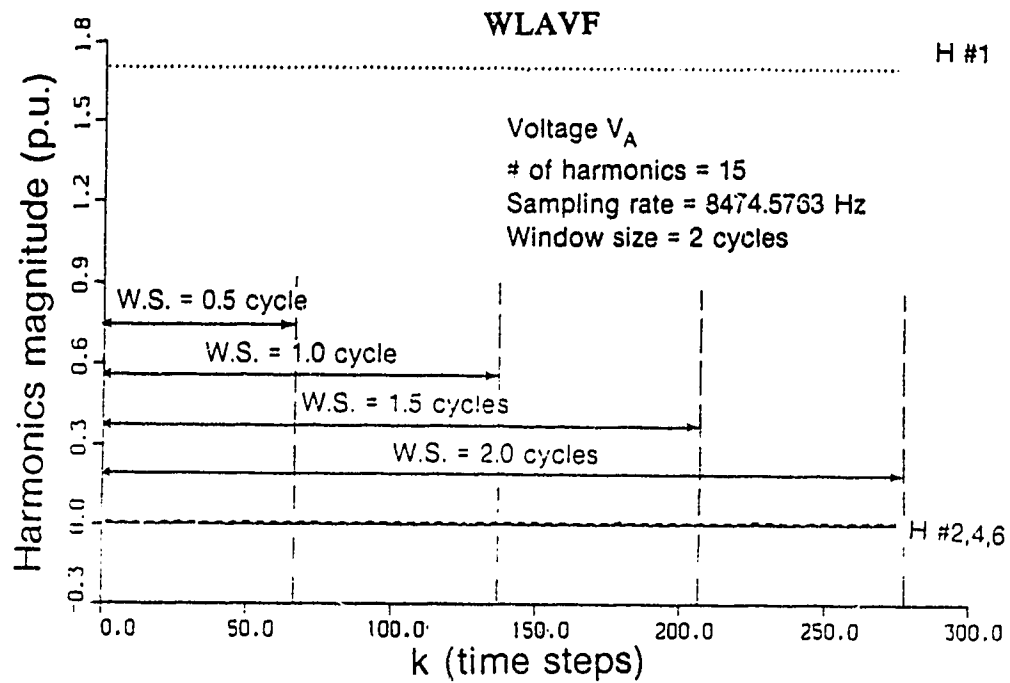


Fig. 5.28 Harmonics magnitude of V_A versus time steps at different window sizes.

For comparison with KF see page 154

WLAVF

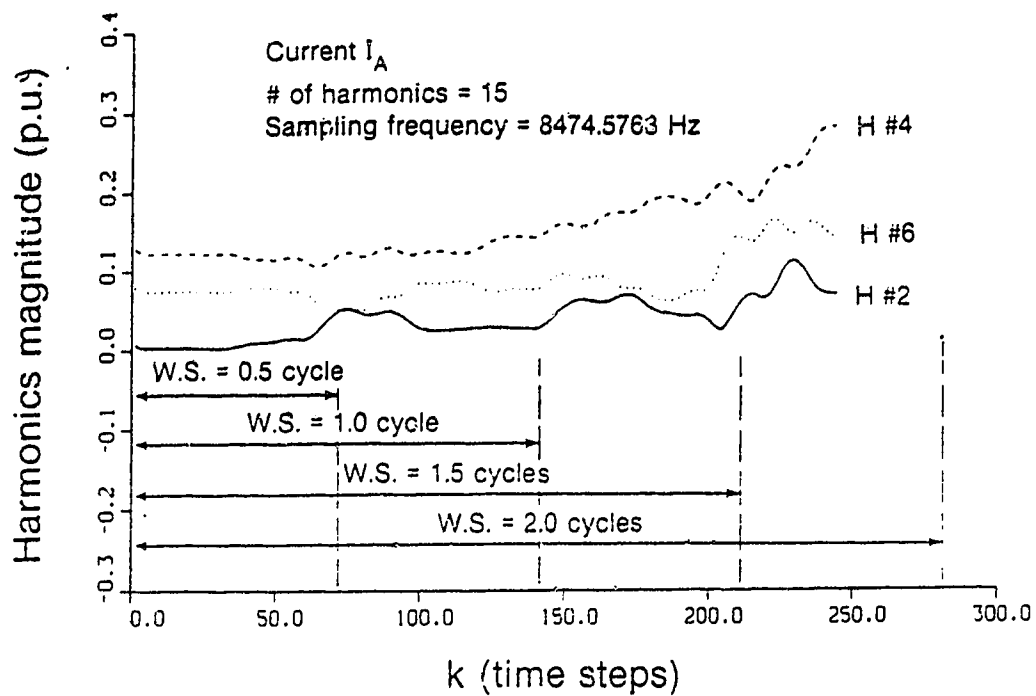


Fig. 5.29 Harmonics magnitude of I_A versus time steps at different window sizes.

For comparison with KF see page 155

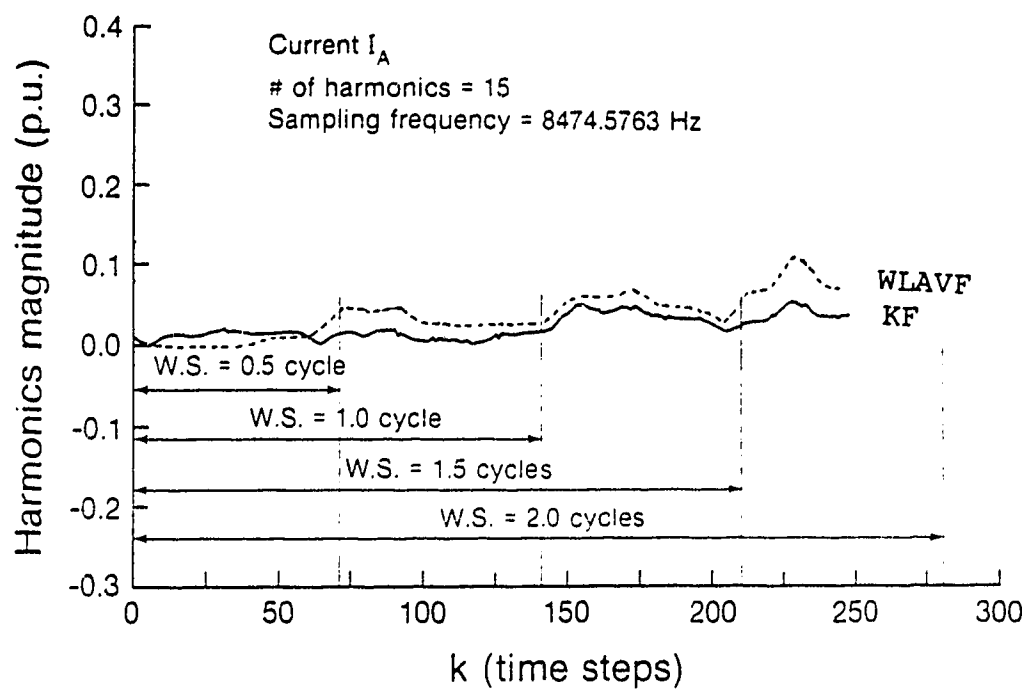


Fig. 5.30 The estimated 2nd harmonic magnitude using KF and WLAVF

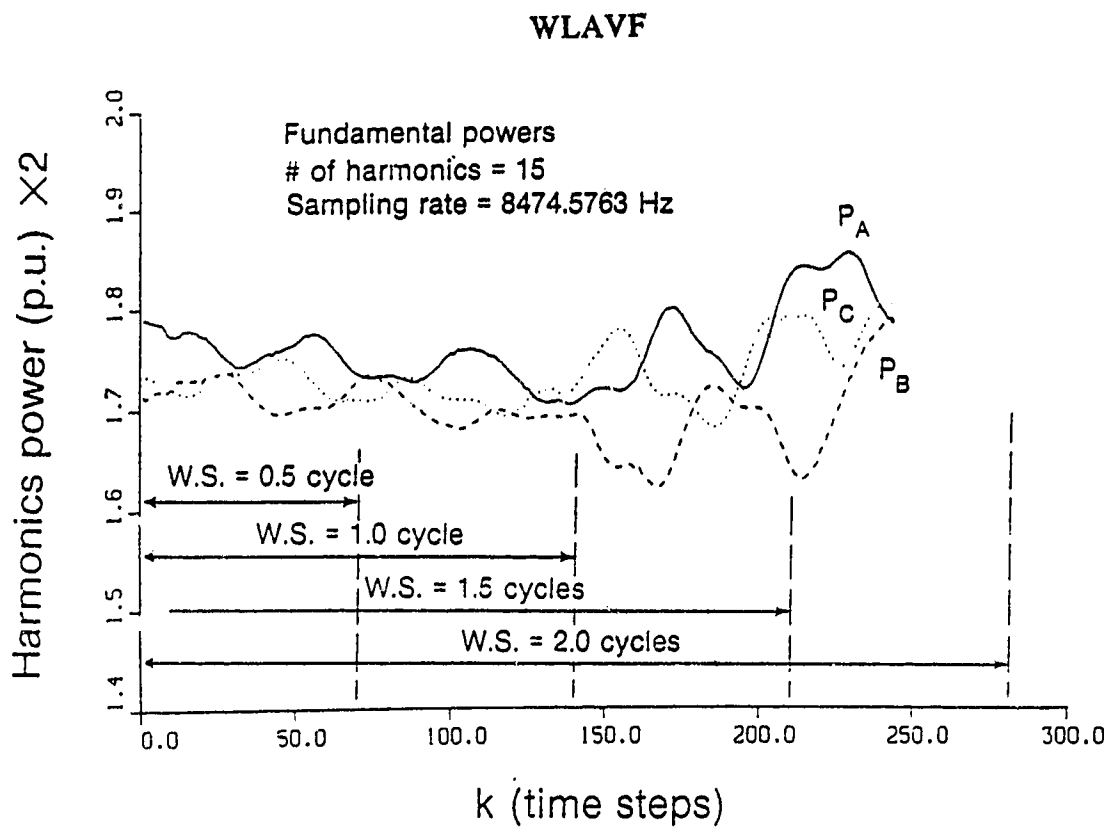


Fig. 5.31 Fundamental powers versus time steps.

For comparison with KF see page 157

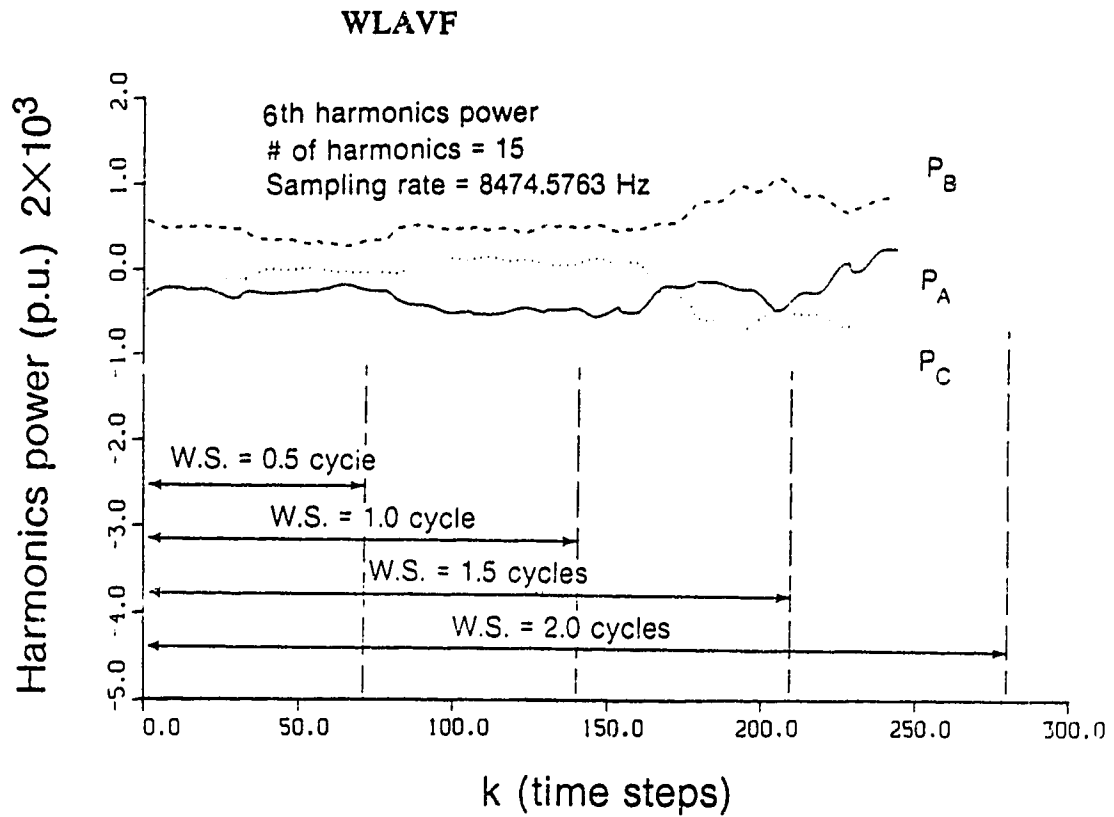


Fig. 5.32 6th harmonic power in the three phases versus time steps at different window sizes.

For comparison with KF see page 159

is kept constant at 2 cycles while the sampling frequency is changing as 8474.57, 4237.28, 2824.85 and 2118.64 Hz. Samples of the results obtained are introduced here. Figures (5.33), (5.34) and (5.35) gives the most effective harmonic magnitudes of the current I_A when the sampling frequency was 2118.64, 2824.85 and 4237.28 Hz respectively, for the same frequencies the sixth harmonic power for phases A, B and C were found and samples of the results are given in figures (5.36) and (5.37). Figure (5.38) gives the estimation of the fourth harmonic magnitude when the three sampling rates are used. In this figure the three curves are shown on a common graph. Examining all these curves indicates that the sampling frequency has a slight effect on the estimate providing that the sampling frequency is still higher than twice the frequency of the highest harmonic considered in the waveform and that is what happened with the KF case.

Effects of number of harmonics

The algorithm was tested for a different number of harmonics considered in the voltage and the current waveforms, the number of harmonics was changed from 7 to 23 with the sampling frequency constant at 8474.57 Hz and the data window size was chosen to be 1 cycle. Figures (5.39), (5.40) and (5.41) give samples of the results obtained. These figures show the variation of the harmonic magnitudes when a different number of harmonics is considered. Examining these curves shows that the number of harmonics considered has a slight effect on the estimate. However, it is better to increase the number of harmonic to reduce the error in the estimate.

WLAVF

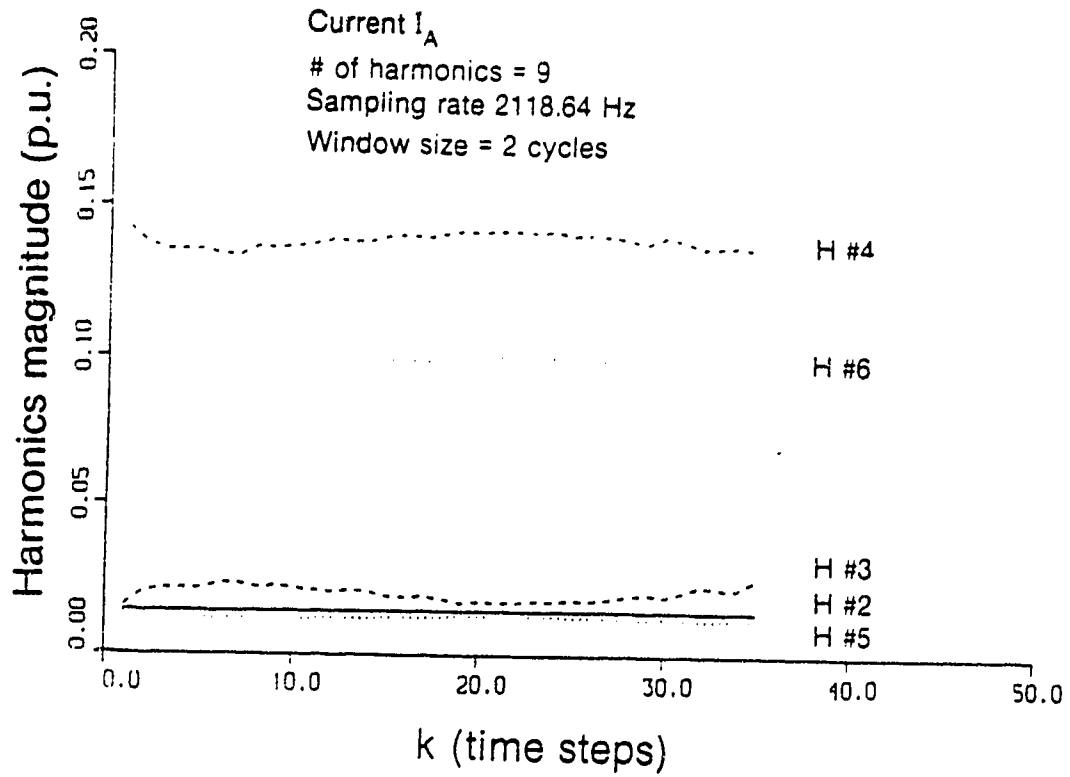


Fig. 5.33 Variation of harmonics magnitude with the time steps.
For comaprison with KF see page 162

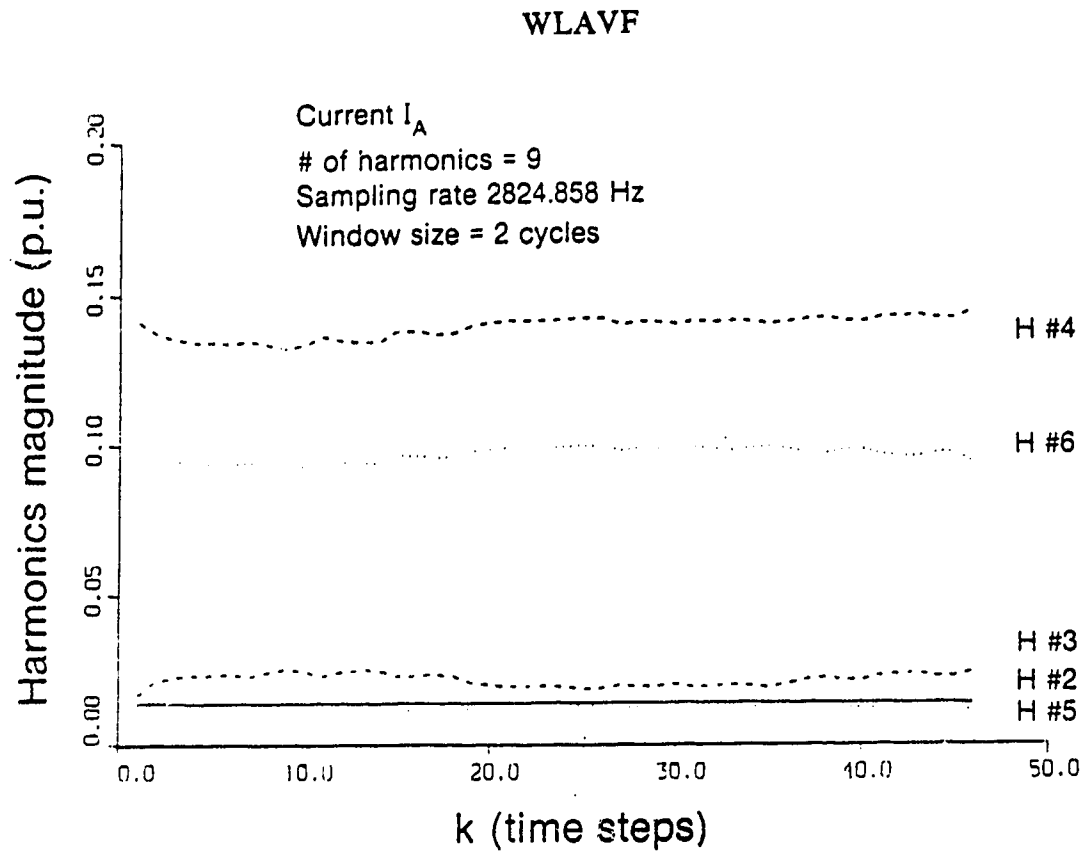


Fig. 5.34 Variation of harmonics magnitude with the time steps
For comparison with KF see page 163

WLAVF

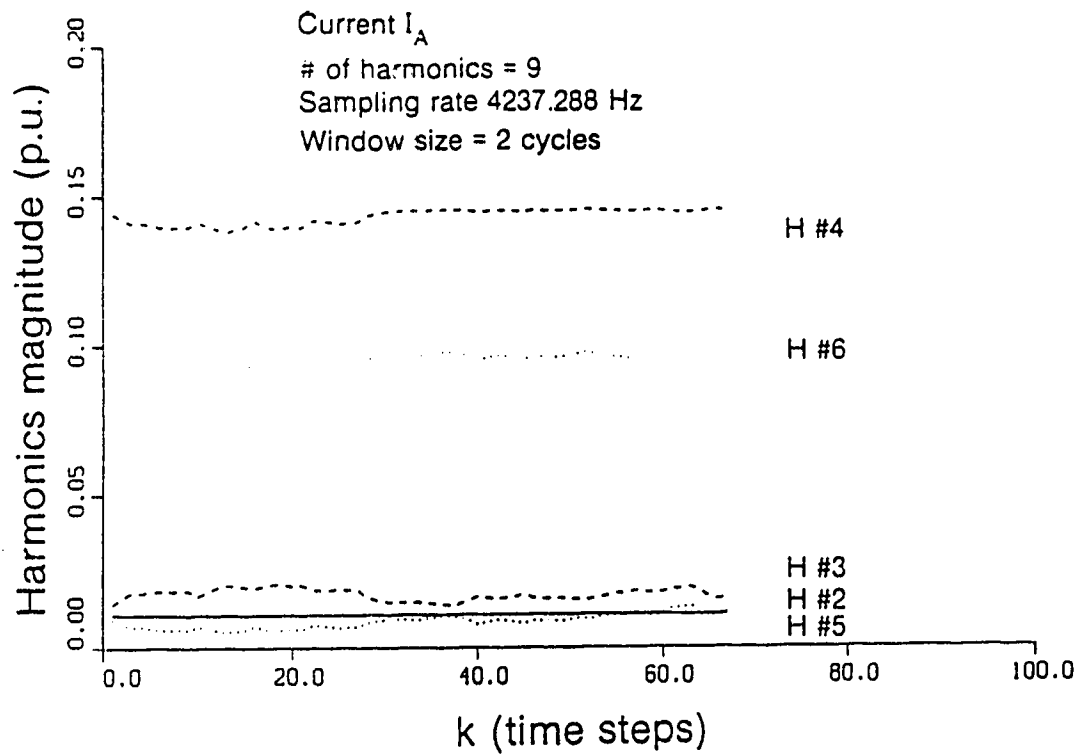


Fig. 5.35 Variation of harmonics magnitude with the time steps.

For comparison with KF see page 164

WLAVF

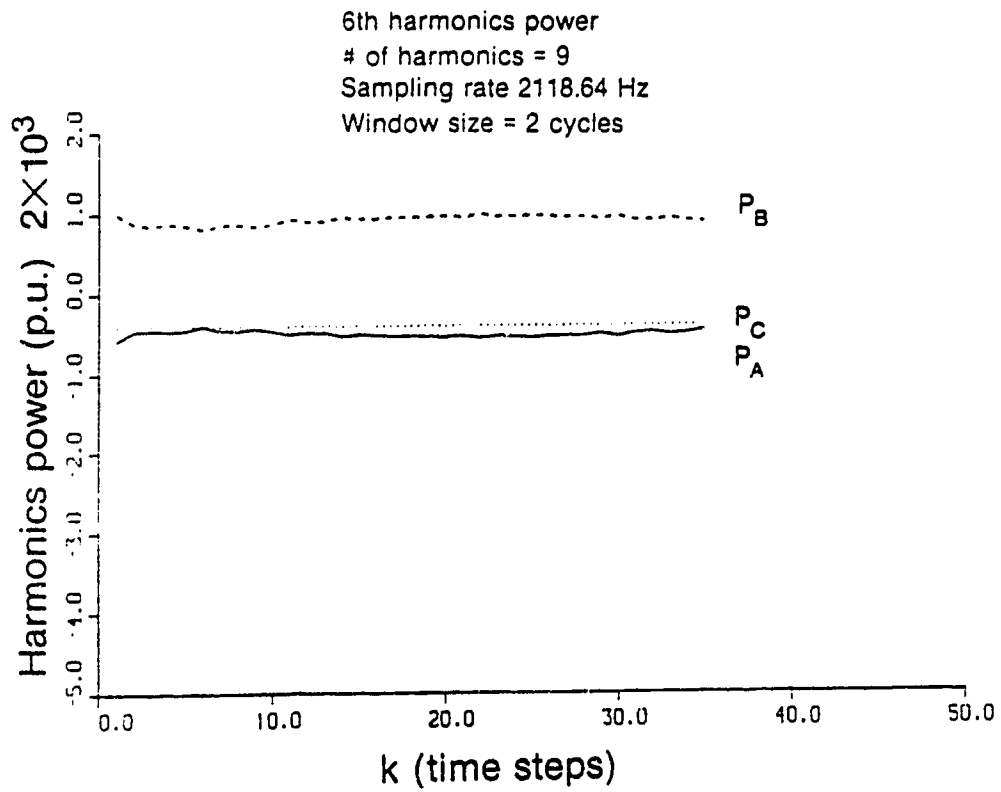


Fig. 5.36 Variation of harmonics power with the time steps samples.

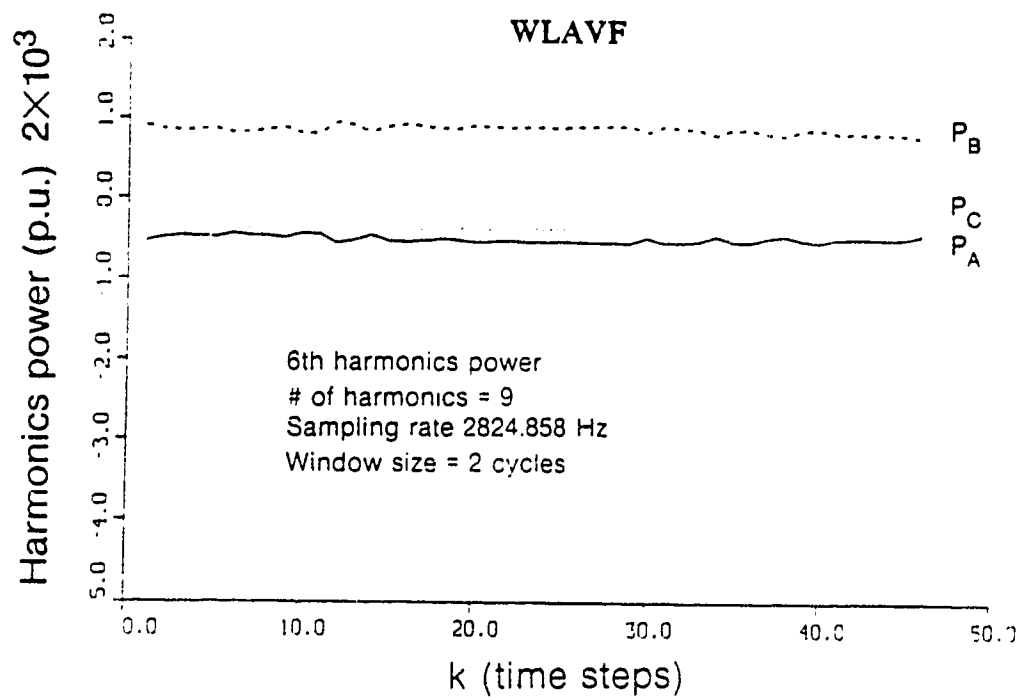


Fig. 5.37 Variation of harmonics power with the time steps.

For comparison with KF see page 166

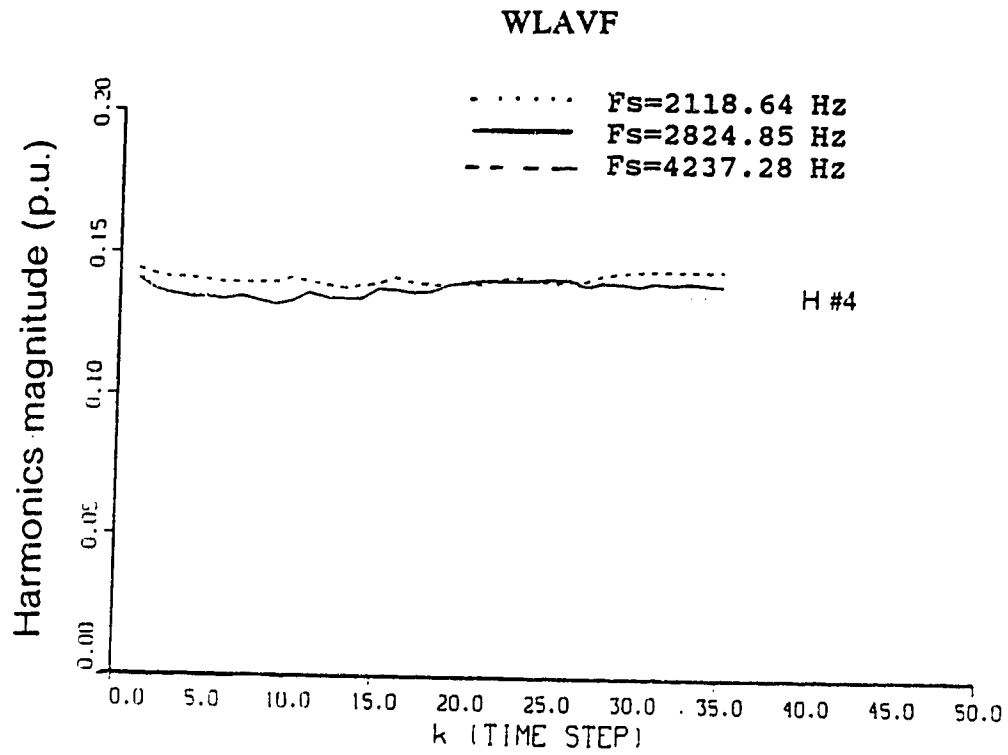


Fig. 5.38 Variations of the harmonic magnitudes
with the sampling frequency

WLAVF

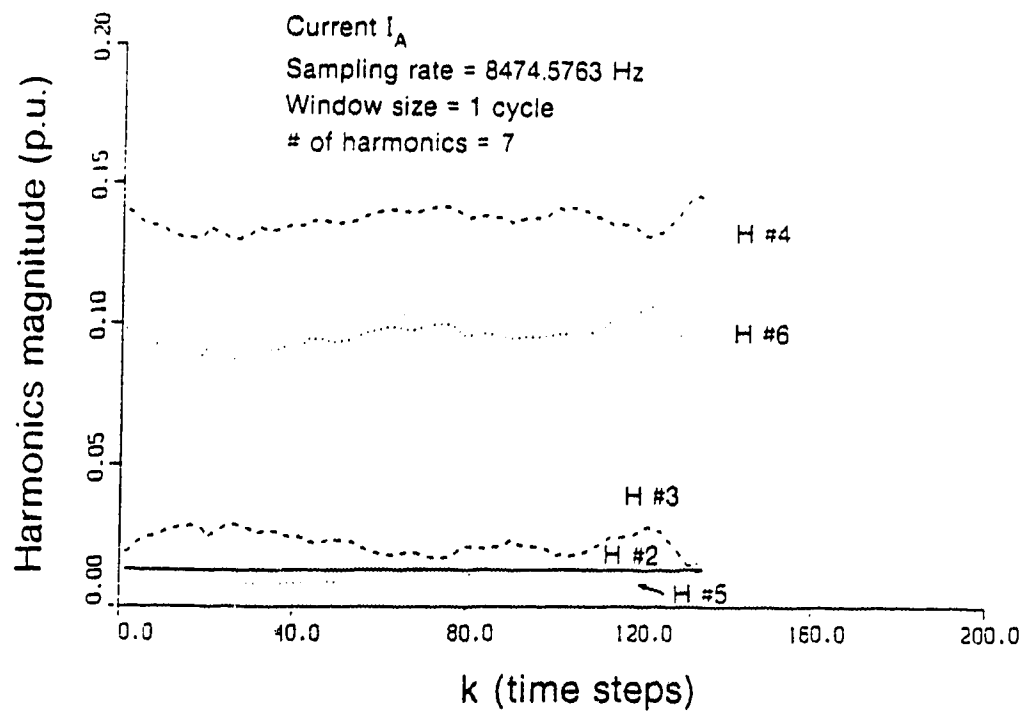


Fig. 5.39 Variation of harmonics magnitude with the time steps.

For comparison with KF see page 168

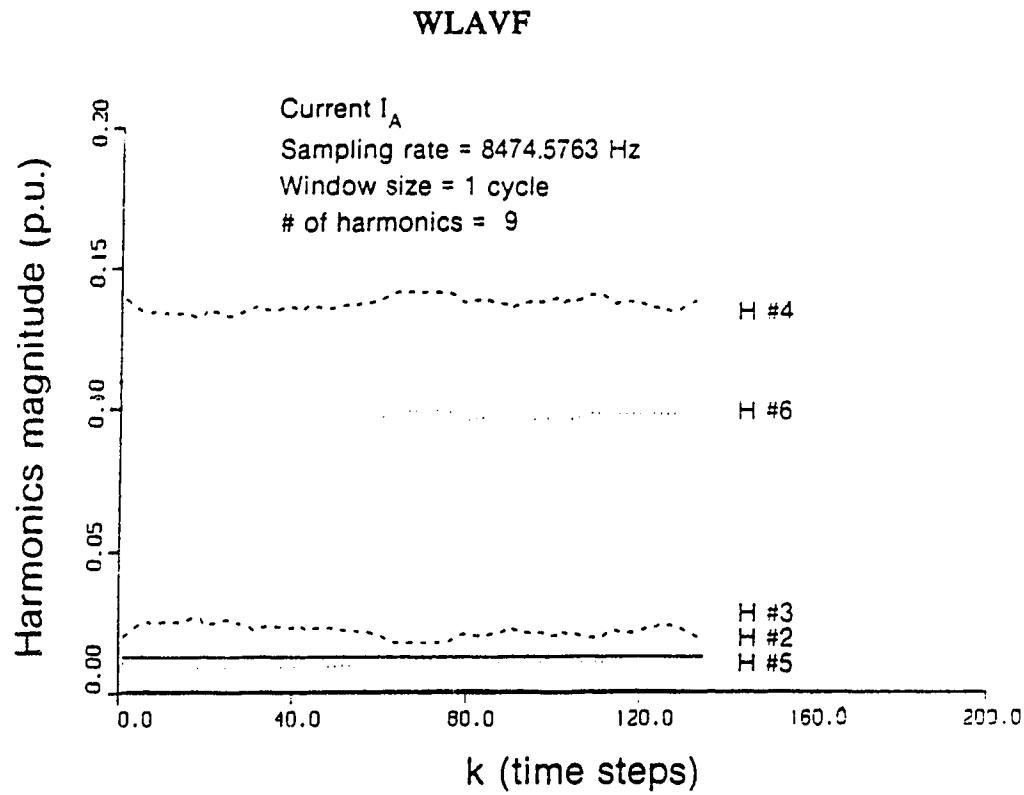


Fig. 5.40 Variation of harmonics magnitude with the time steps.

For comparison with KF see page 169

WLAVF

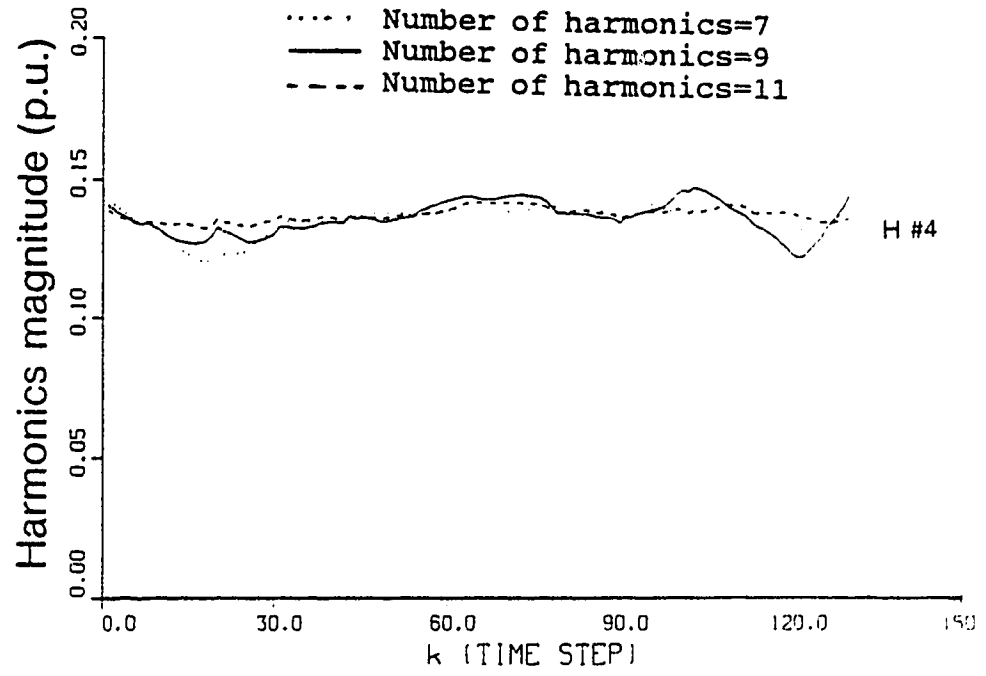


Fig. 5.41 Variations of the harmonic magnitudes with the number of harmonics considered

Subharmonics estimation

Once the harmonic contents of the waveform is identified, the reconstructed waveform can be obtained. Figure (5.42) gives the real current and the reconstructed current for phase A as well as the resultant error. The maximum error in this estimation was found to be about 13%. The error signal is then analyzed to identify the subharmonic parameters. Figure (5.43) gives the subharmonic amplitudes for the subharmonic frequencies of 15 and 30 Hz while figure (5.44) gives the phase angle Φ_2 .

The total error is found by subtracting the combination of the harmonic and the subharmonic contents, total reconstructed, from the actual waveform. This error is given in figure (5.45) and it is clear that this is a very small error with a maximum value of about 3 %.

5.5: Comparison between the KF and the WLAVF

From section 5.4 we can say generally that both filters nearly produce very close results. However, some points could be mentioned here

1. The estimate obtained via the WLAVF algorithm is more damped than that obtained via the KF algorithm. This is probably due to the fact that the WLAVF gain is more damped and reaches steady state faster than the KF gain as shown in figure (5.46).
2. The overall error in the estimate was found to be very close in both cases with a maximum value of about 3%. The overall error for

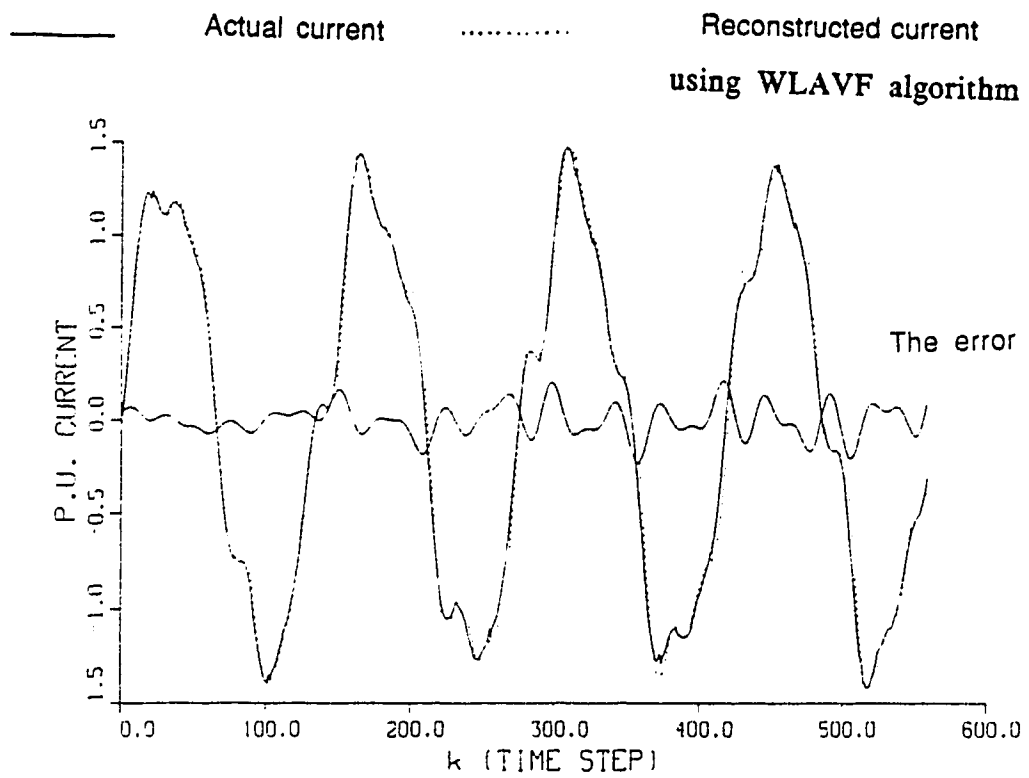


Fig. 5.42 Actual and reconstructed current for phase A
For comparison with KF see page 172

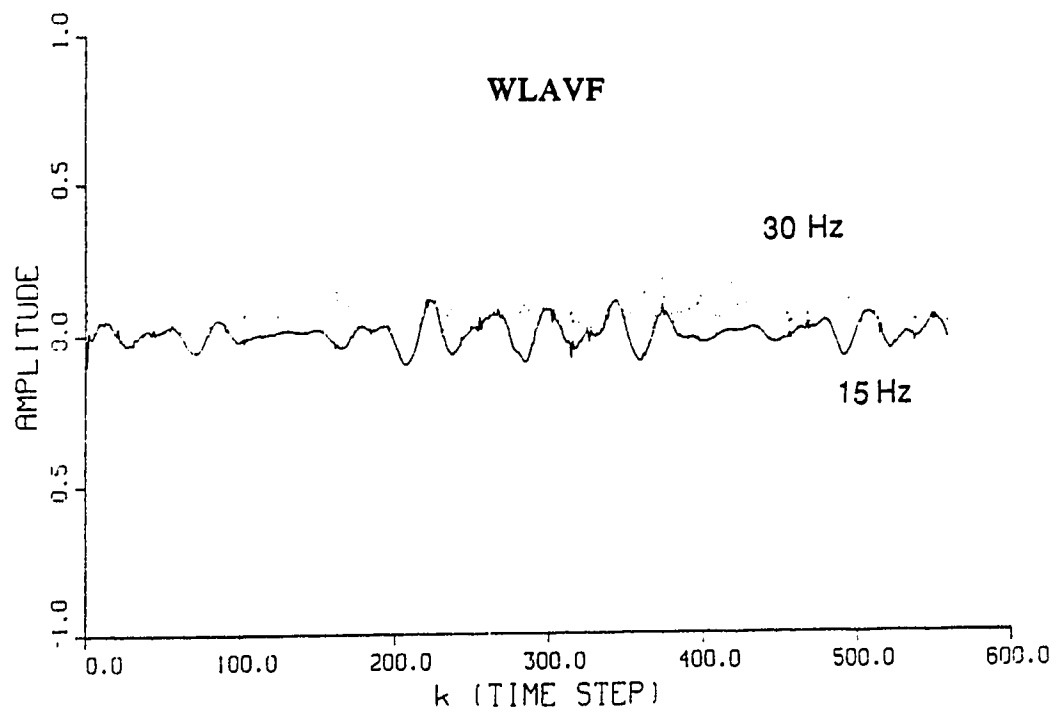


Fig. 5.43 The subharmonic amplitudes

For comparison with KF see page 173

WLAVF

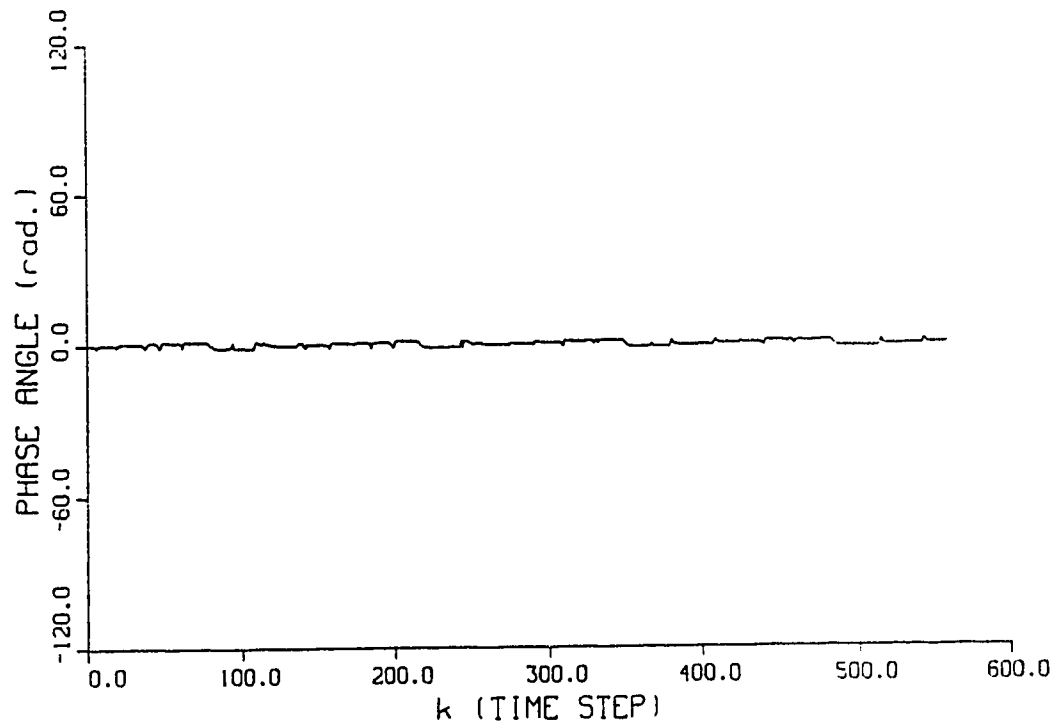


Fig. 5.44 The phase angle of the 30 Hz component

For comparison with KF see page 174

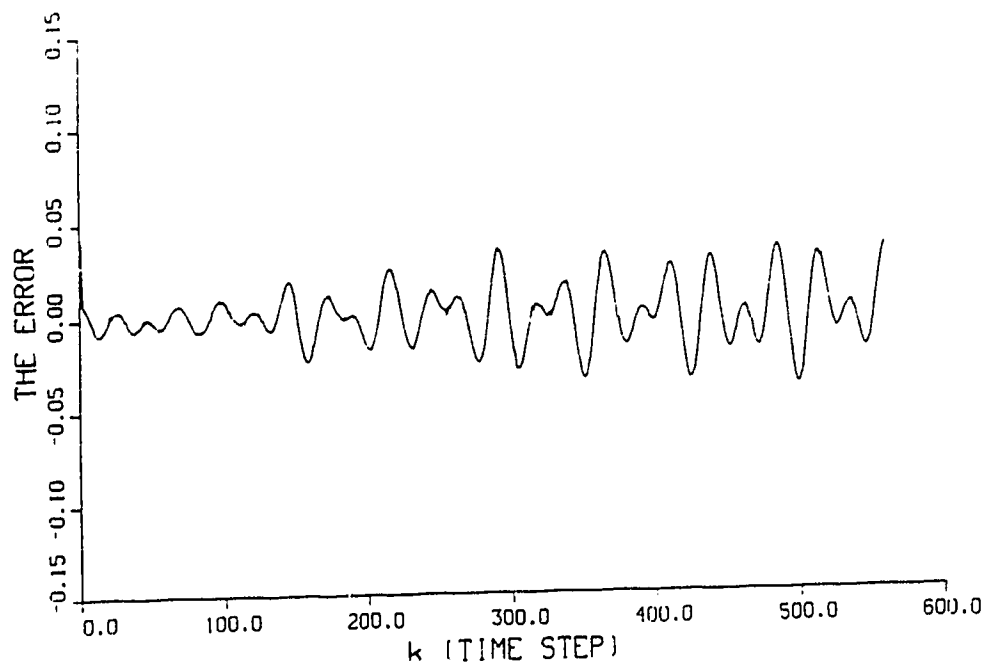


Fig. 5.45 The final error in the estimate using the WLAVF algorithm

For comparison with KF see page 175

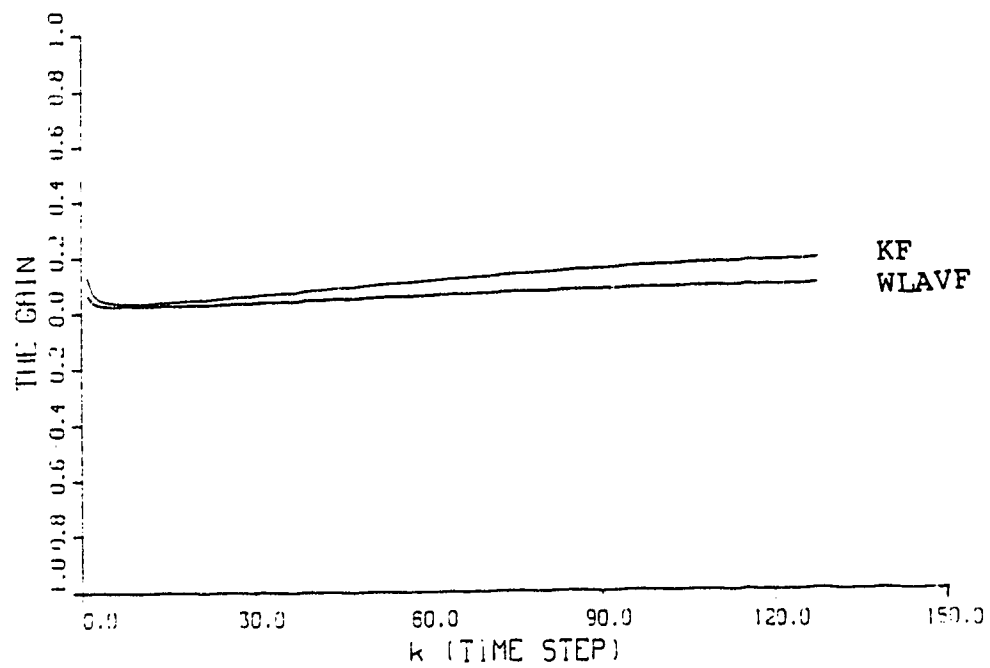


Fig. 5.46 Comparison between the filters gain for the component x_1
(simulated example case, Model 2)

both cases is given in figure (5.47).

3. Both algorithms were found to act similarly when the effects of the data window size, sampling frequency and the number of harmonics were studied.

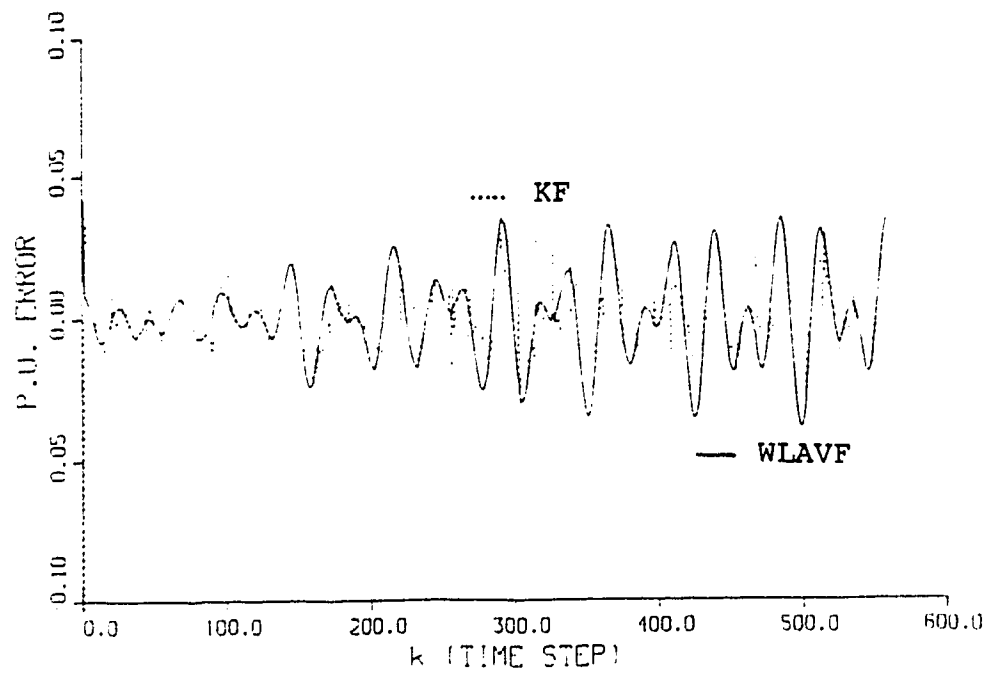


Fig. 5.47 The final error in the estimation using the two filters

CHAPTER VI

SUMMARY AND CONCLUSIONS

SUMMARY

In this study, different state estimation techniques for identifying power system harmonics have been introduced. First, the power system harmonic problem was reviewed in chapter II. This review included, the harmonic sources, harmonic effects and the harmonic measurement techniques.

In chapter III, the mathematical models suitable for solving this problem were developed. These models were classified according to the problem type, harmonic or subharmonic, and also according to the technique used, on-line or off-line.

The static estimation problem was presented in chapter IV. In this chapter different static estimation techniques are introduced. A new application of least squares technique is presented and compared to the discrete Fourier transform. An application of a new non iterative least absolute value technique is presented as well. The chapter was concluded by the results obtained when using these techniques with simulated examples and real data, also a comparison between these techniques was provided.

In chapter V the dynamic estimation problem was presented as well as the Kalman filter and the recently developed weighted least absolute value filter. The algorithms were tested using simulated example and real data. The results were presented and a comparison was

made.

CONCLUSIONS

From the results obtained in the off-line simulation some important remarks can be made as follows

1. The new application of the least squares technique for identifying power system harmonic sources gave an easy alternative to the popular discrete Fourier technique with the same degree of accuracy.
2. The new least absolute value estimator gave a results as good as both the discrete Fourier transform and least squares techniques with superiority in the case of bad data. The application of this new least absolute value technique showed that it is a valuable alternative to the iterative linear programming technique.
- 3 In the case of non-stationary waveforms if each cycle of the data set is considered separately, as suggested, a very good estimate can be obtained.
4. An interesting observation made during the off-line simulation, was that the second least squares solution in the way to get the least absolute value estimation was, in most cases, very close to the LAV solution hence, this can be considered as an improvement in the least squares estimation.

5. It is obvious that in the case of stationary waveforms the static techniques are preferable over the dynamic ones.

In the on-line simulation the results obtained reveal that

1. The dynamic filters are superior in the case of non-stationary waveforms.

2. The new least absolute value filter appeared as an alternative to the Kalman filter with almost the same computational time and a high degree of accuracy. The LAVF would give even better results when the error distribution is non-Gaussian.

SUGGESTIONS FOR FUTURE INVESTIGATIONS

During the course of the research, the following points have been detected and they are suggested here as subjects for future work in the same area.

1. This work can be extended to identify the harmonic sources in a multibus system. The transient waveforms can be analyzed, as well, and the amplitudes and the frequencies can be identified.

2. This theoretical work could be repeated experimentally especially the parts with the LAV filters and compared to the theoretical work done in this thesis. A complete simulation can be made using an induction motor with variable speed drive and a signal from the

voltage and the currents can be recorded in a digital form. The digitized waveforms can then be analyzed using on or off line filtering algorithms. After detecting the harmonic content, a suitable circuits can be built to reduce the distortion level or to limit it to the standard levels.

3. A continuation of the theoretical work can be in the form of deriving the mathematical model for the extended weighted least absolute value filter to solve the non linear problems and compare the performance to that of the Kalman filter.

REFERENCES

- [1] T.C.Shuter, H.T.Volkommer and T.L.Kirkpatrick, "Survey of Harmonic Levels on the American Electric Power Distribution System", IEEE Trans. on Power Delivery, Vol.4, No.4, pp. 2204-2213, 1989.
- [2] IEEE Power System Harmonics working Group Report, "Bibliography on Power System Harmonics, Part I and Part II" IEEE Trans. on Power Apparatus and Systems, Vol.PAS-103, No.9, pp.2460-2478, 1984
- [3] R.H.Kitchin, "A New Method for Digital-Computer Evaluation of Converter Harmonics In Power Systems Using State-Variable Analysis", IEEE Proc. Vol.128, Pt C, No.4, pp.196-207, 1981.
- [4] M.F.McGranaghan, J.H.Shaw and R.E.Owen, "Measuring Voltage And Current Harmonics on Distribution Systems", IEEE. Trans.on PAS, Vol.PAS-100, No.7, pp.3599-3608, 1981.
- [5] K.Olejniczak and G.T.Heydt, "Basic Mechanisms of Generation and Flow of Harmonic Signals in Balanced and Unbalanced Three Phase Power Systems", IEEE. Trans., PWRD-4, No.4, pp.2162-2170, 1989.
- [6] IEEE Working Group on Power System Harmonics," Power System Harmonic: An Overview" IEEE Trans. on PAS, Vol.102, No.8, pp.2455-2460, 1983.
- [7] J.Arrillaga, D.A.Bradley and P.S.Bodger, "Power System Harmonics". John Wiley & Sons, 1985, New York.
- [8] G.D.Breuer et al., "HVDC-AC Harmonic Interaction, Part I. Development of A Harmonic Measurement System, Hardware and Software", IEEE Trans., Vol.PAS-101, pp.701-708, 1982.
- [9] G.D.Breuer et al., "HVDC-AC Harmonic Interaction, Part II. AC System Harmonic Model With Comparison of Calculated and Measured Data", IEEE Trans., Vol. PAS-101, pp.709-718, 1982.
- [10] J.A.Orr, D.Cyganski, A.E.Emanud and R.T.Saleh, "Design of A System for Automated Measurement and Statistics calculation of Voltage and Current Harmonics", IEEE Trans., PWRD-1, pp.23-30, 1986.
- [11] G.T.Heydt, " Identification of Harmonic Sources by A State Estimation Technique", IEEE Trans., PWRD-4, pp.569-576, 1989.
- [12] D.Crevier and A.Marcier, "Estimation of Higher Frequency Network Equivalent Impedance By Harmonic Analysis of Natural Waveforms", IEEE Trans. on PAS, VOL.PAS-97, No.2, pp.424-431,1978.
- [13] A.A. Girgis, W.B. Chang and E.B. Makram, "A Digital Recursive Measurement Scheme for on-line Tracking of Power System Harmonics." IEEE Trans. on Power Delivery, Vol.6., No.3, pp.1153-1160, 1991.

- [14] H.Jeffereys, "Theory of probability", Oxford University press. London, 1939.
- [15] G.S.Christensen, S.A.Soliman and A.Rouhi, "A New Technique for Curve Fitting Based on Minimum Absolute Deviations", Computational Statistical and Data Analysis, Vol.6, No.4, pp.341-351, 1988.
- [16] S.Persaud, "A Study of Parameter Estimation Techniques in Short-Term Load Forecasting", M.Sc. Thesis, University of Alberta, 1991.
- [17] E.J.Scholssmacher, "An Iterative Technique for Absolute Deviations curve fitting", Journal of the American Statistical Ass. Vol.68, No.344, pp.867-869, 1973.
- [18] O.J.Karst, "Linear Curve Fitting Using Least Absolute Deviations", Journal of the American Statistical Ass., Vol.53, pp.118-132, 1958.
- [19] I.Barrodale and F.D.K.Roberts, "An Improved Algorithm for Discrete L_1 Linear Approximations", SIAM J.of Numer. Anal., Vol10, No.5, pp.839-848, 1973.
- [20] I.Barrodale and F.D.K.Roberts, "An Efficient Algorithm for Discrete L_1 Linear Approximation With Linear Constrains", SIAM Journal of Num. Anal., Vol.15, No.3, pp.603-611, 1978.
- [21] S.A.Soliman, G.S.Christensen and A.Rouhi, "A New Technique for Curve Fitting Based on Least absolute Value", Computational Statistical & Data Analysis ,6, pp341-351, 1988.
- [22] G.S.Christensen, S.A.Soliman and A.Rouhi, "A New Technique for Unconstrained and Constrained Linear LAV Parameter Estimation", Canadian J. Elec. & Comp. Eng., Vol14, No.1, pp.24-30, 1989.
- [23] V.A.Sposito and M.L.Hand, "Using An Approximate L_1 Estimator", Communications in statistics - Simulation and Computation, Vol.B6(3), pp.263-268, 1977
- [24] G.F.McCormick and V.A.Sposito, "Using the L_2 estimation in L_1 estimation", SIAM J. of Num. Anal. Vol.13, No.3, pp.337-343, 1976.
- [25] Center of Research in Eng. & Applied Science, University of New Brunswick, "Power System Harmonics: A Review and Assessment of problems", Report to Canadian Electrical Association, Vol.1-Technical Document, Report No.415 U 474, March 1986.
- [26] S.A.Soliman, G.S.Christensen, D.H.Kelly and K.M.El-Naggar, "A State Estimation Algorithm for Identification and Measurement of Power System Harmonics", Electrical Power Systems Research J. Vol.19, pp.195-206, 1990.

- [27] K.G.Lee and K.P.Poon, "Analysis of Power System Dynamic Oscillations With Beat Phenomenon By Fourier Transformation", IEEE. Trans. on Power Systems, Vol.5, NO.1, pp.148-153, 1990.
- [28] P.K.Dash and A.M.Sharaf, "Kalman Filtering Approach for Estimation of Power System Harmonics" Proceeding of International conference on Power System Harmonics, pp.34-40, 1989.
- [29] D.Xia and G.T. Heydt, "Harmonic Power Flow Studies. Part I-Formulation and Solution", IEEE. Trans. on Power Systems and Apparatus, Vol.PAS-101, No.6, 1257-1265, 1982.
- [30] G.S.Christensen, S.A.Soliman, D.H.Kelly and K.M.El-Naggar, "Identification and Measurements of Power Systems Harmonics Using Discrete Fourier Transform (DFT)", Accepted for publication to the Electric Machines and Power Systems Journal, 1991.
- [31] L.C.Ludeman, "Fundamentals of Digital Signal Processing", Harper and Row, New York, 1986.
- [32] M.S.Sachdev and M.M.Giray, "A Least error Squares Technique for Determining Power System Frequency", IEEE. Trans. Vol.PAS-104, pp.437-444, 1985.
- [33] M.S.Sachdev and M.A.Baribeau, "A New Algorithm for Digital Impedance Relay", IEEE. Trans., Vol.PAS-98, pp.2232-2240, 1979.
- [34] G.S Christensen, S.A.Soliman and A.Rouhi, "Discussion of an Example Showing That A New Technique for LAV Estimation Breaks Down in Certain Cases", Computational Statistical and Data Analysis, Vol.19, pp.203-213, 1991.
- [35] N.Liu, "Frequency Estimation in Power Systems", M.Sc. Thesis, University of Alberta, 1989.
- [36] A.H.Rouhi, "A New Power System State Estimator", M.Sc. Thesis, University of Alberta, 1988.
- [37] S.A.Soliman, G.S.Christensen and S.S.Fouda, "On The Application of the Least Absolute Value Parameter Estimation Algorithm to Distance Relaying", Electric Power Systems Research, pp.23-35, 1990.
- [38] S.A.Soliman, S.E.A.Emam and G.S.Christensen, "A New Algorithm for Optimal Parameter Estimation of Synchronous Machine from Frequency Test Based on LAV Approximation", Canadian Journal of Electrical and Computer Engineering, Vol.14, No.3, pp.98-102, 1989.
- [39] R.F.Stengel, "Stochastic Optimal Control Theory and applications", John Wiley & Sons, 1986.
- [40] R.E.Kalman, "A New Approach to Linear Filtering and Prediction

Problems", Journal of Basic Engineering, Trans. of The ASME, pp.35-45, March 1960.

[41] A.E.Bryson and Y.C.Ho, "Applied Optimal Control", Blaisdell Pub. Comp., 1969.

[42] R.G.Brown, "Introduction to Random Signal Analysis and Kalman Filtering", John Wiley & Sons, 1983.

[43] G.S.Christensen and S.A.Soliman, "Optimal Filtering of Linear Discrete Systems Based On Least Absolute Value Approximation", Automatica, Vol.26, No.2, pp.389-395, 1990.

[44] F.L.Lewis, "Optimal Estimation With An Introduction To Stochastic Control Theory", Wiley, New York, 1986.

[45] A.P.Sage and G.W.Husa, Adaptive Filtering With Unknown Prior Statistics", Proc. of The Joint Automotive Control Conference, pp.670-679, 1969.

[46] G.T.Heydt, "The Identification and Analysis of Harmonic Signal In Electric Power Systems", Int.Journal of Energy System, Vol.11, No.1, pp.20-24, 1991.

[47] K.L.Sharma and A.K.Mahalanabis, "Harmonic Analysis Via Kalman Filtering Technique", Proc. of IEEE., Vol.61, No.3, pp.391-392, 1973.

[48] A.P.Sage and C.C.White, III, "Optimum Systems Control", New Jersey, 1977.

[49] D.E.Catlin, "Estimation, Control and the Discrete Kalman Filter", Applied Mathematical Sciences, Springer-Verlag, New York, 1989.

[50] N.B.Jones and J.D.Mck.Watson, "Digital Signal Processing Principles, Devices and Applications", Peter Peregrinus, London U.K., 1990.

APPENDIX I

The full wave rectifier circuit is shown in figure I.1. The equations of the input and output waveforms are given as

$$V_{in}(t) = V_m \sin(\omega t) \quad \text{and}$$

$$V_{out}(t) = | V_m \sin(\omega t) | .$$

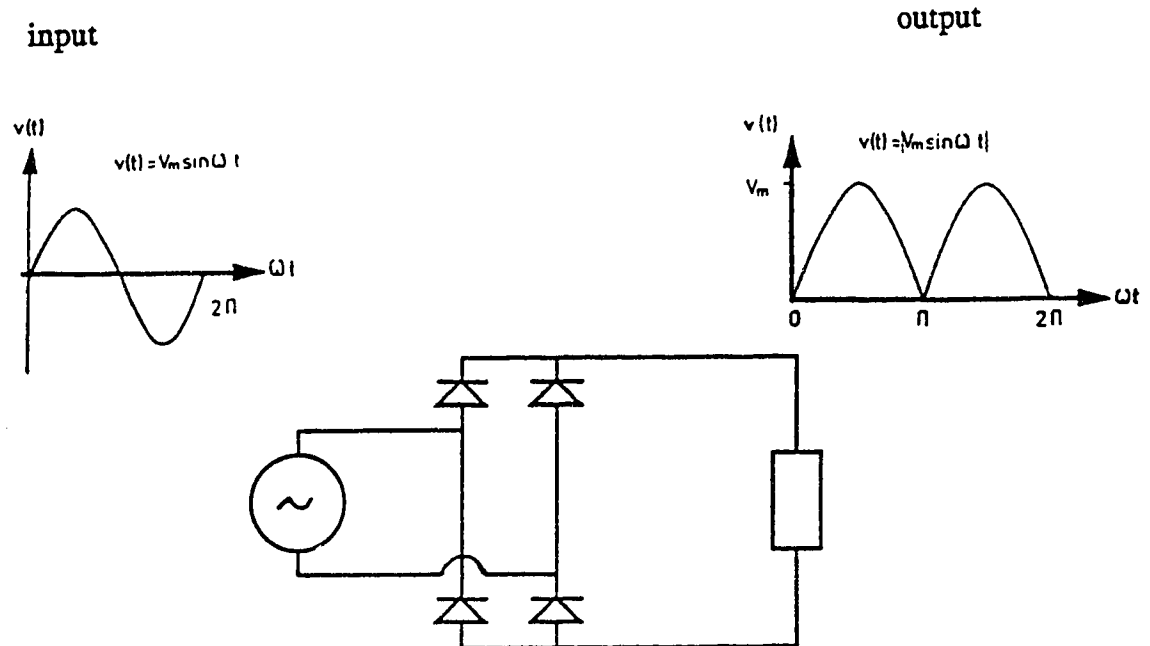


Fig. I.1 The full wave rectifier circuit

According to Fourier analysis, V_{out} can be expressed as

$$V_{out}(t) = a_0 + \sum_{n=1}^{\infty} (a_n \cos n\omega t + b_n \sin n\omega t)$$

where $a_0 = \frac{1}{T} \int_0^T V(\omega t) d(\omega t) ,$

$$a_n = \frac{2}{T} \int_0^T V(\omega t) \cos n\omega t d(\omega t) ,$$

$$b_n = \frac{2}{T} \int_0^T V(\omega t) \sin n\omega t d(\omega t) ,$$

and T is the periodic time.

The analysis of the full wave rectified voltage (output voltage) gives the Fourier coefficients as

$$a_0 = \frac{2 V_m}{\pi} ,$$

$$a_n = \frac{4 V_m}{\pi(n^2 - 1)} \quad \text{for} \quad n=2,4,6,\dots ,$$

$$a_n = 0 \quad \text{for} \quad n=1,3,5,\dots , \text{ and}$$

$$b_n = 0 .$$

APPENDIX II

The actual data provided by ALBERTA POWER LIMITED is for a dynamic load. The load is a variable frequency drive controlling a 3000 HP induction motor connected to an oil pipe line compressor. The solid state drive is of 12 puls design with harmonic filtering. The data given is the phase voltage V_A and the three phase currents at different speeds of the motor. The electrical description of the load is given as follows:

POWER = 3000 HP , and

VOLTAGE = 25 K.V.

At the point of measurement there are voltage transformer and current transformers with the following data:

CURRENT TRANSFORMER TURNS RATIO = 60 , and

VOLTAGE TRANSFORMER TURNS RATIO = (120)*101 .

The sampling rate is 118 micro seconds with 4096 samples (about 29 cycles).

A sample of the waveforms given for the voltage and current is shown earlier in the body of the thesis (pages 90 and 91) .

The per unit system used in this thesis is based on the following

quantities at the motor side:

$$\text{Base K.V.A} = 3000 \times 746/3 = 746 \text{ K.V.A} ,$$

$$\text{Base voltage} = 25/\sqrt{3} = 14.43 \text{ K.V.} , \text{ and}$$

$$\text{Base current} = \frac{2238}{\sqrt{3} \ 25} = 51.684 \text{ Amperes.}$$

Thus in the low tension side of the transformers the base values will be:

$$\text{Base voltage} = \frac{14.43}{120 \times 101} = 1.2 \text{ Volts} , \text{ and}$$

$$\text{Base current} = \frac{51.684}{60} = 0.8614 \text{ Amperes} .$$